

EUROPEAN ORGANISATION FOR NUCLEAR RESEARCH (CERN)



Submitted to: JHEP



CERN-PH-EP-2015-070
14th August 2015

Search for heavy Majorana neutrinos with the ATLAS detector in pp collisions at $\sqrt{s} = 8$ TeV

The ATLAS Collaboration

Abstract

A search for heavy Majorana neutrinos in events containing a pair of high- p_T leptons of the same charge and high- p_T jets is presented. The search uses 20.3 fb^{-1} of pp collision data collected with the ATLAS detector at the CERN Large Hadron Collider with a centre-of-mass energy of $\sqrt{s} = 8$ TeV. The data are found to be consistent with the background-only hypothesis based on the Standard Model expectation. In the context of a Type-I seesaw mechanism, limits are set on the production cross-section times branching ratio for production of heavy Majorana neutrinos in the mass range between 100 and 500 GeV. The limits are subsequently interpreted as limits on the mixing between the heavy Majorana neutrinos and the Standard Model neutrinos. In the context of a left-right symmetric model, limits on the production cross-section times branching ratio are set with respect to the masses of heavy Majorana neutrinos and heavy gauge bosons W_R and Z' .

© 2015 CERN for the benefit of the ATLAS Collaboration.

Reproduction of this article or parts of it is allowed as specified in the CC-BY-3.0 license.

arXiv:1506.06020v2 [hep-ex] 13 Aug 2015

Contents

1	Introduction	2
2	The ATLAS detector	4
3	Background and signal simulation	5
4	Data sample and event selection	6
4.1	Object reconstruction and selection	6
4.2	Lepton isolation criteria	7
4.3	General event selection	8
4.4	Selection criteria for mTISM signal events	8
4.5	Selection criteria for LRSM W_R and Z' signal events	9
5	Background estimation	9
5.1	Background from prompt same-sign leptons	10
5.2	Background from prompt opposite-sign leptons	11
5.3	Background from fake and non-prompt leptons	11
5.4	Validation of background estimates	12
6	Systematic uncertainties	16
6.1	Background uncertainties	16
6.2	Uncertainties on MC simulation	16
6.3	Signal-specific modelling uncertainties	18
7	Results	18
7.1	Results in the mTISM signal region	18
7.2	Results in the LRSM signal region	20
8	Conclusions	25

1 Introduction

The discovery of mixing between generations of neutrinos [1] has established that at least two of the neutrinos have small non-zero masses. A unique feature of neutrinos compared to other fermions in the Standard Model (SM) is that neutrinos could be their own anti-particles, so-called Majorana fermions. If this is realised in nature, then the unusually low mass scale of the light neutrinos could be generated by a seesaw mechanism [2–7] which would imply the existence of yet unobserved heavy Majorana neutrino states. The nature of Majorana neutrinos would explicitly allow for lepton number violation.

In this paper, a search is presented for heavy Majorana neutrinos using the ATLAS detector at the Large Hadron Collider (LHC). The data sample was collected in 2012 during $\sqrt{s} = 8$ TeV pp collisions and corresponds to an integrated luminosity of 20.3 fb^{-1} . Heavy Majorana neutrinos with masses above 50 GeV are considered. In this regime, the production and subsequent decay of heavy Majorana neutrinos could lead to a final state containing exactly two charged leptons, where the leptons may have the same or opposite charge in equal fractions of the heavy neutrino decays. Only lepton pairs of the same charge

(same-sign) are considered as there is a smaller expected SM background for pairs of same-sign leptons than for pairs of leptons of opposite charge (opposite-sign). The search includes the ee and $\mu\mu$ final states.

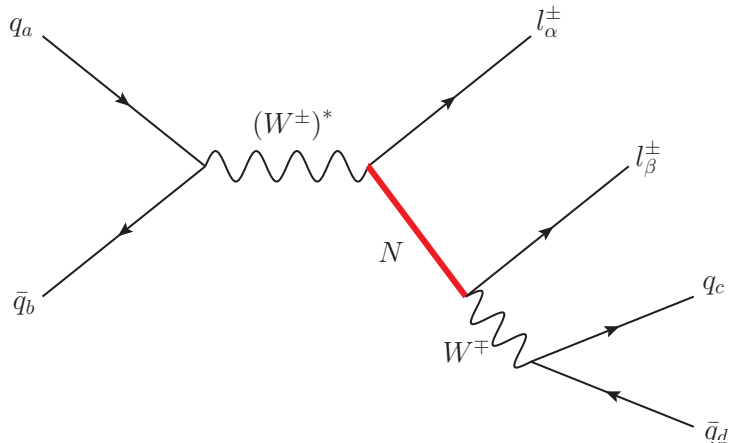


Figure 1: The tree-level diagram for the production of a heavy Majorana neutrino (N) in the mTISM model. Lepton flavour is denoted by α and β . Lepton flavour is assumed to be conserved, such that $\alpha = \beta$. The W boson produced from the N decay is on-shell and, in this case, decays hadronically.

The search is guided by two theoretical models. In the first model, the SM is extended in the simplest way to include right-handed neutrinos [8], such that light neutrino masses are generated by a Type-I seesaw mechanism or by radiative corrections [9]. In this minimal Type-I seesaw mechanism (mTISM), the heavy Majorana neutrinos, N , can be produced via an off-shell W boson, $pp \rightarrow (W^\pm)^* \rightarrow \ell^\pm N$. Due to previous limits [10, 11], the heavy neutrino is assumed to be more massive than the W boson and therefore subsequently decays to an on-shell W boson and a lepton. The on-shell W boson produced in the decay of the heavy neutrino predominantly decays into a quark–antiquark ($q\bar{q}$) pair. The final state in this case contains two opposite-sign or same-sign leptons and at least two high- p_T jets, where p_T is the transverse momentum with respect to the beam direction.¹ The tree-level process is illustrated in figure 1. The free parameters in this model are the mixing between the heavy Majorana neutrinos and the Standard Model neutrinos, $V_{\ell N}$, and the masses of the heavy neutrinos, m_N . In this framework, LEP has set direct limits for $m_N < m_Z$ [10, 11] and CMS has set direct limits for $90 < m_N < 200$ GeV in ee final states [12] and $40 < m_N < 500$ GeV in $\mu\mu$ final states [13].

The second model is the left-right symmetric model (LRSM) [4, 14–16], where a right-handed symmetry $SU(2)_R$ is added to the SM. The symmetry $SU(2)_R$ is assumed to be the right-handed analogue of the SM $SU(2)_L$ symmetry. In this model, heavy gauge bosons $V_R = \{W_R, Z'\}$ are also predicted and, in this analysis, the heavy gauge bosons are assumed to be more massive than the heavy neutrinos, such that they are kinematically allowed to decay into final states including heavy neutrinos. These can be produced in the decays of heavy gauge bosons according to $W_R \rightarrow N\ell$ and $Z' \rightarrow NN$ and can subsequently decay via an off-shell W_R boson into a lepton and a $q\bar{q}$ pair, $N \rightarrow \ell W_R^*$ with $W_R^* \rightarrow q\bar{q}'$. The tree-level processes are shown in figure 2. A previous ATLAS search in this framework has excluded $m_{W_R} < 2.3$ TeV for

¹ ATLAS uses a right-handed coordinate system, with its origin at the nominal interaction point in the centre of the detector. The z -axis points along the beam direction, the x -axis from the interaction point to the centre of the LHC ring, and the y -axis upwards. In the transverse plane, cylindrical coordinates (r, ϕ) are used, where ϕ is the azimuthal angle around the beam direction. The pseudorapidity η is defined via the polar angle θ as $\eta = -\ln \tan(\theta/2)$.

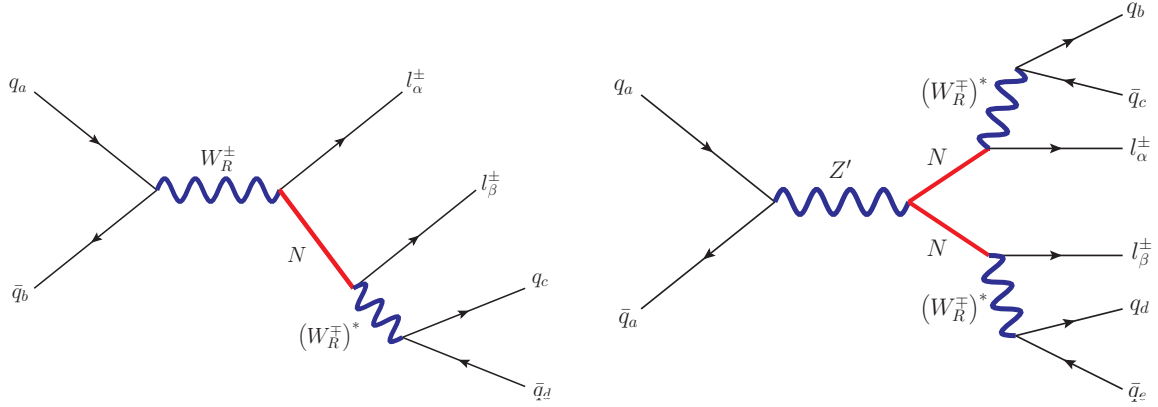


Figure 2: The tree-level diagrams for the production of a heavy Majorana neutrino (N) in the LRSM model, in which heavy gauge bosons W_R and Z' are also incorporated. Lepton flavour is denoted by α and β . Lepton flavour is assumed to be conserved, such that $\alpha = \beta$. The W_R boson produced from the N decay is off-shell and, in this case, decays hadronically.

$m_{W_R} - m_N > 0.3$ TeV at 95% confidence level (CL) [17]. A more recent search performed by CMS has excluded $m_{W_R} < 3.0$ TeV for $m_{W_R} - m_N > 0.05$ TeV at 95% CL [18]. There are no such limits for the production of heavy neutrinos from Z' boson decays.

Both the mTISM and LRSM models produce final states containing two same-sign leptons and high- p_T jets, but the kinematic characteristics of the events are quite different. In the mTISM final state, one can reconstruct the resonant SM W boson from the jets originating from the tree-level $q\bar{q}$ pair, whereas in the LRSM final states, one can instead reconstruct the masses of the heavy gauge bosons. Furthermore, the energy scales of the two models are largely separate. The energy scale of mTISM final states is set by the heavy neutrino mass, which, based on the LEP constraints [10, 11], is assumed to be greater than 100 GeV. Instead, the energy scale of LRSM final states is set by the masses of the heavy bosons, which, motivated by the earlier heavy neutrino searches, are assumed to be greater than 400 GeV. For these reasons, the event selection criteria are optimised separately for each model, although a common object selection is used in both cases.

2 The ATLAS detector

The ATLAS detector [19] surrounds the interaction point and covers nearly the entire solid angle. The detector consists of an inner detector (ID) tracking system, electromagnetic and hadronic calorimeters, and a muon spectrometer (MS) that surrounds the other detector systems. The ID tracking system consists of a silicon pixel detector, a silicon microstrip tracker, both covering $|\eta| < 2.5$, and a transition radiation tracker covering $|\eta| < 2.0$. The ID tracker is immersed in a 2 T axial magnetic field provided by a superconducting solenoid magnet. The electromagnetic accordion calorimeter is composed of lead and liquid-argon (LAr) and provides coverage for $|\eta| < 3.2$. Hadronic calorimetry is provided by steel and scintillator tile calorimeters for $|\eta| < 1.7$ and copper and LAr calorimeters for $1.5 < |\eta| < 3.2$. Additional LAr calorimeters with copper and tungsten absorbers cover the forward region. The MS consists of dedicated trigger chambers covering $|\eta| < 2.4$ and precision tracking detectors covering $|\eta| < 2.7$. A system of three superconducting toroids (one in the barrel, two in the end-caps), with eight coils each,

provides the magnetic field for the MS. A three-level trigger system is used to collect the data. The first-level trigger (L1) is implemented in hardware, using a subset of detector information to reduce the event rate to no more than 75 kHz. This is followed by two software-based trigger levels (L2 and EF), which together further reduce the event rate to less than 1 kHz.

3 Background and signal simulation

There are several SM interactions that can produce pairs of isolated charged leptons from vector boson decays, specifically from Drell–Yan and diboson processes and also from the decay products of top quarks. These processes are modelled using events produced by Monte Carlo (MC) generators. A summary of the primary MC generators used in this paper to model the background processes is presented in table 1. Processes that contribute to the background with pairs of same-sign leptons are indicated by the label ‘SS’ and processes which contribute with pairs of opposite-sign leptons, which are included in the charge-misidentification background estimate (section 5.2), are indicated by the label ‘OS’. The MC samples are normalised using the best available theoretical cross-sections, typically next-to-leading order or next-to-next-to-leading order in QCD.

The production of top quark pairs and the production of a single top-quark in association with a W boson are simulated using MC@NLO 4.0.3 [20, 21] with the CT10 PDF set [22]. The production of single Z boson and diboson ($W^\pm W^\mp$, WZ and ZZ) events are simulated using SHERPA 1.4.1 [23] with the CT10 PDF set. These samples include contributions from virtual photons, with the requirement for electron pairs to satisfy $m_{e^+e^-} > 0.1$ GeV. No requirement is made on $m_{\mu^+\mu^-}$. The SHERPA samples include leading-order matrix elements for the production of up to three additional partons. The matching between the matrix elements and the parton shower is achieved using the CKKW method [24]. The process $qq \rightarrow q'q'W^\pm W^\pm$ is generated using MADGRAPH 2.1.1 [25] with the MSTW 2008 PDF set [26]. The production of gauge bosons in association with top quark pairs is also simulated with MADGRAPH 2.1.1 using the CTEQ6L1 PDF set.

Table 1 also shows how the various signal processes are modelled. Signal events in the mTISM model are generated at leading order in QCD using the ALPGEN 2.14 MC generator [27, 28] with the CTEQ6L1 PDF set. The events are generated for heavy Majorana neutrino masses between 100 and 500 GeV. Final states which contain exactly two prompt leptons $\{ee, \mu\mu\}$ with same-sign charge are produced.

The PYTHIA 8.170 generator [29] is used to generate LRSM events at leading order in QCD. It is assumed in the model that the coupling between heavy gauge bosons and the heavy neutrino is equal to the coupling between the respective SM gauge bosons and light neutrinos. Similarly, the couplings of the new gauge bosons and the quarks are assumed to be equal to the couplings between the SM gauge bosons and the quarks. In the PYTHIA implementation of this process, all of the decay products of heavy neutrinos are distributed isotropically and so the heavy neutrino decays are independent of m_{W_R} , with the assumption that $m_{W_R} > m_N$. In this approximation, the decay of the Z' boson is also independent of m_{W_R} . The events are generated with W_R boson masses between 0.6 TeV and 4.5 TeV and Z' boson masses between 0.4 TeV and 3.6 TeV. At each Z' and W_R mass point, the heavy neutrino mass is varied upward from 50 GeV to at most 100 GeV below the mass of the heavy gauge boson. At each mass point, a sample is generated assuming no mixing between the heavy neutrinos, which results in final states containing same-flavour leptons $\{ee, \mu\mu, \tau\tau\}$.

Process	OS/SS	Generator	Parton shower	PDF set	
Background processes					
Wt	OS	MC@NLO	HERWIG	CT10	
$t\bar{t}$					
Z		SHERPA	SHERPA		
$W^\pm W^\mp$					
WZ	SS	MADGRAPH	PYTHIA		MSTW 2008
ZZ					
$W^\pm W^\pm jj$					
$t\bar{t} + W/Z$				CTEQ6L1	
Signal processes					
$W^\pm \rightarrow \ell^\pm N$	SS	ALPGEN	PYTHIA	CTEQ6L1	
$W_R^\pm \rightarrow \ell^\pm N$		PYTHIA		MSTW 2008	
$Z' \rightarrow NN$					

Table 1: Overview of primary MC samples used for the simulation of signal and background processes. The category labelled ‘OS/SS’ refers to whether the process leads to pairs of opposite-sign (OS) or same-sign (SS) leptons. As described in section 5.2, OS MC samples are used in the prediction of the charge-misidentification background.

Parton showering, fragmentation, hadronisation and the modelling of the underlying event for all MADGRAPH and ALPGEN samples are performed with PYTHIA 8.165 and for MC@NLO samples with HERWIG 6.520 [30] and JIMMY 4.31 [31].

The effect of multiple pp collisions in the same or different bunch crossings is incorporated into the simulation by overlaying minimum-bias events generated using PYTHIA 8 onto hard-scatter events, where the number of additional interactions is distributed in the same way as in data. All the background samples are produced using a simulation of the ATLAS detector [32] based on GEANT4 [33]. The signal samples are processed through a fast simulation using a parameterisation of the performance of the ATLAS electromagnetic and hadronic calorimeters [34], and GEANT4 in the ID and MS. Both the signal and background samples are then processed with the same reconstruction software as the data. Small differences between data and MC simulation in the lepton reconstruction, identification and trigger efficiencies are corrected for by using specific data-driven measurements.

4 Data sample and event selection

The events used were selected from pp collision data with an integrated luminosity of 20.3 fb^{-1} collected by ATLAS in 2012. Quality criteria are applied to suppress non-collision backgrounds such as cosmic-ray muons, beam-related backgrounds, and spurious noise in the calorimeters.

4.1 Object reconstruction and selection

The search uses reconstructed electrons, muons, jets and a measurement of the missing transverse momentum.

Electrons are required to satisfy tight identification requirements [35] and to have $p_T > 20$ GeV and $|\eta| < 2.47$. Any electron in the transition region between the barrel and end-cap calorimeters ($1.37 < |\eta| < 1.52$) is rejected. In order to avoid double counting electrons as jets, the nearest jet within $\Delta R(e, \text{jet}) = 0.2$ of an electron and with $p_T < 2E_T$, where $E_T = E \sin \theta$ is the transverse energy deposited by the electron, is rejected.

Muons are required to be reconstructed in the MS and successfully matched to a good-quality track in the ID [36]. It is required that muons have $p_T > 20$ GeV and $|\eta| < 2.5$. In order to suppress muons with misidentified charge, it is required that there is a consistent measurement of charge in the MS and ID. Muons with $p_T < 80$ GeV are required to be well separated from jets, such that $\Delta R(\mu, \text{jet}) > 0.4$, where $\Delta R = \sqrt{(\Delta\eta)^2 + (\Delta\phi)^2}$.

Jets are reconstructed using the anti- k_r clustering algorithm [37, 38] with the radius parameter set to 0.4. Jets are calibrated [39, 40] using an energy- and η -dependent simulation-based calibration scheme, with in-situ corrections based on data. The impact of multiple overlapping pp interactions is accounted for using a technique that provides an event-by-event and jet-by-jet correction [41]. Events are rejected if any jet is identified as originating from beam-halo effects or calorimeter noise. Jets are required to have $p_T > 20$ GeV and $|\eta| < 2.8$. The p_T requirement is chosen in order to maximise the acceptance for the mTISM model. For jets with $p_T < 50$ GeV within the acceptance of the tracking detector ($|\eta| < 2.4$), the ‘jet vertex fraction’ (JVF) [42] is required to be greater than 0.5. The jet vertex fraction is calculated by summing the p_T of tracks associated with the jet and matched to the selected primary vertex, and dividing it by the sum of the p_T of all tracks associated with the jet.

The primary vertex of the event is defined as the reconstructed vertex with the highest $\sum p_T^2$, consistent with the beam spot position, where the sum is over all tracks associated with the candidate primary vertex.

The missing transverse momentum, E_T^{miss} , is used to identify invisible particles such as light neutrinos that escape detection. The E_T^{miss} quantity is calculated as the magnitude of the negative vector sum of all reconstructed particles momenta, including muons, electrons, photons, and jets, as well as clusters of calorimeter cells, not associated with these objects.

4.2 Lepton isolation criteria

Backgrounds due to misidentified leptons and non-prompt leptons, which are described in detail in section 5.3, can be suppressed by requiring that leptons are isolated from other activity in the event. Because of the different background compositions for electrons compared to muons and of the different response of the detector to isolated electrons and muons from prompt sources, different isolation criteria are used for the two lepton flavours.

Electrons are required to satisfy $(p_T^{\text{C}2} + 1 \text{ GeV})/E_T < 0.05$ and $E_T^{\text{C}3}/E_T < 0.05$, where $p_T^{\text{C}2}$ is the sum of the p_T of all tracks within a cone of $\Delta R = 0.2$ around the electron, excluding the electron track itself, and $E_T^{\text{C}3}$ is the sum of the transverse energy in a cone of $\Delta R = 0.3$ around the electron, excluding the electron itself. The criteria are looser at high electron E_T in order to maintain high efficiency.

Muons with $p_T < 80$ GeV are required to have $p_T^{\text{C}3}/p_T < 0.05$ and $E_T^{\text{C}2}/p_T < 0.05$, where $p_T^{\text{C}3}$ is the sum of the p_T of all tracks within a cone of $\Delta R = 0.3$ around the muon, excluding the muon track itself, and $E_T^{\text{C}2}$ is the sum of transverse energy measured in the calorimeter within a cone of $\Delta R = 0.2$ around the muon, excluding energy deposits associated with the muon track. For muons with $p_T > 80$ GeV

the requirements are relaxed in order to maintain high efficiency. Muons with $p_T > 80$ GeV are either required to satisfy $E_T^{C2}/p_T < 0.05$, or if they are within $\Delta R = 0.4$ of a jet they can additionally be selected if $(m_{\mu j} - m_j) > 10$ GeV, where m_j is the reconstructed mass of the jet closest to the muon and $m_{\mu j}$ is the invariant mass of the jet and the muon. The latter criterion is efficient for the decay of a boosted heavy neutrino decaying into a muon and a $q\bar{q}$ pair, while rejecting a large fraction of misidentified muons.

Both the muons and electrons must satisfy a set of requirements on the impact parameters at the primary vertex in order to further suppress leptons originating from heavy-flavour decays. They are required to have a transverse impact parameter, d_0 , which satisfies $|d_0| < 0.2$ mm and $|d_0|/\sigma(d_0) < 3$, where $\sigma(d_0)$ is the uncertainty on d_0 . It is also required that the product of the longitudinal impact parameter (z_0) and the sine of the polar angle of the lepton (θ) satisfy $|z_0 \sin \theta| < 2$ mm.

4.3 General event selection

The events are required to satisfy one of a suite of triggers [43] that select events with either one or two high- p_T leptons. This analysis uses single-lepton (e or μ) triggers with a 24 GeV p_T threshold. The analysis also uses a dimuon trigger for events in which one muon has satisfied a p_T threshold of 20 GeV and a second muon has satisfied a threshold of 8 GeV. The choice of triggers is found to maintain the highest possible signal efficiency in each channel across the presented range of heavy neutrino masses. The electron (muon) trigger efficiencies for offline selected electrons (muons) are $\gtrsim 94\%$ (70%) and $\gtrsim 85\%$ (90%) in the barrel and end-cap, respectively. The total efficiency for a single electron (muon) within the detector acceptance to satisfy the full lepton selection described in sections 4.1 and 4.2, including the trigger requirement, is approximately 54% (70%).

The highest- p_T lepton in an event is required to satisfy $p_T > 25$ GeV. The choice of lepton p_T threshold is dictated by the trigger requirements. It is required that at least one lepton with $p_T > 25$ GeV is matched to one of the described triggers. In the case of the event being selected by the dimuon trigger, two muons must be matched to the trigger. Any other leptons must satisfy $p_T > 20$ GeV.

Events are required to contain exactly two leptons from $\{ee, \mu\mu\}$ with same-sign charge, where the two leptons must have ID tracks associated with the same vertex. To remove the small background arising from muon bremsstrahlung in the ID or in the first layers of the EM calorimeter, events are rejected if a muon's ID track is also reconstructed as an electron. Backgrounds from WZ and ZZ decays are suppressed by rejecting events which contain an additional lepton, where the additional lepton is selected with looser identification requirements and no requirements on the isolation variables. The impact of the latter criterion on the signal efficiency is negligible compared to the overall uncertainty on the signal acceptance.

4.4 Selection criteria for mTISM signal events

The signal region for the mTISM model is defined for events containing, in addition to the two leptons, at least two jets. The invariant mass, m_{jj} , of the two highest- p_T jets is required to lie in the range $60 < m_{jj} < 100$ GeV. This selects events consistent with an on-shell W boson decaying to a $q\bar{q}$ pair. The invariant mass of the two leptons ($m_{\ell\ell}$) is required to be greater than 40 GeV, a selection that has high efficiency for the signal over the full range of m_N values considered. In the ee channel, the charge-misidentification background (described in section 5.2) is suppressed by requiring that the invariant mass of the two leptons is outside a window around the Z boson mass, $|m_{\ell\ell} - m_Z| > 20$ GeV. Backgrounds

due to electroweak processes producing same-sign leptons are dominated by those including at least one light neutrino, particularly those arising from diboson production processes. Such backgrounds may have high E_T^{miss} compared to the mTISM signal, so the events in the signal region are required to have $E_T^{\text{miss}} < 40$ GeV.

The total efficiency (including the detector acceptance) for signal events to satisfy all selection criteria is lower in ee events than in $\mu\mu$ events as electrons have lower efficiency to satisfy the identification and isolation criteria. The efficiency for leptons in mTISM signal events to satisfy the object selection increases as a function of the lepton p_T . The total efficiency therefore increases as a function of m_N , from approximately 0.5% to 24% in the ee channel and 3% to 30% in the $\mu\mu$ channel.

4.5 Selection criteria for LRSM W_R and Z' signal events

The signal region for heavy neutrinos produced in the decays of W_R bosons is defined for events containing at least one jet. To exploit the high energy scale of the signal events it is required that $m_{\ell\ell} > 110$ GeV and the invariant mass of the system consisting of the two leptons and one or two jets must satisfy $m_{\ell\ell j(j)} > 400$ GeV. If the event contains more than two jets, the two highest- p_T jets are used.

The signal region for heavy neutrinos produced in the decays of Z' bosons uses the same requirement on the dilepton mass, but requires at least two jets and the invariant mass of the system consisting of the two leptons and two to four jets must satisfy $m_{\ell\ell jj(jj)} > 200$ GeV. If the event contains more than four jets, the four highest- p_T jets are used. A lower invariant mass of the system of 200 GeV is considered in the search for Z' bosons compared to the value of 400 GeV used for W_R bosons since previous searches for heavy neutrinos have already set strong constraints for $m_{W_R} < 400$ GeV [17], whereas there are no such limits for Z' production.

Allowing only one jet in the W_R decay or two jets in the Z' decay (rather than two and four respectively) increases the signal efficiency for the case when the heavy neutrino is boosted ($m_{V_R} \gg m_N$) so that the $q\bar{q}$ pair produced in the decay of the off-shell W_R results in a single jet reconstructed in the detector. For $m_{V_R} \gg m_N$, up to 60% of events contain only one jet in W_R events or two jets in the case of Z' decays. The total selection efficiency for LRSM events depends on the masses m_{V_R} and m_N and also the ratio m_{V_R}/m_N . The total efficiency (including the detector acceptance) ranges from approximately 0.5% to 25% in the ee channel, and from approximately 1.5% to 30% in the $\mu\mu$ channel. For small values of m_N/m_{V_R} , the efficiency decreases rapidly and is below 15% for $m_N/m_{V_R} < 0.1$, because the heavy neutrino decay products are highly boosted and the leptons are less isolated.

5 Background estimation

The background is evaluated in the signal regions according to three categories of lepton pairs. The first two categories describe the contribution due to leptons originating from SM processes that produce prompt isolated leptons. The first category, labelled as ‘prompt’ in the following and discussed in section 5.1, corresponds to irreducible background from true same-sign prompt lepton pairs. The second category, labelled as ‘charge-flip’ in the following and discussed in section 5.2, corresponds to true opposite-sign prompt lepton pairs, in which one lepton has its charge mismeasured. The third category, labelled as ‘non-prompt’ in the following and discussed in section 5.3, corresponds to one or both leptons being either a non-prompt lepton from semileptonic heavy-flavour decays, a jet misidentified as a lepton or, in

the case of electrons, photons misidentified as leptons. The first category of background events are entirely estimated using the SS MC samples described in section 3, the second category is estimated using OS MC samples in conjunction with a measurement in the data of the charge misidentification rate and the third category is estimated from data.

5.1 Background from prompt same-sign leptons

The background from SM processes that lead to two same-sign prompt leptons is referred to as the prompt background and is estimated using the MC samples described in section 3. The largest contribution to the SM background in the signal regions originates from WZ and ZZ events. Other prompt contributions were estimated to be negligible; these include processes involving the production of three electroweak gauge bosons or of a Higgs boson. The simulation of the WZ and ZZ backgrounds is validated by selecting events with either three or four charged leptons satisfying the selection cuts described in section 4.3. These events arise predominantly from WZ and ZZ production, respectively, with a negligible contribution expected from the signal processes. The expected and observed jet multiplicity and leading jet p_T distributions for these events are shown in figure 3. The number of events predicted by the simulation is found to be in good agreement with the data and the kinematic properties of the events are adequately described by the simulation.

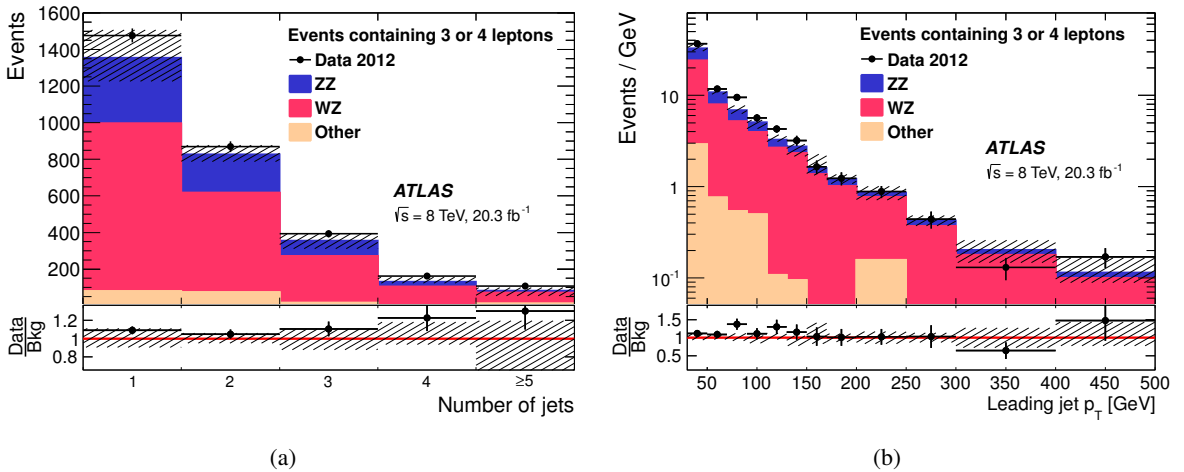


Figure 3: Distribution of (a) the number of jets and (b) the leading jet p_T in events containing any combination of exactly three or four leptons. The events must contain one lepton with $p_T > 25$ GeV and all other leptons must satisfy $p_T > 20$ GeV. The contribution labelled ‘Other’ is from processes described in section 5.1 (with MC samples described in section 3), other than the contributions from WZ and ZZ , which are labelled separately. The shaded bands indicate the experimental uncertainties on the total expected background, including all contributions described in section 6.2, but not including any uncertainty on the WZ and ZZ cross-sections. The lower plots show the ratio of data to the total expected background.

5.2 Background from prompt opposite-sign leptons

SM processes that produce opposite-sign leptons can also enter into the signal regions if the charge of one lepton is incorrectly measured in the detector. This is referred to as the ‘charge-flip’ background and includes pairs of opposite sign-leptons produced in $t\bar{t}$, $W^\pm W^\mp$ and Z processes. The MC samples used to model these processes are described in section 3.

The probability for a charge-flip event to occur is measured using $Z \rightarrow \mu\mu$ and $Z \rightarrow ee$ events, which are identified using events, which have exactly two leptons with an invariant mass close to the mass of the Z boson. For muons, the charge-flip rate is estimated by comparing the two independent measurements of the muon charge in the MS and the ID. The charge-flip rate is found, as expected from simulation, to be consistent with zero, and contributes a negligible number of events to the expected background.

There is however a sizeable charge-flip rate for electrons, due to bremsstrahlung photons produced in the ID and subsequently converting to electron pairs. A sample of $Z \rightarrow ee$ events in data is used to perform a single maximum-likelihood fit, which extracts the electron charge-flip rate as a function of η [44]. The contribution to these events from fake and non-prompt electrons (see section 5.3) is subtracted from the data sample prior to the fit. The measured rate, which is strongly correlated to the amount of material traversed by the electron in the ID, is found to be approximately 10^{-4} for electrons within the barrel region ($|\eta| < 1.0$), increasing to 10^{-2} at the edge of the detector acceptance ($|\eta| = 2.47$). The data-to-MC ratio of the measured electron charge-flip rate is used as a correction factor to the charge-flip rate obtained in the simulation. The p_T -dependence of the charge-flip rate is therefore directly taken from the MC simulation.

5.3 Background from fake and non-prompt leptons

Events where jets or photons are misidentified as leptons (‘fakes’) or events with non-prompt leptons which originate from semileptonic heavy-flavour decays constitute a significant background, which is referred to as the non-prompt background. These processes include $W + \text{jets}$ and $t\bar{t}$ production, where one lepton originates from a vector boson decay and the other lepton is misidentified or from a non-prompt decay. This background cannot be reliably predicted from MC simulation and is estimated directly in each of the signal regions, using the data-driven matrix method [45]. The matrix-method characterises leptons which satisfy ‘loose’ identification criteria as being from prompt or fake/non-prompt sources according to their probabilities to satisfy the full lepton identification criteria.

A ‘loose’ electron is defined with an identification requirement that is relaxed from the ‘tight’ to ‘medium’ operating point compared to the standard electron selection described in section 4.1. The selection criteria for a ‘loose’ muon are identical to the full selection described in section 4.1, with the same requirements on the impact parameters described in section 4.2 but without a requirement to satisfy any isolation criteria.

The measurement of the probabilities r and f for ‘loose’ leptons from prompt or fake/non-prompt sources respectively to satisfy the full lepton identification criteria are the key factors in the estimate of the non-prompt backgrounds. The probabilities r are measured in $Z \rightarrow \ell\ell$ events as these events are dominated by prompt leptons.

The probabilities f are measured in a selection of events which contain a large number of fake and non-prompt leptons. In these control samples, any residual prompt background is subtracted using MC estimates, and low-mass hadronic resonances are excluded by requiring $m_{\ell\ell} > 15$ GeV. For electrons, the probabilities are measured in events with at least one jet and with exactly one electron. To suppress events containing W decays it is required that $|\Delta\phi(e, E_T^{\text{miss}})| < 0.5$ and $E_T^{\text{miss}} + m_T < 40$ GeV, where m_T is the transverse mass.² The probabilities for muons are measured in events containing pairs of muons chosen with transverse impact parameter requirements which differ from the standard selection, such that $|d_0| < 10$ mm and $|d_0/\sigma(d_0)| > 5$. This sample of pairs of muons is expected to have a composition similar to the signal region, making it suitable for the measurement of f . A correction factor is applied to f for muons to account for the fact that muons with high $|d_0/\sigma(d_0)|$ have a lower probability than muons with low $|d_0/\sigma(d_0)|$ to satisfy the isolation criteria. The correction factor of approximately 1.4 is measured using $b\bar{b}$ and $t\bar{t}$ MC simulation.

A validation region is defined for same-sign $\mu\mu$ events which have satisfied the dimuon trigger (section 4.3) with one muon satisfying $p_T > 25$ GeV and the second satisfying $10 \text{ GeV} < p_T < 20$ GeV. As the p_T of the second muon is relatively low, this region is dominated by non-prompt background events. The jet multiplicity measured in events in this region is compared to the expected background as shown in figure 4. The overall level of agreement is within one standard deviation for up to five jets in the event.

5.4 Validation of background estimates

The validation of prompt, charge-flip and non-prompt background estimates is considered in this section.

The combined background estimate can be evaluated using events containing exactly two same-sign leptons and no jets. This sample of events is orthogonal to each of the different signal regions described in sections 4.4 and 4.5, and is expected to contain only a negligible contribution from possible signal events. Comparisons of the distributions of the E_T^{miss} and lepton p_T as measured in data and estimated from the background predictions from the three sources described above are shown in figure 5. The overall agreement between data and background prediction is within approximately one standard deviation in both the ee and $\mu\mu$ channels.

An additional sample of events is considered, which fully includes all signal regions. This region is defined for events containing exactly two same-sign leptons, with no requirement on the number of jets in the event. The contamination from signal events in this sample is less than 2% of the total background in

² $m_T = \sqrt{2p_T E_T^{\text{miss}}(1 - \cos(\Delta\phi(e, E_T^{\text{miss}})))}$, where p_T refers to the electron.

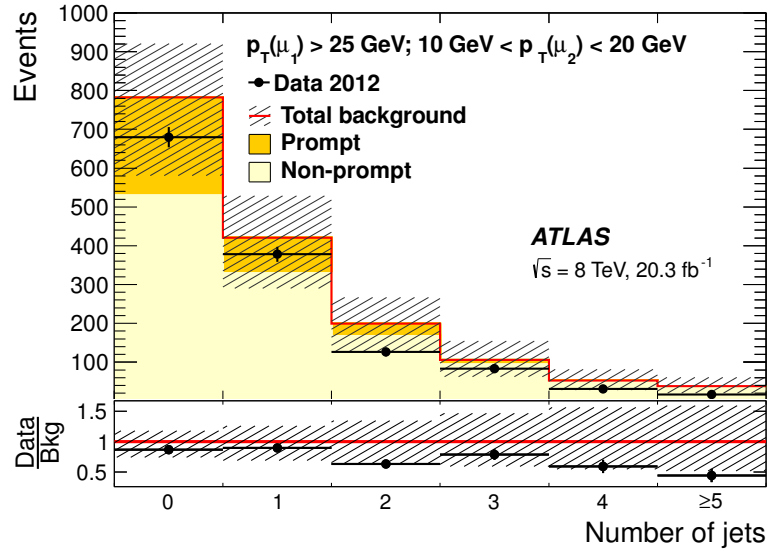
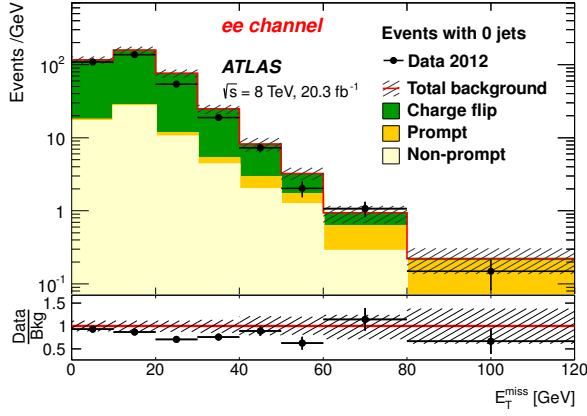
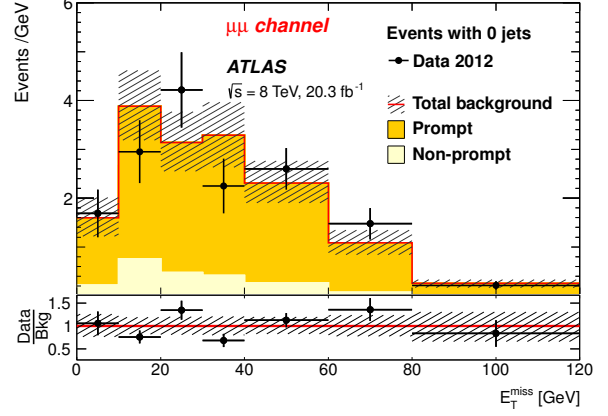


Figure 4: Distribution of the number of jets in a validation region consisting of events containing exactly two same-sign muons with one muon satisfying $p_T > 25 \text{ GeV}$ and the second satisfying $10 \text{ GeV} < p_T < 20 \text{ GeV}$. The shaded bands indicate the total uncertainty, including all contributions described in section 6, on the total expected background and the lower plots show the ratio of data to the total expected background.

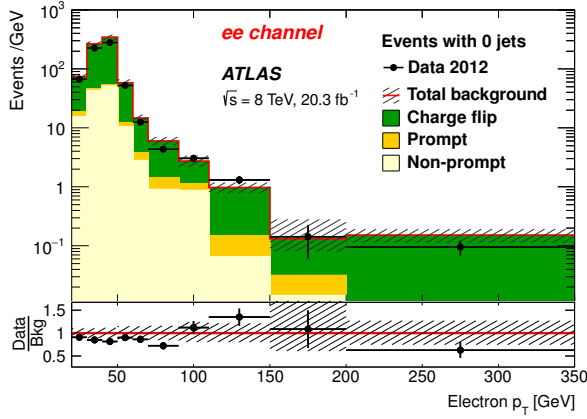
both channels. The distributions of the leading jet p_T and the number of jets in these events, in the ee and $\mu\mu$ channels, as measured in data and estimated from the background predictions from the three sources described above, are shown in figure 6. The overall agreement between data and prediction in the two channels is within approximately one standard deviations.



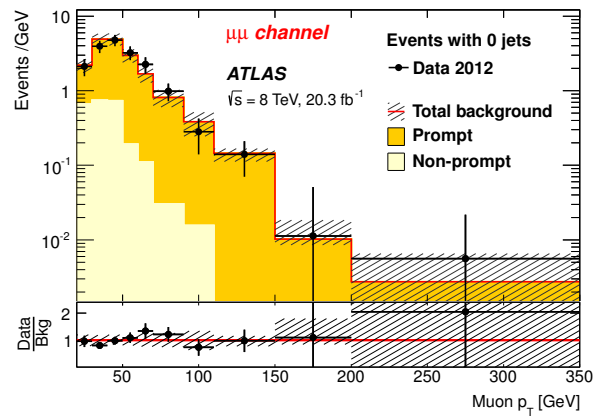
(a)



(b)

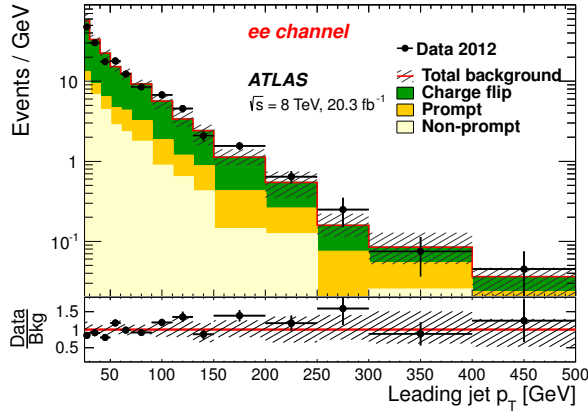


(c)

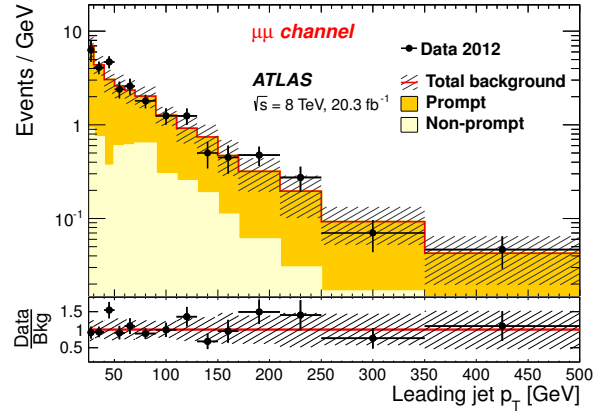


(d)

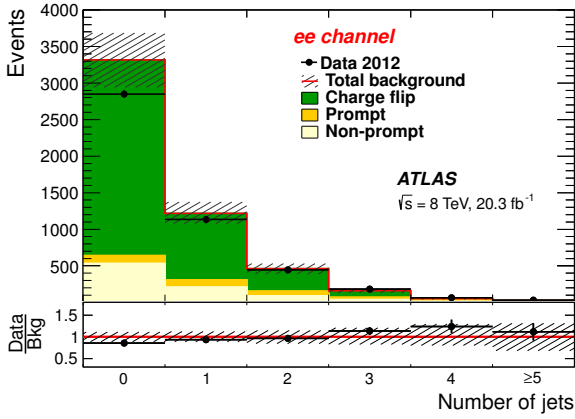
Figure 5: The E_T^{miss} (top) and lepton p_T (bottom) distributions for the ee (left) and $\mu\mu$ (right) channels in a validation region consisting of events with exactly two same-sign leptons and no jets. The shaded bands indicate the total uncertainty, including all contributions described in section 6, on the total expected background and the lower plots show the ratio of data to the total expected background.



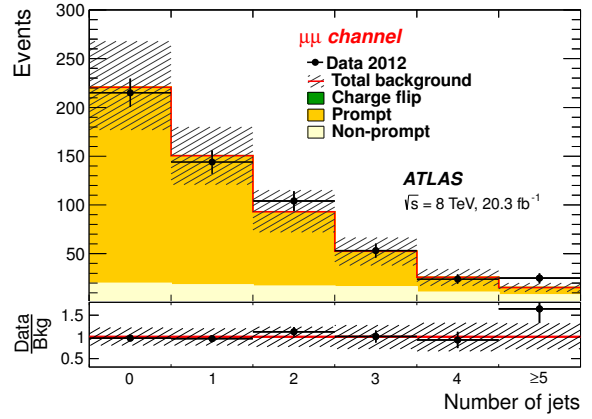
(a)



(b)



(c)



(d)

Figure 6: The distribution of the transverse momentum p_T of the leading jet (top) and the distribution of the number of jets (bottom) for the ee (left) and $\mu\mu$ (right) channels in a validation region consisting of events with exactly two same-sign leptons. The shaded bands indicate the total uncertainty, including all contributions described in section 6, on the total expected background and the lower plots show the ratio of data to the total expected background.

6 Systematic uncertainties

The background estimates and signal efficiencies are subject to several systematic uncertainties. The relative size of the uncertainties on the total background estimates in the mTISM and LRSM signal regions are detailed in tables 2 and 3 respectively. Since the tables show the size of each uncertainty relative to the total background estimate, the impact of each uncertainty depends on the background composition in the different channels (see section 7 and tables 4 and 5).

6.1 Background uncertainties

The systematic uncertainty on the estimate of the non-prompt background is dominated by the uncertainties on the measurements of the rates for leptons from fake and non-prompt sources to satisfy the lepton identification criteria. This uncertainty is dominated by the effect of the choice of control region definition on the measured probabilities, as well as the statistical uncertainty on determining the probabilities. The total uncertainty on the non-prompt background in the ee ($\mu\mu$) channel varies from 30 – 48% (41 – 45%), depending on the signal region.

The charge-flip background is only relevant for the ee channel (see section 5.2) and its uncertainty is dominated by the statistical precision with which the charge-flip rate is determined from the available data. There is, additionally, a non-negligible contribution to the total uncertainty due to the modelling of the subtraction of the non-prompt background, although this is correlated with the uncertainty on the non-prompt background. Since the charge-flip background uses MC simulation, the systematic uncertainties discussed in section 6.2 also apply to the charge-flip background. The total uncertainty on the charge-flip background varies from 18 – 46%, depending on the signal region.

The uncertainty on the normalisation of the backgrounds originating from WZ and ZZ processes is derived from the diboson control region described in section 5.1. This uncertainty is taken to be either the difference between the data and the prediction or the statistical uncertainty from the limited data statistics, whichever is largest. The uncertainty is applied as a function of the number of jets, leading to uncertainties of 10 – 14%, depending on the signal region. The uncertainty on the cross-section of other background processes from MC estimates is taken from the uncertainties on the theoretical cross-sections. The combined effect of the diboson normalisation and theoretical cross-section uncertainties is labelled as ‘Prompt normalisation’ in tables 2 and 3.

Another source of uncertainty is due to the MC statistical uncertainty. In the mTISM signal region this is particularly large in the ee channel due to the small number of events in the $Z \rightarrow ee$ MC sample in this region.

6.2 Uncertainties on MC simulation

The following uncertainties are applied to all MC-derived predictions. In addition to affecting the prompt and charge-flip background estimates, these uncertainties also apply to the signal simulation.

The systematic uncertainty on the jet energy scale has an important effect on both the signal and background processes, as the signal-region event selection includes requirements on quantities that are reconstructed from jet kinematics [40]. The uncertainty on the jet energy scale is notably asymmetric in the mTISM signal region (table 2) compared to the LRSM signal region (table 3) due to the dependency on

	ee	$\mu\mu$
Non-prompt	± 7	± 14
Charge-flip	± 7	–
Prompt normalisation	± 2	± 10
MC statistics	± 14	± 8
Jet energy scale	+8/–22	+7/–12
E_T^{miss}	+2/–3	+6/–3
Jet energy resolution	± 4	± 3
Jet vertex fraction	+2/–6	+4/–5
Lepton uncertainties	± 2	+2/–3
Luminosity	± 2	± 1
Total	+20/–29	+21/–24

Table 2: A breakdown of the relative uncertainty on the total background (given in %) in the mTISM signal region. The various sources of systematic uncertainty are described in Section 6.

	ee		$\mu\mu$	
	W_R	Z'	W_R	Z'
Non-prompt	± 12	± 15	+10/–9	+13/–11
Charge-flip	+5/–4	+4/–3	–	–
Prompt normalisation	± 5	+5/–4	± 18	± 14
MC statistics	± 7	± 6	± 5	± 4
Jet energy scale	+8/–9	+5/–4	± 5	+5/–4
Jet energy resolution	± 0.9	± 0.6	± 1.2	± 0.2
Jet vertex fraction	± 1	± 2	+0.9/–0.1	+2.4/–1.1
Lepton uncertainties	+2/–1	+2.7/–1	± 2	± 2
Luminosity	± 1	+1.5/–1	± 1	± 1
Total	± 18	± 18	± 21	+20/–19

Table 3: A breakdown of the relative uncertainty on the total background (given in %) in the LRSM signal regions. The various sources of systematic uncertainty are described in Section 6.

the leading dijet mass in the mTISM signal region definition described in section 4.4. The uncertainty due to the JES on the sum of the prompt and charge-flip backgrounds varies from 6 – 28%, depending on the signal region. The modelling of the missing transverse momentum (E_T^{miss}) [46] is included as a systematic uncertainty in the mTISM signal region (table 2) as there is a dependence on this quantity in the signal region definition described in section 4.4. Other smaller systematic uncertainties include the uncertainty on the jet energy resolution [47], the jet vertex fraction requirement, uncertainties on lepton identification efficiencies, energy / momentum scales and resolutions ($\text{'Lepton uncertainties'}$) [35, 36] and the uncertainty on the luminosity measurement ('Luminosity') [48].

6.3 Signal-specific modelling uncertainties

In addition to the uncertainties associated with the MC simulation of background processes, there are systematic modelling uncertainties associated with the signal MC samples. An uncertainty is considered for the signal MC simulation to reflect the choice of parton shower model. The nominal parton shower model that is used for all signal MC samples is PYTHIA 8.165. The total number of events in the signal region when the signal MC generator is interfaced to PYTHIA is compared to the number of events when the generator is interfaced to HERWIG 6.520. The variation in the signal efficiency is measured to be approximately 5%. The uncertainty due to the parton distribution functions on the signal acceptance is found to be approximately 5% for the mTISM signal samples and approximately 7% for the LRSM signal samples.

A systematic uncertainty is also considered to cover the effect of using the fast detector simulation described in section 3. Two versions of the MC signal, one with a full detector simulation and the other with the standard fast detector simulation, are compared in each lepton channel, for a single signal mass point. The difference in the efficiency to select signal events, approximately 4%, is assigned as an uncertainty.

7 Results

The numbers of events measured in data are compared to the expected numbers of background events in the signal regions, with the intention of interpreting an excess of events in data in terms of a heavy Majorana neutrino in the mTISM or LRSM models.

7.1 Results in the mTISM signal region

The observed and predicted distributions of the invariant mass of the two highest- p_T jets (m_{jj}) in events satisfying the mTISM selection criteria, excluding the criteria on m_{jj} ($60 \text{ GeV} < m_{jj} < 100 \text{ GeV}$) are presented in figure 7. The shapes of the distributions show good agreement between data and expectation. The numbers of expected and observed events in the mTISM signal region (indicated by arrows in figure 7) are shown in table 4. There is no excess of events relative to the expectation. The observed yields in the data are used to set 95% CL upper limits on the production cross-section times branching ratio, $\sigma \times \text{Br}(pp \rightarrow \ell^\pm N \rightarrow \ell^\pm \ell^\pm q \bar{q}')$, of heavy neutrinos to electrons or muons, using the profile-likelihood test statistic [49, 50] and the CL_s method [51]. The systematic uncertainties are included in the test statistic as nuisance parameters. Each systematic uncertainty is assumed to be uncorrelated with all other systematic uncertainties. The limits are shown as a function of m_N in figure 8 and are translated into limits

on the mixing parameter, $|V_{\ell N}|^2$, between the heavy neutrino and the SM neutrino, separately for the ee and $\mu\mu$ channels. The extraction of the limits on the mixing parameters uses the leading-order cross-section for the signal process and no uncertainties are included on the signal cross-section. The extraction furthermore assumes that only the lightest of the heavy neutrinos contributes to the cross-section and that the masses of the other heavy neutrino species are sufficiently high that the effect of interference is negligible.

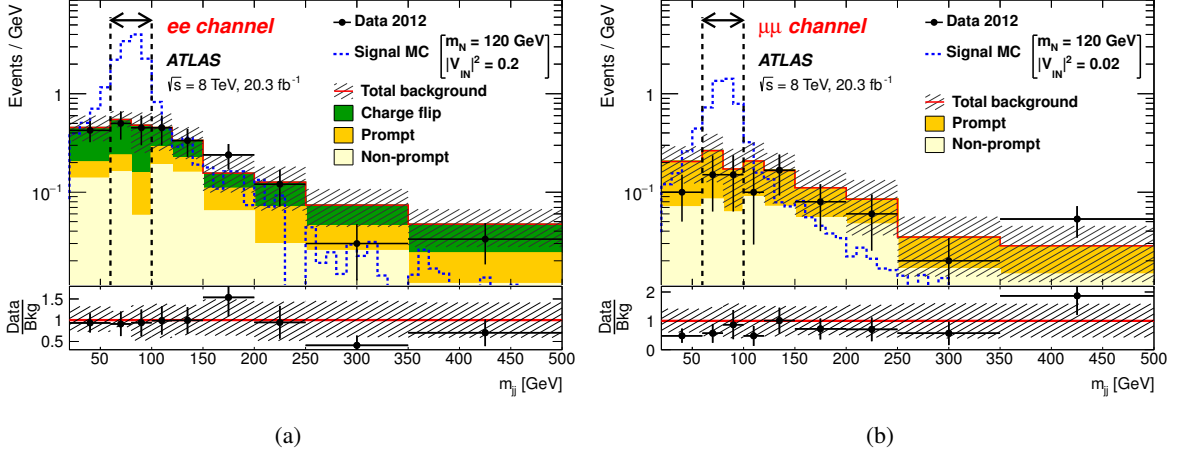


Figure 7: Invariant mass of the two highest- p_T jets (m_{jj}) in events satisfying the mTISM signal region criteria (excluding the m_{jj} criteria) for (a) ee and (b) $\mu\mu$ events. Events satisfying all selection criteria are in the region indicated by the arrows. The expected mTISM signal distribution for $m_N = 120$ GeV is shown by the dashed (blue) histogram. The values of the mixing parameter $|V_{\ell N}|^2$ are chosen such that the signal distribution is clearly visible, $|V_{eN}|^2 = 0.2$ for (a) and $|V_{\mu N}|^2 = 0.02$ for (b). The shaded bands indicate the total uncertainty, including all contributions described in section 6, on the total expected background and the lower plots show the ratio of data to the total expected background.

	ee	$\mu\mu$
Prompt	$3.5^{+0.9}_{-1.7}$	$5.8^{+1.3}_{-1.7}$
Charge-flip	13^{+3}_{-6}	< 0.02
Non-prompt	4.3 ± 1.8	2.9 ± 1.3
Total background	21^{+4}_{-6}	8.7 ± 2.0
Data	19	6
Signal ($m_N = 120$ GeV)	18	6.6
Signal ($m_N = 240$ GeV)	30	5.3

Table 4: Total event yields measured in data and predicted for signal and background processes in the mTISM signal region. The uncertainties shown on the various backgrounds correspond to the total uncertainty. The expected number of mTISM signal events are calculated for $m_N = 120$ GeV (with $|V_{\ell N}|^2$ equal to 0.03 and 0.003 in the ee and $\mu\mu$ channels respectively) and $m_N = 240$ GeV (with $|V_{\ell N}|^2$ equal to 0.2 and 0.02 in the ee and $\mu\mu$ channels respectively). The values of the mixing parameters $|V_{\ell N}|^2$ are chosen to be close to the expected limit shown in figure 8. For backgrounds that have zero expected events, the 95% CL upper limit is shown.

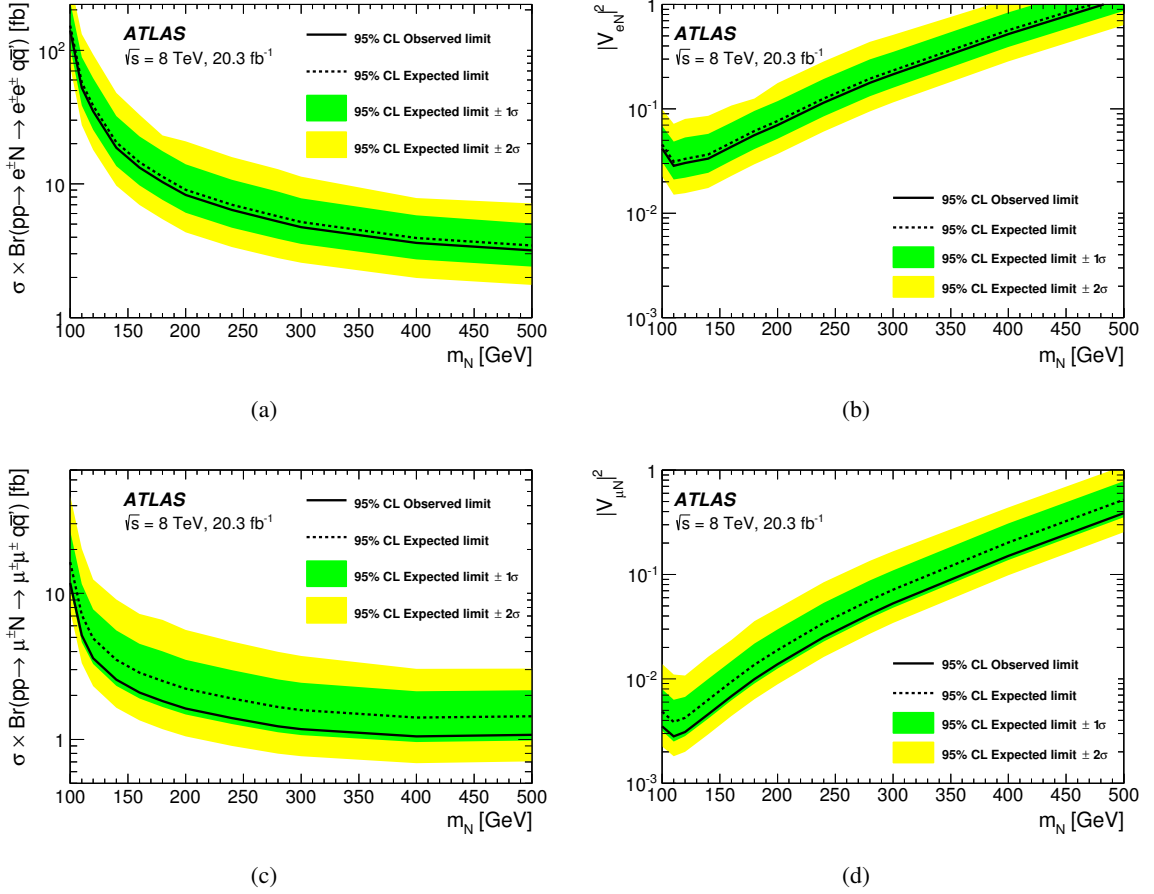


Figure 8: Observed and expected 95% confidence level upper limits on the cross-section times branching ratio for the production of mTISM heavy Majorana neutrinos as a function of the heavy neutrino mass for (a) the ee channel and (c) the $\mu\mu$ channel. The limits on the mixing between the heavy Majorana neutrinos and the SM neutrinos are shown in (b) and (d). Values larger than the solid black line are excluded by this analysis.

7.2 Results in the LRSM signal region

The observed and expected numbers of events for the LRSM signal regions are shown in table 5. There are no excesses observed above the expected numbers of background events.

The LRSM signal is expected to produce a peak in the invariant mass of the decay products of the heavy gauge boson. This would be observed in the invariant mass distribution $m_{\ell\ell_{j(j)}} (m_{\ell\ell_{j(j)j}})$ in the W_R (Z') signal regions, as described in section 4. The observed and predicted distributions are shown in figures 9 and 10. Binned likelihood fits are performed to the invariant mass distributions and the profile-likelihood test statistic is used to assess the compatibility of the data with the background-only and signal-plus-background hypotheses. No significant excess is observed in the data compared to the background expectation and 95% CL upper limits on the cross-section of the production of heavy gauge bosons decaying to heavy neutrinos within the LRSM are set using the CL_s method. The expected and observed cross-section exclusion limits as a function of the masses of the heavy gauge bosons and heavy neutrino are shown for example mass points for both channels, ee and $\mu\mu$, in table 6. The full cross-section limits

for all analysed mass points are available in HepData.³ Exclusion contours are also set in the $\{m_{W_R}, m_N\}$ plane, and are shown in figure 11. The contours are found by comparing the cross-section limits to the leading-order cross-sections for the signal processes and no uncertainties are included on the signal cross-sections. For this interpretation there is assumed to be no mixing between lepton flavours and three cases are investigated: the first two cases assume a single heavy neutrino being kinematically accessible and being of either electron or muon flavour, which leads to events expected in one of the ee and $\mu\mu$ channels, respectively. The limits are stronger in the $\mu\mu$ channel at low heavy neutrino mass, due to the higher signal acceptance discussed in Section 4.5. As the efficiency of the LRSM signal is low in the ee channel for $m_{W_R} \gg m_N$, the limit in this region is weaker. Finally the case where two degenerate neutrinos are present is investigated, leading to events expected in both the ee and $\mu\mu$ channels. The expected limits for this scenario are slightly stronger than either of the individual channel scenarios. The sharp changes in the expected and observed limits visible in figure 11 originate from the interpolation between the limited number of mass points for which the limits are extracted.

	ee		$\mu\mu$	
	W_R	Z'	W_R	Z'
Prompt	26 ± 5	34 ± 6	33 ± 8	42 ± 10
Charge-flip	44 ± 11	44^{+10}_{-8}	< 0.03	< 0.03
Non-prompt	23 ± 11	33^{+11}_{-10}	9.8^{+5}_{-4}	17^{+8}_{-7}
Total background	93 ± 16	111^{+16}_{-14}	43 ± 9	60^{+13}_{-12}
Data	94	106	44	55
Signal	2.4	5.2	2.9	7.7

Table 5: Total event yields measured in data and predicted for signal and background processes in the LRSM signal regions. The uncertainties shown on the various backgrounds correspond to the total uncertainty. The number of LRSM signal events are calculated for $\{m_{W_R}; m_N\} = \{2600; 1950\}$ GeV and $\{m_{Z'}; m_N\} = \{2200; 550\}$ GeV. For backgrounds that have zero expected events, the 95% CL upper limit is shown.

³ <http://hepdata.cedar.ac.uk/>

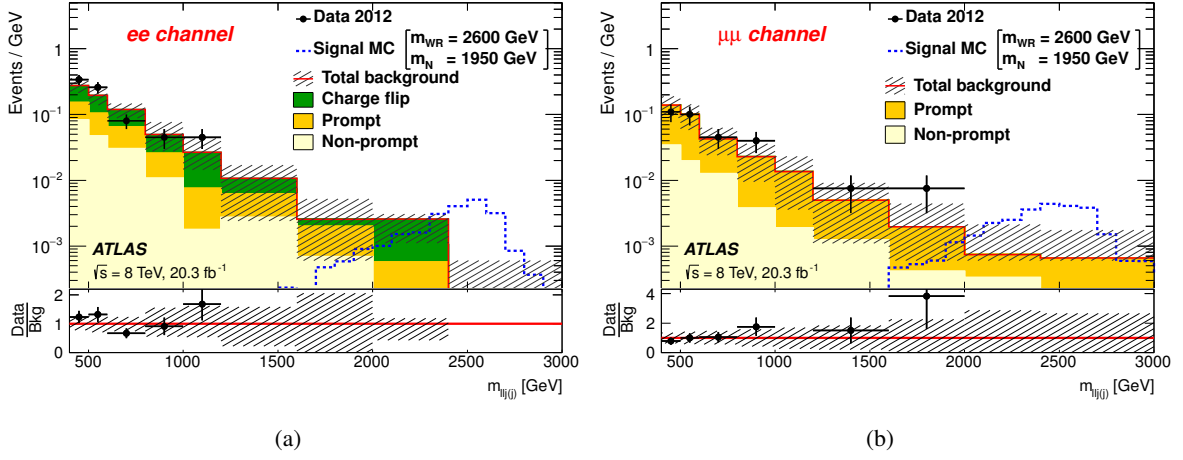


Figure 9: Invariant mass of two leading leptons and up to two leading jets after applying additional W_R selection criteria (two same-sign leptons, at least one jet, $m_{\ell\ell} > 110$ GeV and $m_{\ell\ell j(j)} > 400$ GeV), for the ee -channel (a) and $\mu\mu$ -channel (b). A finely binned LRSM signal sample is represented by the dashed (blue) histogram corresponding to $m_{W_R} = 2600$ GeV and $m_N = 1950$ GeV. The shaded bands indicate the total uncertainty, including all contributions described in section 6, on the total expected background and the lower plots show the ratio of data to the total expected background.

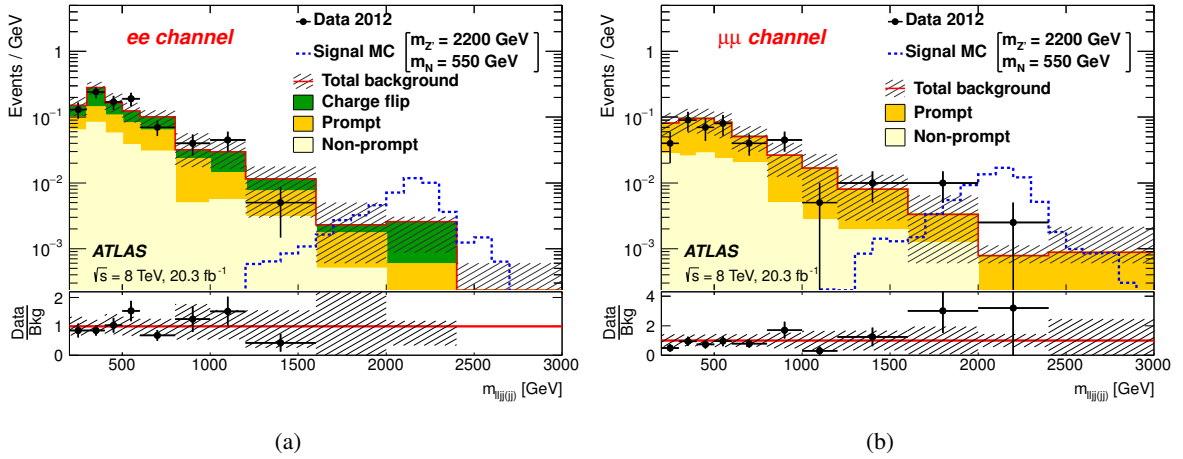


Figure 10: Invariant mass of two leading leptons and up to four leading jets after applying additional Z' selection criteria (two same-sign leptons, at least two jets, $m_{\ell\ell} > 110$ GeV and $m_{\ell\ell j(jj)} > 200$ GeV), for the ee -channel (a) and $\mu\mu$ -channel (b). A finely binned LRSM signal sample is represented by the dashed (blue) histogram corresponding to $m_{Z'} = 2200$ GeV and $m_N = 550$ GeV. The shaded bands indicate the total uncertainty, including all contributions described in section 6, on the total expected background and the lower plots show the ratio of data to the total expected background.

m_{V_R} [GeV]	m_N [GeV]	Efficiency [%]	Expected limit [fb]	Expected limit $\pm 1\sigma$ [fb]	Expected limit $\pm 2\sigma$ [fb]	Observed limit [fb]
$W_R ee$						
1400	50	0.80	100	130/70	190/49	65
1400	1050	22	2.2	3.1/1.5	3.8/1.1	1.7
2300	50	0.39	400	530/250	780/160	320
2300	1725	23	0.87	1.1/0.64	1.8/0.44	0.56
2900	50	1.2	140	210/98	270/71	160
2900	2175	23	0.85	1.1/0.62	1.7/0.43	0.54
$W_R \mu\mu$						
1400	50	19	1.8	2.8/1.2	3.5/0.88	2.1
1400	1050	26	1.2	1.7/0.83	2.2/0.59	1.1
2300	50	18	1.4	2.2/0.91	3.2/0.63	2.1
2300	1725	26	0.85	1.3/0.55	1.8/0.38	1.3
2900	50	15	2.2	3.5/1.4	5.4/0.99	3.4
2900	2175	25	0.87	1.4/0.57	1.8/0.39	1.3
$Z' ee$						
1000	50	0.27	500	740/340	920/240	440
1000	375	14	5.2	6.6/3.8	8.3/2.8	4.2
2000	50	0.091	1100	1600/770	2000/560	1300
2000	750	17	2.8	3.6/2.0	4.8/1.5	2.6
2400	50	0.16	570	780/400	970/290	550
2400	900	17	2.9	3.6/2.0	4.8/1.5	2.6
$Z' \mu\mu$						
1000	50	11	4.8	7.2/3.2	10/2.2	8.5
1000	375	24	2.2	3.2/1.5	4.6/1.1	3.8
2000	50	15	2.7	4.0/1.8	5.8/1.3	3.4
2000	750	23	1.7	2.6/1.2	3.3/0.83	2.2
2400	50	12	3.7	5.6/2.5	7.0/1.8	4.8
2400	900	24	1.7	2.5/1.2	3.3/0.82	2.2

Table 6: Expected and observed 95% CL limits for the production of LRSM W_R or Z' , with subsequent decay into a heavy Majorana neutrino in the ee and $\mu\mu$ channels for several example mass points. Also shown is the event selection efficiency (including the detector acceptance). The full results for all analysed mass points are available in HepData.

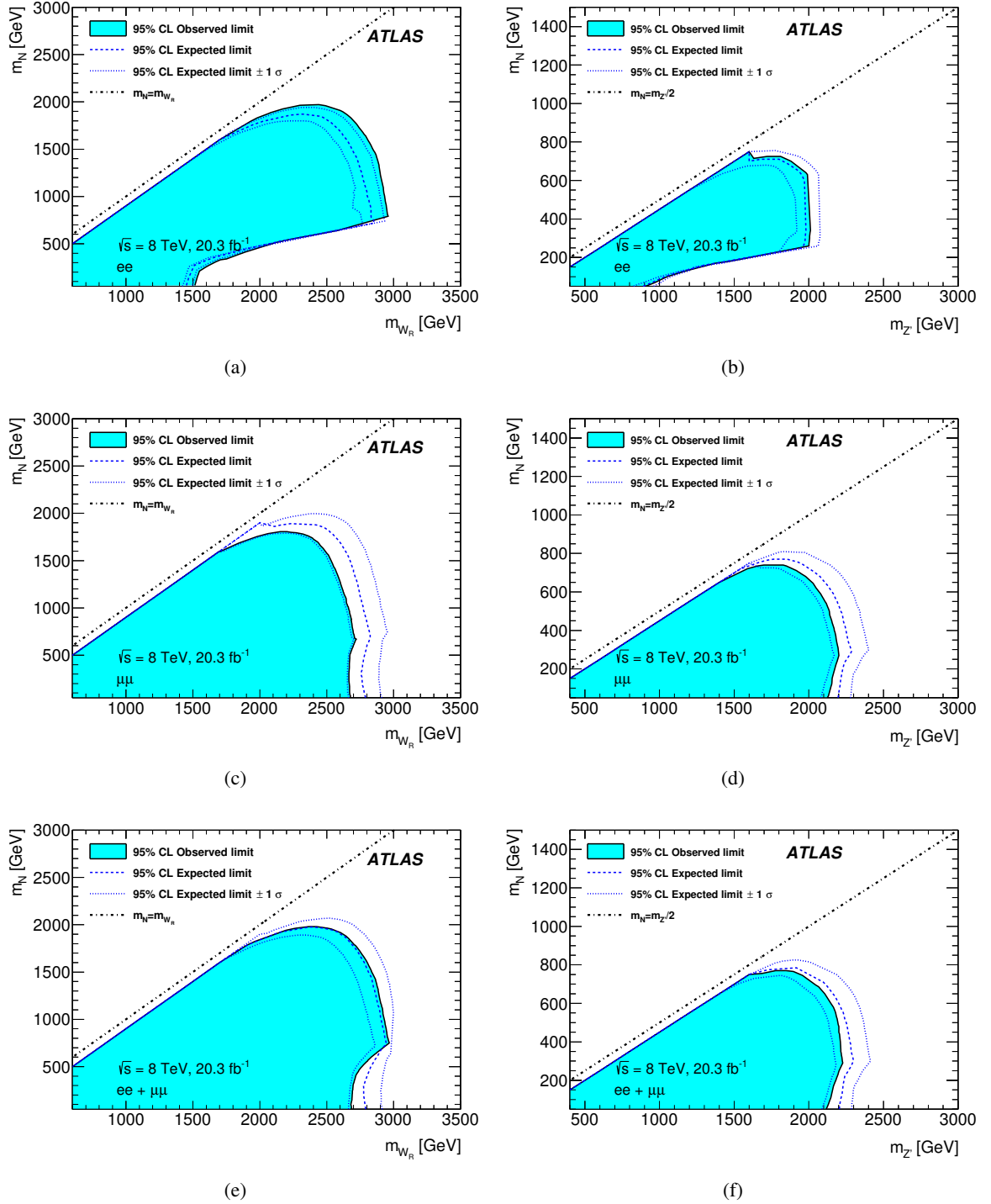


Figure 11: Observed and expected exclusion contour at 95% confidence level as a function of the mass of a heavy Majorana neutrino and of a W_R (left) or Z' boson (right) within the LRSM. The limits in (a) and (b) show the scenario where the heavy neutrino has electron flavour and those in (c) and (d) show the scenario where it has muon flavour. The limits in (e) and (f) show the case of two degenerate neutrinos, one has electron flavour, and the other muon flavour (no mixing between lepton flavours is assumed).

8 Conclusions

The proton–proton collision data sample with a centre-of-mass energy of 8 TeV collected by ATLAS with an integrated luminosity of 20.3 fb^{-1} has been used to search for the production of heavy Majorana neutrinos. The selected events contain two same-sign charged leptons and high- p_T jets. Two final selection criteria were used to provide sensitivity to two different benchmark models, the first being a minimal extension of the SM, mTISM, and the second being a left-right symmetric extension of the SM, LRSM. The background expectation in the signal regions is estimated using a combination of data-driven methods and MC simulation.

No significant excess of events is observed above the SM background, and limits are set for each model. In the framework of a mTISM, limits are set on the cross-section times branching ratio and the mixing between heavy neutrinos and SM neutrinos as a function of the heavy neutrino mass. The observed limits exclude mixing parameters as low as $|V_{\mu N}|^2 = 0.0028$ and $|V_{eN}|^2 = 0.029$. In the framework of an LRSM, limits are set on heavy Majorana neutrino masses in the range 50 GeV to 2000 GeV for heavy gauge boson masses above 400 GeV.

Acknowledgements

We thank CERN for the very successful operation of the LHC, as well as the support staff from our institutions without whom ATLAS could not be operated efficiently.

We acknowledge the support of ANPCyT, Argentina; YerPhI, Armenia; ARC, Australia; BMWFW and FWF, Austria; ANAS, Azerbaijan; SSTC, Belarus; CNPq and FAPESP, Brazil; NSERC, NRC and CFI, Canada; CERN; CONICYT, Chile; CAS, MOST and NSFC, China; COLCIENCIAS, Colombia; MSMT CR, MPO CR and VSC CR, Czech Republic; DNRF, DNSRC and Lundbeck Foundation, Denmark; EPLANET, ERC and NSRF, European Union; IN2P3-CNRS, CEA-DSM/IRFU, France; GNSF, Georgia; BMBF, DFG, HGF, MPG and AvH Foundation, Germany; GSRT and NSRF, Greece; RGC, Hong Kong SAR, China; ISF, MINERVA, GIF, I-CORE and Benoziyo Center, Israel; INFN, Italy; MEXT and JSPS, Japan; CNRST, Morocco; FOM and NWO, Netherlands; BRF and RCN, Norway; MNiSW and NCN, Poland; GRICES and FCT, Portugal; MNE/IFA, Romania; MES of Russia and NRC KI, Russian Federation; JINR; MSTB, Serbia; MSSR, Slovakia; ARRS and MIZŠ, Slovenia; DST/NRF, South Africa; MINECO, Spain; SRC and Wallenberg Foundation, Sweden; SER, SNSF and Cantons of Bern and Geneva, Switzerland; NSC, Taiwan; TAEK, Turkey; STFC, the Royal Society and Leverhulme Trust, United Kingdom; DOE and NSF, United States of America.

The crucial computing support from all WLCG partners is acknowledged gratefully, in particular from CERN and the ATLAS Tier-1 facilities at TRIUMF (Canada), NDGF (Denmark, Norway, Sweden), CC-IN2P3 (France), KIT/GridKA (Germany), INFN-CNAF (Italy), NL-T1 (Netherlands), PIC (Spain), ASGC (Taiwan), RAL (UK) and BNL (USA) and in the Tier-2 facilities worldwide.

References

- [1] W. Alberico and S. Bilenyk, *Neutrino oscillations, masses and mixing*, *Phys. Part. Nucl.* **35** (2004) 297–323, [arXiv:hep-ph/0306239](https://arxiv.org/abs/hep-ph/0306239) [[hep-ph](https://arxiv.org/abs/hep-ph/0306239)], and references therein.

- [2] P. Minkowski, $\mu \rightarrow e\gamma$ at a rate of one out of 10^9 muon decays?, *Phys. Lett. B* **67** (1977) 421 – 428.
- [3] M. Gell-Mann, P. Ramond, and R. Slansky, *Supergravity: Proceedings of the Supergravity Stony Brook Workshop, New York, 1979*, 315.
- [4] R. N. Mohapatra and G. Senjanovic, *Neutrino Mass and Spontaneous Parity Violation*, *Phys. Rev. Lett.* **44** (1980) 912.
- [5] R. N. Mohapatra and G. Senjanovic, *Neutrino Masses and Mixings in Gauge Models with Spontaneous Parity Violation*, *Phys. Rev. D* **23** (1981) 165.
- [6] A. Davidson and K. C. Wali, *Family Mass Hierarchy From Universal Seesaw Mechanism*, *Phys. Rev. Lett.* **60** (1988) 1813.
- [7] J. Schechter and J. W. F. Valle, *Neutrino Masses in $SU(2) \times U(1)$ Theories*, *Phys. Rev. D* **22** (1980) 2227.
- [8] A. Atre, T. Han, S. Pascoli, and B. Zhang, *The Search for Heavy Majorana Neutrinos*, *JHEP* **05** (2009) 030, [arXiv:0901.3589](https://arxiv.org/abs/0901.3589) [hep-ph].
- [9] A. Pilaftsis, *Radiatively induced neutrino masses and large Higgs neutrino couplings in the standard model with Majorana fields*, *Z. Phys. C* **55** (1992) 275–282, [arXiv:hep-ph/9901206](https://arxiv.org/abs/hep-ph/9901206) [hep-ph].
- [10] DELPHI Collaboration, Abreu, P. et al., *Search for neutral heavy leptons produced in Z decays*, *Z. Phys. C* **74** (1997) 57–71.
- [11] L3 Collaboration, Adriani, O. et al., *Search for isosinglet neutral heavy leptons in Z^0 decays*, *Phys. Lett. B* **295** (1992) 371–382.
- [12] CMS Collaboration, *Search for heavy Majorana neutrinos in $\mu^+\mu^+[\mu^-\mu^-]$ and $e^+e^+[e^-e^-]$ events in pp collisions at $\sqrt{s} = 7$ TeV*, *Phys. Lett. B* **717** (2012) 109–128, [arXiv:1207.6079](https://arxiv.org/abs/1207.6079) [hep-ex].
- [13] CMS Collaboration, *Search for heavy Majorana neutrinos in $\mu^\pm\mu^\pm$ +jets events in proton-proton collisions at $\sqrt{s} = 8$ TeV*, CERN-PH-EP-2015-001. CMS-EXO-12-057-003. [arXiv:1501.05566](https://arxiv.org/abs/1501.05566) [hep-ex].
- [14] J. C. Pati and A. Salam, *Lepton Number as the Fourth Color*, *Phys. Rev. D* **10** (1974) 275–289.
- [15] R. N. Mohapatra, *Unification and Supersymmetry*. Springer-Verlag, 3rd edition. 2002.
- [16] R. N. Mohapatra and P. B. Pal, *Massive Neutrinos in Physics and Astrophysics*. World Scientific, 3rd edition. 2004.
- [17] ATLAS Collaboration, *Search for heavy neutrinos and right-handed W bosons in events with two leptons and jets in pp collisions at $\sqrt{s} = 7$ TeV with the ATLAS detector*, *Eur. Phys. J. C* **72** (2012) 2056, [arXiv:1203.5420](https://arxiv.org/abs/1203.5420) [hep-ex].
- [18] CMS Collaboration, *Search for heavy neutrinos and W bosons with right-handed couplings in proton proton collisions at $\sqrt{s} = 8$ TeV*, *Eur. Phys. J. C* **74** (2014) 3149, [arXiv:1407.3683](https://arxiv.org/abs/1407.3683) [hep-ex].
- [19] ATLAS Collaboration, *The ATLAS Experiment at the CERN Large Hadron Collider*, *JINST* **3** (2008) S08003.

- [20] S. Frixione and B. R. Webber, *Matching NLO QCD computations and parton shower simulations*, *JHEP* **06** (2002) 029, [arXiv:hep-ph/0204244](#) [[hep-ph](#)].
- [21] S. Frixione, E. Laenen, P. Motylinski, B. R. Webber, and C. D. White, *Single-top hadroproduction in association with a W boson*, *JHEP* **0807** (2008) 029, [arXiv:0805.3067](#) [[hep-ph](#)].
- [22] M. Guzzi, P. Nadolsky, E. Berger, H.-L. Lai, F. Olness, and C.-P. Yuan, *CT10 parton distributions and other developments in the global QCD analysis*, [arXiv:1101.0561](#) [[hep-ph](#)].
- [23] S. Höche, F. Krauss, M. Schönherr, and F. Siegert, *Event generation with SHERPA 1.1*, *JHEP* **02** (2009) 007, [arXiv:0811.4622](#) [[hep-ph](#)].
- [24] S. Catani, F. Krauss, B. R. Webber, and R. Kuhn, *QCD Matrix Elements + Parton Showers*, *JHEP* **11** (2001) 063, [hep-ph/0109231](#) [[hep-ph](#)].
- [25] F. Maltoni and T. Stelzer, *MadEvent: automatic event generation with MadGraph*, *JHEP* **02** (2003) 027, [0208156](#) [[hep-ph](#)].
- [26] A. Martin, W. Stirling, R. Thorne, and G. Watt, *Parton distributions for the LHC*, *Eur.Phys.J.* **C63** (2009) 189–285, [arXiv:0901.0002](#) [[hep-ph](#)].
- [27] M.L. Mangano et al., *ALPGEN, a generator for hard multiparton processes in hadronic collisions*, *JHEP* **07** (2003) 001, [arXiv:0206293](#) [[hep-ph](#)].
- [28] F. del Aguila, J. Aguilar-Saavedra, and R. Pittau, *Heavy neutrino signals at large hadron colliders*, *JHEP* **07** (2007) 047, [arXiv:0703261](#) [[hep-ph](#)].
- [29] T. Sjöstrand et al., *An Introduction to PYTHIA 8.2*, *Comput. Phys. Commun.* **191** (2015) 159–177, [arXiv:1410.3012](#) [[hep-ph](#)].
- [30] G. Corcella et al., *HERWIG 6: an event generator for hadron emission reactions with interfering gluons (including supersymmetric processes)*, *JHEP* **01** (2001) 010, [arXiv:hep-ph/0011363](#) [[hep-ph](#)].
- [31] J. Butterworth, J. R. Forshaw, and M. Seymour, *Multiparton interactions in photoproduction at HERA*, *Z.Phys.* **C72** (1996) 637–646, [arXiv:hep-ph/9601371](#) [[hep-ph](#)].
- [32] ATLAS Collaboration, *The ATLAS Simulation Infrastructure*, *Eur. Phys. J. C* **70** (2010) 823–874, [1005.4568](#) [[hep-ex](#)].
- [33] S. Agostinelli et al., *Geant4 - a simulation toolkit*, *Nucl. Instrum. Meth.* **506** (2003) 250 – 303.
- [34] ATLAS Collaboration, *The ATLAS calorimeter simulation FastCaloSim*, *J. Phys* **331** (2011) 032053.
- [35] ATLAS Collaboration, *Electron reconstruction and identification efficiency measurements with the ATLAS detector using the 2011 LHC proton-proton collision data*, *Eur. Phys. J.* **C74** (2014) 2941, [arXiv:1404.2240](#) [[hep-ph](#)].
- [36] ATLAS Collaboration, *Measurement of the muon reconstruction performance of the ATLAS detector using 2011 and 2012 LHC proton-proton collision data*, *Eur. Phys. J.* **C74** (2014) 3130, [arXiv:1407.3935](#) [[hep-ex](#)].
- [37] M. Cacciari and G. P. Salam, *Dispelling the N^3 myth for the Kt jet-finder*, *Phys. Lett. B* **641** (2006) 57 – 61, [arXiv:hep-ph/0512210](#) [[hep-ph](#)].

- [38] M. Cacciari, G. P. Salam, and G. Soyez, *The anti- k_t jet clustering algorithm*, *JHEP* **04** (2008) 063, [arXiv:0802.1189 \[hep-ph\]](#).
- [39] ATLAS Collaboration, *Jet energy measurement and its systematic uncertainty in proton-proton collisions at $\sqrt{s} = 7$ TeV with the ATLAS detector*, *Eur. Phys. J. C* **75** (2015) 17, [arXiv:1406.0076 \[hep-ex\]](#).
- [40] ATLAS Collaboration, *Single hadron response measurement and calorimeter jet energy scale uncertainty with the ATLAS detector at the LHC*, *Eur. Phys. J. C* **73** (2013) 2305, [arXiv:1203.1302 \[hep-ex\]](#).
- [41] M. Cacciari and G. P. Salam, *Pileup subtraction using jet areas*, *Phys. Lett. B* **659** (2008) 119 – 126, [arXiv:0707.1378 \[hep-ph\]](#).
- [42] ATLAS Collaboration, *Pile-up subtraction and suppression for jets in ATLAS*, ATLAS-CONF-2013-083. <https://cds.cern.ch/record/1570994>.
- [43] ATLAS Collaboration, *Performance of the ATLAS Trigger System*, *JINST* **7** (2012) C01092, [arXiv:1110.1530 \[hep-ex\]](#).
- [44] ATLAS Collaboration, *Search for same-sign top-quark production and fourth-generation down-type quarks in pp collisions at $\sqrt{s} = 7$ TeV with the ATLAS detector*, *JHEP* **04** (2012) 069, [arXiv:1202.5520 \[hep-ex\]](#).
- [45] ATLAS Collaboration, *Measurement of the top quark-pair production cross section with ATLAS in pp collisions at $\sqrt{s} = 7$ TeV*, *Eur. Phys. J. C* **71** (2011) 1577, [arXiv:1012.1792 \[hep-ex\]](#).
- [46] *Performance of missing transverse momentum reconstruction in proton-proton collisions at $\sqrt{s} = 7$ TeV with ATLAS*, *Eur. Phys. J. C* **72** (2012) 1–35, [arXiv:1108.5602 \[hep-ex\]](#).
- [47] ATLAS Collaboration, *Jet energy resolution in proton-proton collisions at $\sqrt{s} = 7$ TeV recorded in 2010 with the ATLAS detector*, *Eur. Phys. J. C* **73** (2013) 2306, [arXiv:1210.6210 \[hep-ex\]](#).
- [48] ATLAS Collaboration, *Improved luminosity determination in pp collisions at $\sqrt{s} = 7$ TeV using the ATLAS detector at the LHC*, *Eur. Phys. J. C* **73** (2013) 2518, [arXiv:1302.4393 \[hep-ex\]](#).
- [49] G. Cowan, K. Cranmer, E. Gross, and O. Vitells, *Asymptotic formulae for likelihood-based tests of new physics*, *Eur. Phys. J. C* **71** (2011) 1554, [arXiv:1007.1727 \[physics.data-an\]](#).
- [50] G. Cowan, K. Cranmer, E. Gross, and O. Vitells, *Erratum to: Asymptotic formulae for likelihood-based tests of new physics*, *Eur. Phys. J. C* **73** (2013).
- [51] A. L. Read, *Presentation of search results: the CL_s technique*, *J. Phys* **G28** (2002) 2693.

The ATLAS Collaboration

G. Aad⁸⁵, B. Abbott¹¹³, J. Abdallah¹⁵², S. Abdel Khalek¹¹⁷, O. Abdinov¹¹, R. Aben¹⁰⁷, B. Abi¹¹⁴, M. Abolins⁹⁰, O.S. AbouZeid¹⁵⁹, H. Abramowicz¹⁵⁴, H. Abreu¹⁵³, R. Abreu³⁰, Y. Abulaiti^{147a,147b}, B.S. Acharya^{165a,165b,a}, L. Adamczyk^{38a}, D.L. Adams²⁵, J. Adelman¹⁰⁸, S. Adomeit¹⁰⁰, T. Adye¹³¹, T. Agatonovic-Jovin¹³, J.A. Aguilar-Saavedra^{126a,126f}, M. Agustoni¹⁷, S.P. Ahlen²², F. Ahmadov^{65,b}, G. Aielli^{134a,134b}, H. Akerstedt^{147a,147b}, T.P.A. Åkesson⁸¹, G. Akimoto¹⁵⁶, A.V. Akimov⁹⁶, G.L. Alberghi^{20a,20b}, J. Albert¹⁷⁰, S. Albrand⁵⁵, M.J. Alconada Verzini⁷¹, M. Aleksa³⁰, I.N. Aleksandrov⁶⁵, C. Alexa^{26a}, G. Alexander¹⁵⁴, G. Alexandre⁴⁹, T. Alexopoulos¹⁰, M. Alhroob¹¹³, G. Alimonti^{91a}, L. Alio⁸⁵, J. Alison³¹, B.M.M. Allbrooke¹⁸, L.J. Allison⁷², P.P. Allport⁷⁴, J. Almond⁸⁴, A. Aloisio^{104a,104b}, A. Alonso³⁶, F. Alonso⁷¹, C. Alpigiani⁷⁶, A. Altheimer³⁵, B. Alvarez Gonzalez⁹⁰, M.G. Alvigi^{104a,104b}, K. Amako⁶⁶, Y. Amaral Coutinho^{24a}, C. Amelung²³, D. Amidei⁸⁹, S.P. Amor Dos Santos^{126a,126c}, A. Amorim^{126a,126b}, S. Amoroso⁴⁸, N. Amram¹⁵⁴, G. Amundsen²³, C. Anastopoulos¹⁴⁰, L.S. Ancu⁴⁹, N. Andari³⁰, T. Andeen³⁵, C.F. Anders^{58b}, G. Anders³⁰, K.J. Anderson³¹, A. Andreazza^{91a,91b}, V. Andrei^{58a}, X.S. Anduaga⁷¹, S. Angelidakis⁹, I. Angelozzi¹⁰⁷, P. Anger⁴⁴, A. Angerami³⁵, F. Anghinolfi³⁰, A.V. Anisenkov^{109,c}, N. Anjos¹², A. Annovi^{124a,124b}, M. Antonelli⁴⁷, A. Antonov⁹⁸, J. Antos^{145b}, F. Anulli^{133a}, M. Aoki⁶⁶, L. Aperio Bella¹⁸, G. Arabidze⁹⁰, Y. Arai⁶⁶, J.P. Araque^{126a}, A.T.H. Arce⁴⁵, F.A. Arduh⁷¹, J-F. Arguin⁹⁵, S. Argyropoulos⁴², M. Arik^{19a}, A.J. Armbruster³⁰, O. Arnaez³⁰, V. Arnal⁸², H. Arnold⁴⁸, M. Arratia²⁸, O. Arslan²¹, A. Artamonov⁹⁷, G. Artoni²³, S. Asai¹⁵⁶, N. Asbah⁴², A. Ashkenazi¹⁵⁴, B. Åsman^{147a,147b}, L. Asquith¹⁵⁰, K. Assamagan²⁵, R. Astalos^{145a}, M. Atkinson¹⁶⁶, N.B. Atlay¹⁴², B. Auerbach⁶, K. Augsten¹²⁸, M. Auresseau^{146b}, G. Avolio³⁰, B. Axen¹⁵, M.K. Ayoub¹¹⁷, G. Azuelos^{95,d}, M.A. Baak³⁰, A.E. Baas^{58a}, C. Bacci^{135a,135b}, H. Bachacou¹³⁷, K. Bachas¹⁵⁵, M. Backes³⁰, M. Backhaus³⁰, P. Bagiacchi^{133a,133b}, P. Bagnaia^{133a,133b}, Y. Bai^{33a}, T. Bain³⁵, J.T. Baines¹³¹, O.K. Baker¹⁷⁷, P. Balek¹²⁹, T. Balestri¹⁴⁹, F. Balli⁸⁴, E. Banas³⁹, Sw. Banerjee¹⁷⁴, A.A.E. Bannoura¹⁷⁶, H.S. Bansil¹⁸, L. Barak¹⁷³, E.L. Barberio⁸⁸, D. Barberis^{50a,50b}, M. Barbero⁸⁵, T. Barillari¹⁰¹, M. Barisonzi^{165a,165b}, T. Barklow¹⁴⁴, N. Barlow²⁸, S.L. Barnes⁸⁴, B.M. Barnett¹³¹, R.M. Barnett¹⁵, Z. Barnovska⁵, A. Baroncelli^{135a}, G. Barone⁴⁹, A.J. Barr¹²⁰, F. Barreiro⁸², J. Barreiro Guimarães da Costa⁵⁷, R. Bartoldus¹⁴⁴, A.E. Barton⁷², P. Bartos^{145a}, A. Bassalat¹¹⁷, A. Basye¹⁶⁶, R.L. Bates⁵³, S.J. Batista¹⁵⁹, J.R. Batley²⁸, M. Battaglia¹³⁸, M. Bauge^{133a,133b}, F. Bauer¹³⁷, H.S. Bawa^{144,e}, J.B. Beacham¹¹¹, M.D. Beattie⁷², T. Beau⁸⁰, P.H. Beauchemin¹⁶², R. Beccherle^{124a,124b}, P. Bechtel²¹, H.P. Beck^{17,f}, K. Becker¹²⁰, S. Becker¹⁰⁰, M. Beckingham¹⁷¹, C. Becot¹¹⁷, A.J. Beddall^{19b}, A. Beddall^{19b}, V.A. Bednyakov⁶⁵, C.P. Bee¹⁴⁹, L.J. Beamster¹⁰⁷, T.A. Beermann¹⁷⁶, M. Begel²⁵, J.K. Behr¹²⁰, C. Belanger-Champagne⁸⁷, P.J. Bell⁴⁹, W.H. Bell⁴⁹, G. Bella¹⁵⁴, L. Bellagamba^{20a}, A. Bellerive²⁹, M. Bellomo⁸⁶, K. Belotskiy⁹⁸, O. Beltramello³⁰, O. Benary¹⁵⁴, D. Benckekroun^{136a}, M. Bender¹⁰⁰, K. Bendtz^{147a,147b}, N. Benekos¹⁰, Y. Benhammou¹⁵⁴, E. Benhar Noccioli⁴⁹, J.A. Benitez Garcia^{160b}, D.P. Benjamin⁴⁵, J.R. Bensinger²³, S. Bentvelsen¹⁰⁷, L. Beresford¹²⁰, M. Beretta⁴⁷, D. Berge¹⁰⁷, E. Bergeaas Kuutmann¹⁶⁷, N. Berger⁵, F. Berghaus¹⁷⁰, J. Beringer¹⁵, C. Bernard²², N.R. Bernard⁸⁶, C. Bernius¹¹⁰, F.U. Bernlochner²¹, T. Berry⁷⁷, P. Berta¹²⁹, C. Bertella⁸³, G. Bertoli^{147a,147b}, F. Bertolucci^{124a,124b}, C. Bertsche¹¹³, D. Bertsche¹¹³, M.I. Besana^{91a}, G.J. Besjes¹⁰⁶, O. Bessidskaia Bylund^{147a,147b}, M. Bessner⁴², N. Besson¹³⁷, C. Betancourt⁴⁸, S. Bethke¹⁰¹, A.J. Bevan⁷⁶, W. Bhimji⁴⁶, R.M. Bianchi¹²⁵, L. Bianchini²³, M. Bianco³⁰, O. Biebel¹⁰⁰, S.P. Bieniek⁷⁸, M. Biglietti^{135a}, J. Bilbao De Mendizabal⁴⁹, H. Bilokon⁴⁷, M. Bindi⁵⁴, S. Binet¹¹⁷, A. Bingul^{19b}, C. Bini^{133a,133b}, C.W. Black¹⁵¹, J.E. Black¹⁴⁴, K.M. Black²², D. Blackburn¹³⁹, R.E. Blair⁶, J.-B. Blanchard¹³⁷, J.E. Blanco⁷⁷, T. Blazek^{145a}, I. Bloch⁴², C. Blocker²³, W. Blum^{83,*}, U. Blumenschein⁵⁴, G.J. Bobbink¹⁰⁷, V.S. Bobrovnikov^{109,c}, S.S. Bocchetta⁸¹, A. Bocci⁴⁵, C. Bock¹⁰⁰, C.R. Boddy¹²⁰, M. Boehler⁴⁸, J.A. Bogaerts³⁰,

A.G. Bogdanchikov¹⁰⁹, C. Bohm^{147a}, V. Boisvert⁷⁷, T. Bold^{138a}, V. Boldea^{26a}, A.S. Boldyrev⁹⁹,
 M. Bomben⁸⁰, M. Bona⁷⁶, M. Boonekamp¹³⁷, A. Borisov¹³⁰, G. Borissov⁷², S. Borroni⁴²,
 J. Bortfeldt¹⁰⁰, V. Bortolotto^{60a}, K. Bos¹⁰⁷, D. Boscherini^{20a}, M. Bosman¹², J. Boudreau¹²⁵, J. Bouffard²,
 E.V. Bouhova-Thacker⁷², D. Boumediene³⁴, C. Bourdarios¹¹⁷, N. Bousson¹¹⁴, S. Boutouil^{136d},
 A. Boveia³⁰, J. Boyd³⁰, I.R. Boyko⁶⁵, I. Bozic¹³, J. Bracinik¹⁸, A. Brandt⁸, G. Brandt¹⁵, O. Brandt^{58a},
 U. Bratzler¹⁵⁷, B. Brau⁸⁶, J.E. Brau¹¹⁶, H.M. Braun^{176,*}, S.F. Brazzale^{165a,165c}, K. Brendlinger¹²²,
 A.J. Brennan⁸⁸, L. Brenner¹⁰⁷, R. Brenner¹⁶⁷, S. Bressler¹⁷³, K. Bristow^{146c}, T.M. Bristow⁴⁶,
 D. Britton⁵³, F.M. Brochu²⁸, I. Brock²¹, R. Brock⁹⁰, J. Bronner¹⁰¹, G. Brooijmans³⁵, T. Brooks⁷⁷,
 W.K. Brooks^{32b}, J. Brosamer¹⁵, E. Brost¹¹⁶, J. Brown⁵⁵, P.A. Bruckman de Renstrom³⁹, D. Bruncko^{145b},
 R. Bruneliere⁴⁸, A. Bruni^{20a}, G. Bruni^{20a}, M. Bruschi^{20a}, L. Bryngemark⁸¹, T. Buanes¹⁴, Q. Buat¹⁴³,
 F. Bucci⁴⁹, P. Buchholz¹⁴², A.G. Buckley⁵³, S.I. Buda^{26a}, I.A. Budagov⁶⁵, F. Buehrer⁴⁸, L. Bugge¹¹⁹,
 M.K. Bugge¹¹⁹, O. Bulekov⁹⁸, H. Burckhart³⁰, S. Burdin⁷⁴, B. Burghgrave¹⁰⁸, S. Burke¹³¹,
 I. Burmeister⁴³, E. Busato³⁴, D. Büscher⁴⁸, V. Büscher⁸³, P. Bussey⁵³, C.P. Buszello¹⁶⁷, J.M. Butler²²,
 A.I. Butt³, C.M. Buttar⁵³, J.M. Butterworth⁷⁸, P. Butti¹⁰⁷, W. Buttinger²⁵, A. Buzatu⁵³,
 S. Cabrera Urbán¹⁶⁸, D. Caforio¹²⁸, O. Cakir^{4a}, P. Calafiura¹⁵, A. Calandri¹³⁷, G. Calderini⁸⁰,
 P. Calfayan¹⁰⁰, L.P. Caloba^{24a}, D. Calvet³⁴, S. Calvet³⁴, R. Camacho Toro⁴⁹, S. Camarda⁴²,
 D. Cameron¹¹⁹, L.M. Caminada¹⁵, R. Caminal Armadans¹², S. Campana³⁰, M. Campanelli⁷⁸,
 A. Campoverde¹⁴⁹, V. Canale^{104a,104b}, A. Canepa^{160a}, M. Cano Bret⁷⁶, J. Cantero⁸², R. Cantrill^{126a},
 T. Cao⁴⁰, M.D.M. Capeans Garrido³⁰, I. Caprini^{26a}, M. Caprini^{26a}, M. Capua^{37a,37b}, R. Caputo⁸³,
 R. Cardarelli^{134a}, T. Carli³⁰, G. Carlino^{104a}, L. Carminati^{91a,91b}, S. Caron¹⁰⁶, E. Carquin^{32a},
 G.D. Carrillo-Montoya^{146c}, J.R. Carter²⁸, J. Carvalho^{126a,126c}, D. Casadei⁷⁸, M.P. Casado¹²,
 M. Casolino¹², E. Castaneda-Miranda^{146b}, A. Castelli¹⁰⁷, V. Castillo Gimenez¹⁶⁸, N.F. Castro^{126a,g},
 P. Catastini⁵⁷, A. Catinaccio³⁰, J.R. Catmore¹¹⁹, A. Cattai³⁰, G. Cattani^{134a,134b}, J. Caudron⁸³,
 V. Cavaliere¹⁶⁶, D. Cavalli^{91a}, M. Cavalli-Sforza¹², V. Cavasinni^{124a,124b}, F. Ceradini^{135a,135b},
 B.C. Cerio⁴⁵, K. Cerny¹²⁹, A.S. Cerqueira^{24b}, A. Cerri¹⁵⁰, L. Cerrito⁷⁶, F. Cerutti¹⁵, M. Cerv³⁰,
 A. Cervelli¹⁷, S.A. Cetin^{19c}, A. Chafaq^{136a}, D. Chakraborty¹⁰⁸, I. Chalupkova¹²⁹, P. Chang¹⁶⁶,
 B. Chapleau⁸⁷, J.D. Chapman²⁸, D. Charfeddine¹¹⁷, D.G. Charlton¹⁸, C.C. Chau¹⁵⁹,
 C.A. Chavez Barajas¹⁵⁰, S. Cheatham¹⁵³, A. Chegwiddden⁹⁰, S. Chekanov⁶, S.V. Chekulaev^{160a},
 G.A. Chelkov^{65,h}, M.A. Chelstowska⁸⁹, C. Chen⁶⁴, H. Chen²⁵, K. Chen¹⁴⁹, L. Chen^{33d,i}, S. Chen^{33c},
 X. Chen^{33f}, Y. Chen⁶⁷, H.C. Cheng⁸⁹, Y. Cheng³¹, A. Cheplakov⁶⁵, E. Cheremushkina¹³⁰,
 R. Cherkaoui El Moursli^{136e}, V. Chernyatin^{25,*}, E. Cheu⁷, L. Chevalier¹³⁷, V. Chiarella⁴⁷, J.T. Childers⁶,
 A. Chilingarov⁷², G. Chiodini^{73a}, A.S. Chisholm¹⁸, R.T. Chislett⁷⁸, A. Chitan^{26a}, M.V. Chizhov⁶⁵,
 S. Chouridou⁹, B.K.B. Chow¹⁰⁰, D. Chromek-Burckhart³⁰, M.L. Chu¹⁵², J. Chudoba¹²⁷,
 J.J. Chwastowski³⁹, L. Chytka¹¹⁵, G. Ciapetti^{133a,133b}, A.K. Ciftci^{4a}, D. Cinca⁵³, V. Cindro⁷⁵,
 A. Ciocio¹⁵, Z.H. Citron¹⁷³, M. Ciubancan^{26a}, A. Clark⁴⁹, P.J. Clark⁴⁶, R.N. Clarke¹⁵, W. Cleland¹²⁵,
 C. Clement^{147a,147b}, Y. Coadou⁸⁵, M. Cobal^{165a,165c}, A. Coccaro¹³⁹, J. Cochran⁶⁴, L. Coffey²³,
 J.G. Cogan¹⁴⁴, B. Cole³⁵, S. Cole¹⁰⁸, A.P. Colijn¹⁰⁷, J. Collot⁵⁵, T. Colombo^{58c}, G. Compostella¹⁰¹,
 P. Conde Muiño^{126a,126b}, E. Coniavitis⁴⁸, S.H. Connell^{146b}, I.A. Connelly⁷⁷, S.M. Consonni^{91a,91b},
 V. Consorti⁴⁸, S. Constantinescu^{26a}, C. Conta^{121a,121b}, G. Conti³⁰, F. Conventi^{104a,j}, M. Cooke¹⁵,
 B.D. Cooper⁷⁸, A.M. Cooper-Sarkar¹²⁰, K. Copic¹⁵, T. Cornelissen¹⁷⁶, M. Corradi^{20a}, F. Corriveau^{87,k},
 A. Corso-Radu¹⁶⁴, A. Cortes-Gonzalez¹², G. Cortiana¹⁰¹, G. Costa^{91a}, M.J. Costa¹⁶⁸, D. Costanzo¹⁴⁰,
 D. Côté⁸, G. Cottin²⁸, G. Cowan⁷⁷, B.E. Cox⁸⁴, K. Cranmer¹¹⁰, G. Cree²⁹, S. Crépe-Renaudin⁵⁵,
 F. Crescioli⁸⁰, W.A. Cribbs^{147a,147b}, M. Crispin Ortuzar¹²⁰, M. Cristinziani²¹, V. Croft¹⁰⁶,
 G. Crosetti^{37a,37b}, T. Cuhadar Donszelmann¹⁴⁰, J. Cummings¹⁷⁷, M. Curatolo⁴⁷, C. Cuthbert¹⁵¹,
 H. Czirr¹⁴², P. Czodrowski³, S. D'Auria⁵³, M. D'Onofrio⁷⁴, M.J. Da Cunha Sargedas De Sousa^{126a,126b},
 C. Da Via⁸⁴, W. Dabrowski^{38a}, A. Dafinca¹²⁰, T. Dai⁸⁹, O. Dale¹⁴, F. Dallaire⁹⁵, C. Dallapiccola⁸⁶,
 M. Dam³⁶, J.R. Dandoy³¹, A.C. Daniells¹⁸, M. Danninger¹⁶⁹, M. Dano Hoffmann¹³⁷, V. Dao⁴⁸,

G. Darbo^{50a}, S. Darmora⁸, J. Dassoulas³, A. Dattagupta⁶¹, W. Davey²¹, C. David¹⁷⁰, T. Davidek¹²⁹, E. Davies^{120,l}, M. Davies¹⁵⁴, O. Davignon⁸⁰, P. Davison⁷⁸, Y. Davygora^{58a}, E. Dawe¹⁴³, I. Dawson¹⁴⁰, R.K. Daya-Ishmukhametova⁸⁶, K. De⁸, R. de Asmundis^{104a}, S. De Castro^{20a,20b}, S. De Cecco⁸⁰, N. De Groot¹⁰⁶, P. de Jong¹⁰⁷, H. De la Torre⁸², F. De Lorenzi⁶⁴, L. De Nooij¹⁰⁷, D. De Pedis^{133a}, A. De Salvo^{133a}, U. De Sanctis¹⁵⁰, A. De Santo¹⁵⁰, J.B. De Vivie De Regie¹¹⁷, W.J. Dearnaley⁷², R. Debbe²⁵, C. Debenedetti¹³⁸, D.V. Dedovich⁶⁵, I. Deigaard¹⁰⁷, J. Del Peso⁸², T. Del Prete^{124a,124b}, D. Delgove¹¹⁷, F. Deliot¹³⁷, C.M. Delitzsch⁴⁹, M. Deliyergiyev⁷⁵, A. Dell'Acqua³⁰, L. Dell'Asta²², M. Dell'Orso^{124a,124b}, M. Della Pietra^{104a,j}, D. della Volpe⁴⁹, M. Delmastro⁵, P.A. Delsart⁵⁵, C. Deluca¹⁰⁷, D.A. DeMarco¹⁵⁹, S. Demers¹⁷⁷, M. Demichev⁶⁵, A. Demilly⁸⁰, S.P. Denisov¹³⁰, D. Derendarz³⁹, J.E. Derkaoui^{136d}, F. Derue⁸⁰, P. Dervan⁷⁴, K. Desch²¹, C. Deterre⁴², P.O. Deviveiros³⁰, A. Dewhurst¹³¹, S. Dhaliwal²³, A. Di Ciaccio^{134a,134b}, L. Di Ciaccio⁵, A. Di Domenico^{133a,133b}, C. Di Donato^{104a,104b}, A. Di Girolamo³⁰, B. Di Girolamo³⁰, A. Di Mattia¹⁵³, B. Di Micco^{135a,135b}, R. Di Nardo⁴⁷, A. Di Simone⁴⁸, R. Di Sipio^{20a,20b}, D. Di Valentino²⁹, C. Diaconu⁸⁵, M. Diamond¹⁵⁹, F.A. Dias⁴⁶, M.A. Diaz^{32a}, E.B. Diehl⁸⁹, J. Dietrich¹⁶, T.A. Dietzsch^{58a}, S. Diglio⁸⁵, A. Dimitrievska¹³, J. Dingfelder²¹, P. Dita^{26a}, S. Dita^{26a}, F. Dittus³⁰, F. Djama⁸⁵, T. Djobava^{51b}, J.I. Djuvsland^{58a}, M.A.B. do Vale^{24c}, D. Dobos³⁰, M. Dobre^{26a}, C. Doglioni⁴⁹, T. Doherty⁵³, T. Dohmae¹⁵⁶, J. Dolejsi¹²⁹, Z. Dolezal¹²⁹, B.A. Dolgoshein^{98,*}, M. Donadelli^{24d}, S. Donati^{124a,124b}, P. Dondero^{121a,121b}, J. Donini³⁴, J. Dopke¹³¹, A. Doria^{104a}, M.T. Dova⁷¹, A.T. Doyle⁵³, M. Dris¹⁰, E. Dubreuil³⁴, E. Duchovni¹⁷³, G. Duckeck¹⁰⁰, O.A. Ducu^{26a}, D. Duda¹⁷⁶, A. Dudarev³⁰, L. Dufлот¹¹⁷, L. Duguid⁷⁷, M. Dührssen³⁰, M. Dunford^{58a}, H. Duran Yildiz^{4a}, M. Düren⁵², A. Durglishvili^{51b}, D. Duschinger⁴⁴, M. Dwuznik^{38a}, M. Dyndal^{38a}, K.M. Ecker¹⁰¹, W. Edson², N.C. Edwards⁴⁶, W. Ehrenfeld²¹, T. Eifert³⁰, G. Eigen¹⁴, K. Einsweiler¹⁵, T. Ekelof¹⁶⁷, M. El Kacimi^{136c}, M. Ellert¹⁶⁷, S. Elles⁵, F. Ellinghaus⁸³, A.A. Elliot¹⁷⁰, N. Ellis³⁰, J. Elmsheuser¹⁰⁰, M. Elsing³⁰, D. Emeliyanov¹³¹, Y. Enari¹⁵⁶, O.C. Endner⁸³, M. Endo¹¹⁸, J. Erdmann⁴³, A. Ereditato¹⁷, D. Eriksson^{147a}, G. Ernis¹⁷⁶, J. Ernst², M. Ernst²⁵, S. Errede¹⁶⁶, E. Ertel⁸³, M. Escalier¹¹⁷, H. Esch⁴³, C. Escobar¹²⁵, B. Esposito⁴⁷, A.I. Etiennev¹³⁷, E. Etzion¹⁵⁴, H. Evans⁶¹, A. Ezhilov¹²³, L. Fabbri^{20a,20b}, G. Facini³¹, R.M. Fakhruddinov¹³⁰, S. Falciano^{133a}, R.J. Falla⁷⁸, J. Faltova¹²⁹, Y. Fang^{33a}, M. Fanti^{91a,91b}, A. Farbin⁸, A. Farilla^{135a}, T. Farooque¹², S. Farrell¹⁵, S.M. Farrington¹⁷¹, P. Farthouat³⁰, F. Fassi^{136e}, P. Fassnacht³⁰, D. Fassouliotis⁹, A. Favareto^{50a,50b}, L. Fayard¹¹⁷, P. Federic^{145a}, O.L. Fedin^{123,m}, W. Fedorko¹⁶⁹, S. Feigl³⁰, L. Felgioni⁸⁵, C. Feng^{33d}, E.J. Feng⁶, H. Feng⁸⁹, A.B. Fenyuk¹³⁰, P. Fernandez Martinez¹⁶⁸, S. Fernandez Perez³⁰, S. Ferrag⁵³, J. Ferrando⁵³, A. Ferrari¹⁶⁷, P. Ferrari¹⁰⁷, R. Ferrari^{121a}, D.E. Ferreira de Lima⁵³, A. Ferrer¹⁶⁸, D. Ferrere⁴⁹, C. Ferretti⁸⁹, A. Ferretto Parodi^{50a,50b}, M. Fiascaris³¹, F. Fiedler⁸³, A. Filipčić⁷⁵, M. Filipuzzi⁴², F. Filthaut¹⁰⁶, M. Fincke-Keeler¹⁷⁰, K.D. Finelli¹⁵¹, M.C.N. Fiolhais^{126a,126c}, L. Fiorini¹⁶⁸, A. Firan⁴⁰, A. Fischer², C. Fischer¹², J. Fischer¹⁷⁶, W.C. Fisher⁹⁰, E.A. Fitzgerald²³, M. Flechl⁴⁸, I. Fleck¹⁴², P. Fleischmann⁸⁹, S. Fleischmann¹⁷⁶, G.T. Fletcher¹⁴⁰, G. Fletcher⁷⁶, T. Flick¹⁷⁶, A. Floderus⁸¹, L.R. Flores Castillo^{60a}, M.J. Flowerdew¹⁰¹, A. Formica¹³⁷, A. Forti⁸⁴, D. Fournier¹¹⁷, H. Fox⁷², S. Fracchia¹², P. Francavilla⁸⁰, M. Franchini^{20a,20b}, D. Francis³⁰, L. Franconi¹¹⁹, M. Franklin⁵⁷, M. Fraternali^{121a,121b}, D. Freeborn⁷⁸, S.T. French²⁸, F. Friedrich⁴⁴, D. Froidevaux³⁰, J.A. Frost¹²⁰, C. Fukunaga¹⁵⁷, E. Fullana Torregrosa⁸³, B.G. Fulson¹⁴⁴, J. Fuster¹⁶⁸, C. Gabaldon⁵⁵, O. Gabizon¹⁷⁶, A. Gabrielli^{20a,20b}, A. Gabrielli^{133a,133b}, S. Gadatsch¹⁰⁷, S. Gadomski⁴⁹, G. Gagliardi^{50a,50b}, P. Gagnon⁶¹, C. Galea¹⁰⁶, B. Galhardo^{126a,126c}, E.J. Gallas¹²⁰, B.J. Gallop¹³¹, P. Gallus¹²⁸, G. Galster³⁶, K.K. Gan¹¹¹, J. Gao^{33b,85}, Y.S. Gao^{144,e}, F.M. Garay Walls⁴⁶, F. Garbersson¹⁷⁷, C. García¹⁶⁸, J.E. García Navarro¹⁶⁸, M. Garcia-Sciveres¹⁵, R.W. Gardner³¹, N. Garelli¹⁴⁴, V. Garonne³⁰, C. Gatti⁴⁷, G. Gaudio^{121a}, B. Gaur¹⁴², L. Gauthier⁹⁵, P. Gauzzi^{133a,133b}, I.L. Gavrilenko⁹⁶, C. Gay¹⁶⁹, G. Gaycken²¹, E.N. Gazis¹⁰, P. Ge^{33d}, Z. Gece¹⁶⁹, C.N.P. Gee¹³¹, D.A.A. Geerts¹⁰⁷, Ch. Geich-Gimbel²¹, C. Gemme^{50a}, M.H. Genest⁵⁵, S. Gentile^{133a,133b}, M. George⁵⁴, S. George⁷⁷, D. Gerbaudo¹⁶⁴, A. Gershon¹⁵⁴, H. Ghazlane^{136b}, N. Ghodbane³⁴, B. Giacobbe^{20a}, S. Giagu^{133a,133b},

V. Giangiobbe¹², P. Giannetti^{124a,124b}, F. Gianotti³⁰, B. Gibbard²⁵, S.M. Gibson⁷⁷, M. Gilchriese¹⁵, T.P.S. Gillam²⁸, D. Gillberg³⁰, G. Gilles³⁴, D.M. Gingrich^{3,d}, N. Giokaris⁹, M.P. Giordani^{165a,165c}, F.M. Giorgi^{20a}, F.M. Giorgi¹⁶, P.F. Giraud¹³⁷, D. Giugni^{91a}, C. Giuliani⁴⁸, M. Giulini^{58b}, B.K. Gjelsten¹¹⁹, S. Gkaitatzis¹⁵⁵, I. Gkialas¹⁵⁵, E.L. Gkoukousis¹¹⁷, L.K. Gladilin⁹⁹, C. Glasman⁸², J. Glatzer³⁰, P.C.F. Glaysher⁴⁶, A. Glazov⁴², M. Goblirsch-Kolb¹⁰¹, J.R. Goddard⁷⁶, J. Godlewski³⁹, S. Goldfarb⁸⁹, T. Golling⁴⁹, D. Golubkov¹³⁰, A. Gomes^{126a,126b,126d}, R. Gonçalo^{126a}, J. Goncalves Pinto Firmino Da Costa¹³⁷, L. Gonella²¹, S. González de la Hoz¹⁶⁸, G. Gonzalez Parra¹², S. Gonzalez-Sevilla⁴⁹, L. Goossens³⁰, P.A. Gorbounov⁹⁷, H.A. Gordon²⁵, I. Gorelov¹⁰⁵, B. Gorini³⁰, E. Gorini^{73a,73b}, A. Gorišek⁷⁵, E. Gornicki³⁹, A.T. Goshaw⁴⁵, C. Gössling⁴³, M.I. Gostkin⁶⁵, M. Gouighri^{136a}, D. Goujdami^{136c}, A.G. Goussiou¹³⁹, H.M.X. Grabas¹³⁸, L. Graber⁵⁴, I. Grabowska-Bold^{38a}, P. Grafström^{20a,20b}, K.-J. Grahn⁴², J. Gramling⁴⁹, E. Gramstad¹¹⁹, S. Grancagnolo¹⁶, V. Grassi¹⁴⁹, V. Gratchev¹²³, H.M. Gray³⁰, E. Graziani^{135a}, Z.D. Greenwood^{79,n}, K. Gregersen⁷⁸, I.M. Gregor⁴², P. Grenier¹⁴⁴, J. Griffiths⁸, A.A. Grillo¹³⁸, K. Grimm⁷², S. Grinstein^{12,o}, Ph. Gris³⁴, J.-F. Grivaz¹¹⁷, J.P. Grohs⁴⁴, A. Grohsjean⁴², E. Gross¹⁷³, J. Grosse-Knetter⁵⁴, G.C. Grossi^{134a,134b}, Z.J. Grout¹⁵⁰, L. Guan^{33b}, J. Guenther¹²⁸, F. Guescini⁴⁹, D. Guest¹⁷⁷, O. Gueta¹⁵⁴, E. Guido^{50a,50b}, T. Guillemin¹¹⁷, S. Guindon², U. Gul⁵³, C. Gumpert⁴⁴, J. Guo^{33e}, S. Gupta¹²⁰, P. Gutierrez¹¹³, N.G. Gutierrez Ortiz⁵³, C. Gutsche⁴⁴, N. Guttman¹⁵⁴, C. Guyot¹³⁷, C. Gwenlan¹²⁰, C.B. Gwilliam⁷⁴, A. Haas¹¹⁰, C. Haber¹⁵, H.K. Hadavand⁸, N. Haddad^{136e}, P. Haefner²¹, S. Hageböck²¹, Z. Hajduk³⁹, H. Hakobyan¹⁷⁸, M. Haleem⁴², J. Haley¹¹⁴, D. Hall¹²⁰, G. Halladjian⁹⁰, G.D. Hallowell⁸⁵, K. Hamacher¹⁷⁶, P. Hamal¹¹⁵, K. Hamano¹⁷⁰, M. Hamer⁵⁴, A. Hamilton^{146a}, S. Hamilton¹⁶², G.N. Hamity^{146c}, P.G. Hamnett⁴², L. Han^{33b}, K. Hanagaki¹¹⁸, K. Hanawa¹⁵⁶, M. Hance¹⁵, P. Hanke^{58a}, R. Hanna¹³⁷, J.B. Hansen³⁶, J.D. Hansen³⁶, P.H. Hansen³⁶, K. Hara¹⁶¹, A.S. Hard¹⁷⁴, T. Harenberg¹⁷⁶, F. Hariri¹¹⁷, S. Harkusha⁹², R.D. Harrington⁴⁶, P.F. Harrison¹⁷¹, F. Hartjes¹⁰⁷, M. Hasegawa⁶⁷, S. Hasegawa¹⁰³, Y. Hasegawa¹⁴¹, A. Hasib¹¹³, S. Hassani¹³⁷, S. Haug¹⁷, R. Hauser⁹⁰, L. Hauswald⁴⁴, M. Havranek¹²⁷, C.M. Hawkes¹⁸, R.J. Hawkins³⁰, A.D. Hawkins⁸¹, T. Hayashi¹⁶¹, D. Hayden⁹⁰, C.P. Hays¹²⁰, J.M. Hays⁷⁶, H.S. Hayward⁷⁴, S.J. Haywood¹³¹, S.J. Head¹⁸, T. Heck⁸³, V. Hedberg⁸¹, L. Heelan⁸, S. Heim¹²², T. Heim¹⁷⁶, B. Heinemann¹⁵, L. Heinrich¹¹⁰, J. Hejbal¹²⁷, L. Helary²², M. Heller³⁰, S. Hellman^{147a,147b}, D. Hellmich²¹, C. Helsen³⁰, J. Henderson¹²⁰, R.C.W. Henderson⁷², Y. Heng¹⁷⁴, C. Hengler⁴², A. Henrichs¹⁷⁷, A.M. Henriques Correia³⁰, S. Henrot-Versille¹¹⁷, G.H. Herbert¹⁶, Y. Hernández Jiménez¹⁶⁸, R. Herrberg-Schubert¹⁶, G. Herten⁴⁸, R. Hertenberger¹⁰⁰, L. Hervas³⁰, G.G. Hesketh⁷⁸, N.P. Hessey¹⁰⁷, R. Hickling⁷⁶, E. Higón-Rodríguez¹⁶⁸, E. Hill¹⁷⁰, J.C. Hill²⁸, K.H. Hiller⁴², S.J. Hillier¹⁸, I. Hinchliffe¹⁵, E. Hines¹²², R.R. Hinman¹⁵, M. Hirose¹⁵⁸, D. Hirschbuehl¹⁷⁶, J. Hobbs¹⁴⁹, N. Hod¹⁰⁷, M.C. Hodgkinson¹⁴⁰, P. Hodgson¹⁴⁰, A. Hoecker³⁰, M.R. Hoferkamp¹⁰⁵, F. Hoenig¹⁰⁰, M. Hohlfeld⁸³, T.R. Holmes¹⁵, T.M. Hong¹²², L. Hooft van Huysduynen¹¹⁰, W.H. Hopkins¹¹⁶, Y. Horii¹⁰³, A.J. Horton¹⁴³, J.-Y. Hostachy⁵⁵, S. Hou¹⁵², A. Hoummada^{136a}, J. Howard¹²⁰, J. Howarth⁴², M. Hrabovsky¹¹⁵, I. Hristova¹⁶, J. Hrivnac¹¹⁷, T. Hryn'ova⁵, A. Hrynevich⁹³, C. Hsu^{146c}, P.J. Hsu^{152,p}, S.-C. Hsu¹³⁹, D. Hu³⁵, Q. Hu^{33b}, X. Hu⁸⁹, Y. Huang⁴², Z. Hubacek³⁰, F. Hubaut⁸⁵, F. Huegging²¹, T.B. Huffman¹²⁰, E.W. Hughes³⁵, G. Hughes⁷², M. Huhtinen³⁰, T.A. Hülsing⁸³, N. Huseynov^{65,b}, J. Huston⁹⁰, J. Huth⁵⁷, G. Iacobucci⁴⁹, G. Iakovidis²⁵, I. Ibragimov¹⁴², L. Iconomidou-Fayard¹¹⁷, E. Ideal¹⁷⁷, Z. Idrissi^{136e}, P. Iengo^{104a}, O. Igonkina¹⁰⁷, T. Iizawa¹⁷², Y. Ikegami⁶⁶, K. Ikematsu¹⁴², M. Ikeno⁶⁶, Y. Ilchenko^{31,q}, D. Iliadis¹⁵⁵, N. Ilic¹⁵⁹, Y. Inamaru⁶⁷, T. Ince¹⁰¹, P. Ioannou⁹, M. Iodice^{135a}, K. Iordanidou⁹, V. Ippolito⁵⁷, A. Irls Quiles¹⁶⁸, C. Isaksson¹⁶⁷, M. Ishino⁶⁸, M. Ishitsuka¹⁵⁸, R. Ishmukhametov¹¹¹, C. Issever¹²⁰, S. Istin^{19a}, J.M. Iturbe Ponce⁸⁴, R. Iuppa^{134a,134b}, J. Ivarsson⁸¹, W. Iwanski³⁹, H. Iwasaki⁶⁶, J.M. Izen⁴¹, V. Izzo^{104a}, S. Jabbar³, B. Jackson¹²², M. Jackson⁷⁴, P. Jackson¹, M.R. Jaekel³⁰, V. Jain², K. Jakobs⁴⁸, S. Jakobsen³⁰, T. Jakoubek¹²⁷, J. Jakubek¹²⁸, D.O. Jamin¹⁵², D.K. Jana⁷⁹, E. Jansen⁷⁸, R. Jansky⁶², J. Janssen²¹, M. Janus¹⁷¹, G. Jarlskog⁸¹, N. Javadov^{65,b}, T. Javůrek⁴⁸, L. Jeanty¹⁵, J. Jejelava^{51a,r},

G.-Y. Jeng¹⁵¹, D. Jennens⁸⁸, P. Jenni^{48,s}, J. Jentzsch⁴³, C. Jeske¹⁷¹, S. Jézéquel⁵, H. Ji¹⁷⁴, J. Jia¹⁴⁹, Y. Jiang^{33b}, J. Jimenez Pena¹⁶⁸, S. Jin^{33a}, A. Jinaru^{26a}, O. Jinnouchi¹⁵⁸, M.D. Joergensen³⁶, P. Johansson¹⁴⁰, K.A. Johns⁷, K. Jon-And^{147a,147b}, G. Jones¹⁷¹, R.W.L. Jones⁷², T.J. Jones⁷⁴, J. Jongmanns^{58a}, P.M. Jorge^{126a,126b}, K.D. Joshi⁸⁴, J. Jovicevic¹⁴⁸, X. Ju¹⁷⁴, C.A. Jung⁴³, P. Jussel⁶², A. Juste Rozas^{12,o}, M. Kaci¹⁶⁸, A. Kaczmarzka³⁹, M. Kado¹¹⁷, H. Kagan¹¹¹, M. Kagan¹⁴⁴, S.J. Kahn⁸⁵, E. Kajomovitz⁴⁵, C.W. Kalderon¹²⁰, S. Kama⁴⁰, A. Kamenshchikov¹³⁰, N. Kanaya¹⁵⁶, M. Kaneda³⁰, S. Kaneti²⁸, V.A. Kantserov⁹⁸, J. Kanzaki⁶⁶, B. Kaplan¹¹⁰, A. Kapliy³¹, D. Kar⁵³, K. Karakostas¹⁰, A. Karamaoun³, N. Karastathis^{10,107}, M.J. Kareem⁵⁴, M. Karnevskiy⁸³, S.N. Karpov⁶⁵, Z.M. Karpova⁶⁵, K. Karthik¹¹⁰, V. Kartvelishvili⁷², A.N. Karyukhin¹³⁰, L. Kashif¹⁷⁴, R.D. Kass¹¹¹, A. Kastanas¹⁴, Y. Kataoka¹⁵⁶, A. Katre⁴⁹, J. Katzy⁴², K. Kawagoe⁷⁰, T. Kawamoto¹⁵⁶, G. Kawamura⁵⁴, S. Kazama¹⁵⁶, V.F. Kazanin^{109,c}, M.Y. Kazarinov⁶⁵, R. Keeler¹⁷⁰, R. Kehoe⁴⁰, J.S. Keller⁴², J.J. Kempster⁷⁷, H. Keoshkerian⁸⁴, O. Kepka¹²⁷, B.P. Kerševan⁷⁵, S. Kersten¹⁷⁶, R.A. Keyes⁸⁷, F. Khalil-zada¹¹, H. Khandanyan^{147a,147b}, A. Khanov¹¹⁴, A.G. Kharlamov^{109,c}, A. Khodinov⁹⁸, A. Khomich^{58a}, T.J. Khoo²⁸, V. Khovanskiy⁹⁷, E. Khramov⁶⁵, J. Khubua^{51b,t}, H.Y. Kim⁸, H. Kim^{147a,147b}, S.H. Kim¹⁶¹, N. Kimura¹⁵⁵, O.M. Kind¹⁶, B.T. King⁷⁴, M. King¹⁶⁸, R.S.B. King¹²⁰, S.B. King¹⁶⁹, J. Kirk¹³¹, A.E. Kiryunin¹⁰¹, T. Kishimoto⁶⁷, D. Kisielewska^{38a}, F. Kiss⁴⁸, K. Kiuchi¹⁶¹, E. Kladiva^{145b}, M.H. Klein³⁵, M. Klein⁷⁴, U. Klein⁷⁴, K. Kleinknecht⁸³, P. Klimek^{147a,147b}, A. Klimentov²⁵, R. Klingenberg⁴³, J.A. Klinger⁸⁴, T. Klioutchnikova³⁰, P.F. Klok¹⁰⁶, E.-E. Kluge^{58a}, P. Kluit¹⁰⁷, S. Kluth¹⁰¹, E. Kneringer⁶², E.B.F.G. Knoops⁸⁵, A. Knue⁵³, D. Kobayashi¹⁵⁸, T. Kobayashi¹⁵⁶, M. Kobel⁴⁴, M. Kocian¹⁴⁴, P. Kodys¹²⁹, T. Koffas²⁹, E. Koffeman¹⁰⁷, L.A. Kogan¹²⁰, S. Kohlmann¹⁷⁶, Z. Kohout¹²⁸, T. Kohriki⁶⁶, T. Koi¹⁴⁴, H. Kolanoski¹⁶, I. Koletsou⁵, A.A. Komar^{96,*}, Y. Komori¹⁵⁶, T. Kondo⁶⁶, N. Kondrashova⁴², K. Köneke⁴⁸, A.C. König¹⁰⁶, S. König⁸³, T. Kono^{66,u}, R. Konoplich^{110,v}, N. Konstantinidis⁷⁸, R. Kopeliansky¹⁵³, S. Koperny^{38a}, L. Köpke⁸³, A.K. Kopp⁴⁸, K. Korcyl³⁹, K. Kordas¹⁵⁵, A. Korn⁷⁸, A.A. Korol^{109,c}, I. Korolkov¹², E.V. Korolkova¹⁴⁰, O. Kortner¹⁰¹, S. Kortner¹⁰¹, T. Kosek¹²⁹, V.V. Kostyukhin²¹, V.M. Kotov⁶⁵, A. Kotwal⁴⁵, A. Kourkoumeli-Charalampidi¹⁵⁵, C. Kourkoumelis⁹, V. Kouskoura²⁵, A. Koutsman^{160a}, R. Kowalewski¹⁷⁰, T.Z. Kowalski^{38a}, W. Kozanecki¹³⁷, A.S. Kozhin¹³⁰, V.A. Kramarenko⁹⁹, G. Kramberger⁷⁵, D. Krasnopevtsev⁹⁸, M.W. Krasny⁸⁰, A. Krasznahorkay³⁰, J.K. Kraus²¹, A. Kravchenko²⁵, S. Kreiss¹¹⁰, M. Kretz^{58c}, J. Kretzschmar⁷⁴, K. Kreutzfeldt⁵², P. Krieger¹⁵⁹, K. Krizka³¹, K. Kroeninger⁴³, H. Kroha¹⁰¹, J. Kroll¹²², J. Kroseberg²¹, J. Krstic¹³, U. Kruchonak⁶⁵, H. Krüger²¹, N. Krumnack⁶⁴, Z.V. Krumshteyn⁶⁵, A. Kruse¹⁷⁴, M.C. Kruse⁴⁵, M. Kruskal²², T. Kubota⁸⁸, H. Kucuk⁷⁸, S. Kудay^{4b}, S. Kuehn⁴⁸, A. Kugel^{58c}, F. Kuger¹⁷⁵, A. Kuhl¹³⁸, T. Kuhl⁴², V. Kukhtin⁶⁵, Y. Kulchitsky⁹², S. Kuleshov^{32b}, M. Kuna^{133a,133b}, T. Kunigo⁶⁸, A. Kupco¹²⁷, H. Kurashige⁶⁷, Y.A. Kurochkin⁹², R. Kurumida⁶⁷, V. Kus¹²⁷, E.S. Kuwertz¹⁴⁸, M. Kuze¹⁵⁸, J. Kvita¹¹⁵, T. Kwan¹⁷⁰, D. Kyriazopoulos¹⁴⁰, A. La Rosa⁴⁹, J.L. La Rosa Navarro^{24d}, L. La Rotonda^{37a,37b}, C. Lacasta¹⁶⁸, F. Lacava^{133a,133b}, J. Lacey²⁹, H. Lacker¹⁶, D. Lacour⁸⁰, V.R. Lacuesta¹⁶⁸, E. Ladygin⁶⁵, R. Lafaye⁵, B. Laforge⁸⁰, T. Lagouri¹⁷⁷, S. Lai⁴⁸, L. Lambourne⁷⁸, S. Lammers⁶¹, C.L. Lampen⁷, W. Lampl⁷, E. Lançon¹³⁷, U. Landgraf⁴⁸, M.P.J. Landon⁷⁶, V.S. Lang^{58a}, A.J. Lankford¹⁶⁴, F. Lanni²⁵, K. Lantzsck³⁰, S. Laplace⁸⁰, C. Lapoire³⁰, J.F. Laporte¹³⁷, T. Lari^{91a}, F. Lasagni Manghi^{20a,20b}, M. Lassnig³⁰, P. Laurelli⁴⁷, W. Lavrijsen¹⁵, A.T. Law¹³⁸, P. Laycock⁷⁴, O. Le Dortz⁸⁰, E. Le Guirriec⁸⁵, E. Le Menedeu¹², T. LeCompte⁶, F. Ledroit-Guillon⁵⁵, C.A. Lee^{146b}, S.C. Lee¹⁵², L. Lee¹, G. Lefebvre⁸⁰, M. Lefebvre¹⁷⁰, F. Legger¹⁰⁰, C. Leggett¹⁵, A. Lehan⁷⁴, G. Lehmann Miotto³⁰, X. Lei⁷, W.A. Leight²⁹, A. Leisos^{155,w}, A.G. Leister¹⁷⁷, M.A.L. Leite^{24d}, R. Leitner¹²⁹, D. Lellouch¹⁷³, B. Lemmer⁵⁴, K.J.C. Leney⁷⁸, T. Lenz²¹, B. Lenzi³⁰, R. Leone⁷, S. Leone^{124a,124b}, C. Leonidopoulos⁴⁶, S. Leontsinis¹⁰, C. Leroy⁹⁵, C.G. Lester²⁸, M. Levchenko¹²³, J. Levêque⁵, D. Levin⁸⁹, L.J. Levinson¹⁷³, M. Levy¹⁸, A. Lewis¹²⁰, A.M. Leyko²¹, M. Leyton⁴¹, B. Li^{33b,x}, B. Li⁸⁵, H. Li¹⁴⁹, H.L. Li³¹, L. Li⁴⁵, L. Li^{33e}, S. Li⁴⁵, Y. Li^{33c,y}, Z. Liang¹³⁸, H. Liao³⁴, B. Liberti^{134a}, P. Lichard³⁰, K. Lie¹⁶⁶, J. Liebal²¹,

W. Liebig¹⁴, C. Limbach²¹, A. Limosani¹⁵¹, S.C. Lin^{152,z}, T.H. Lin⁸³, F. Linde¹⁰⁷, B.E. Lindquist¹⁴⁹,
 J.T. Linnemann⁹⁰, E. Lipeles¹²², A. Lipniacka¹⁴, M. Lisovyi⁴², T.M. Liss¹⁶⁶, D. Lissauer²⁵, A. Lister¹⁶⁹,
 A.M. Litke¹³⁸, B. Liu^{152,aa}, D. Liu¹⁵², J. Liu⁸⁵, J.B. Liu^{33b}, K. Liu⁸⁵, L. Liu⁸⁹, M. Liu⁴⁵, M. Liu^{33b},
 Y. Liu^{33b}, M. Livan^{121a,121b}, A. Lleres⁵⁵, J. Llorente Merino⁸², S.L. Lloyd⁷⁶, F. Lo Sterzo¹⁵²,
 E. Lobodzinska⁴², P. Loch⁷, W.S. Lockman¹³⁸, F.K. Loebinger⁸⁴, A.E. Loevschall-Jensen³⁶,
 A. Loginov¹⁷⁷, T. Lohse¹⁶, K. Lohwasser⁴², M. Lokajicek¹²⁷, B.A. Long²², J.D. Long⁸⁹, R.E. Long⁷²,
 K.A. Looper¹¹¹, L. Lopes^{126a}, D. Lopez Mateos⁵⁷, B. Lopez Paredes¹⁴⁰, I. Lopez Paz¹², J. Lorenz¹⁰⁰,
 N. Lorenzo Martinez⁶¹, M. Losada¹⁶³, P. Loscutoff¹⁵, P.J. Lösel¹⁰⁰, X. Lou^{33a}, A. Lounis¹¹⁷, J. Love⁶,
 P.A. Love⁷², N. Lu⁸⁹, H.J. Lubatti¹³⁹, C. Luci^{133a,133b}, A. Lucotte⁵⁵, F. Luehring⁶¹, W. Lukas⁶²,
 L. Luminari^{133a}, O. Lundberg^{147a,147b}, B. Lund-Jensen¹⁴⁸, M. Lungwitz⁸³, D. Lynn²⁵, R. Lysak¹²⁷,
 E. Lytken⁸¹, H. Ma²⁵, L.L. Ma^{33d}, G. Maccarrone⁴⁷, A. Macchiolo¹⁰¹, J. Machado Miguens^{126a,126b},
 D. Macina³⁰, D. Madaffari⁸⁵, R. Madar³⁴, H.J. Maddocks⁷², W.F. Mader⁴⁴, A. Madsen¹⁶⁷, T. Maeno²⁵,
 A. Maevskiy⁹⁹, E. Magradze⁵⁴, K. Mahboubi⁴⁸, J. Mahlstedt¹⁰⁷, S. Mahmoud⁷⁴, C. Maiani¹³⁷,
 C. Maidantchik^{24a}, A.A. Maier¹⁰¹, T. Maier¹⁰⁰, A. Maio^{126a,126b,126d}, S. Majewski¹¹⁶, Y. Makida⁶⁶,
 N. Makovec¹¹⁷, B. Malaescu⁸⁰, Pa. Malecki³⁹, V.P. Maleev¹²³, F. Malek⁵⁵, U. Mallik⁶³, D. Malon⁶,
 C. Malone¹⁴⁴, S. Maltezos¹⁰, V.M. Malyshev¹⁰⁹, S. Malyukov³⁰, J. Mamuzic⁴², B. Mandelli³⁰,
 L. Mandelli^{91a}, I. Mandić⁷⁵, R. Mandrysch⁶³, J. Maneira^{126a,126b}, A. Manfredini¹⁰¹,
 L. Manhaes de Andrade Filho^{24b}, J. Manjarres Ramos^{160b}, A. Mann¹⁰⁰, P.M. Manning¹³⁸,
 A. Manousakis-Katsikakis⁹, B. Mansoulie¹³⁷, R. Mantifel⁸⁷, M. Mantoani⁵⁴, L. Mapelli³⁰, L. March^{146c},
 G. Marchiori⁸⁰, M. Marcisovsky¹²⁷, C.P. Marino¹⁷⁰, M. Marjanovic¹³, F. Marroquim^{24a}, S.P. Marsden⁸⁴,
 Z. Marshall¹⁵, L.F. Marti¹⁷, S. Marti-Garcia¹⁶⁸, B. Martin⁹⁰, T.A. Martin¹⁷¹, V.J. Martin⁴⁶,
 B. Martin dit Latour¹⁴, H. Martinez¹³⁷, M. Martinez^{12,o}, S. Martin-Haugh¹³¹, A.C. Martyniuk⁷⁸,
 M. Marx¹³⁹, F. Marzano^{133a}, A. Marzin³⁰, L. Masetti⁸³, T. Mashimo¹⁵⁶, R. Mashinistov⁹⁶, J. Masik⁸⁴,
 A.L. Maslennikov^{109,c}, I. Massa^{20a,20b}, L. Massa^{20a,20b}, N. Massol⁵, P. Mastrandrea¹⁴⁹,
 A. Mastroberardino^{37a,37b}, T. Masubuchi¹⁵⁶, P. Mättig¹⁷⁶, J. Mattmann⁸³, J. Maurer^{26a}, S.J. Maxfield⁷⁴,
 D.A. Maximov^{109,c}, R. Mazini¹⁵², S.M. Mazza^{91a,91b}, L. Mazzaferro^{134a,134b}, G. Mc Goldrick¹⁵⁹,
 S.P. Mc Kee⁸⁹, A. McCarn⁸⁹, R.L. McCarthy¹⁴⁹, T.G. McCarthy²⁹, N.A. McCubbin¹³¹,
 K.W. McFarlane^{56,*}, J.A. Mcfayden⁷⁸, G. Mchedlize⁵⁴, S.J. McMahon¹³¹, R.A. McPherson^{170,k},
 J. Mechnich¹⁰⁷, M. Medinnis⁴², S. Meehan^{146a}, S. Mehlhase¹⁰⁰, A. Mehta⁷⁴, K. Meier^{58a},
 C. Meineck¹⁰⁰, B. Meirose⁴¹, C. Melachrinou³¹, B.R. Mellado Garcia^{146c}, F. Meloni¹⁷,
 A. Mengarelli^{20a,20b}, S. Menke¹⁰¹, E. Meoni¹⁶², K.M. Mercurio⁵⁷, S. Mergelmeyer²¹, N. Meric¹³⁷,
 P. Mermod⁴⁹, L. Merola^{104a,104b}, C. Meroni^{91a}, F.S. Merritt³¹, H. Merritt¹¹¹, A. Messina^{30,ab},
 J. Metcalfe²⁵, A.S. Mete¹⁶⁴, C. Meyer⁸³, C. Meyer¹²², J-P. Meyer¹³⁷, J. Meyer¹⁰⁷, R.P. Middleton¹³¹,
 S. Migas⁷⁴, S. Miglioranza^{165a,165c}, L. Mijović²¹, G. Mikenberg¹⁷³, M. Mikesikova¹²⁷, M. Mikuž⁷⁵,
 A. Milic³⁰, D.W. Miller³¹, C. Mills⁴⁶, A. Milov¹⁷³, D.A. Milstead^{147a,147b}, A.A. Minaenko¹³⁰,
 Y. Minami¹⁵⁶, I.A. Minashvili⁶⁵, A.I. Mincer¹¹⁰, B. Mindur^{38a}, M. Mineev⁶⁵, Y. Ming¹⁷⁴, L.M. Mir¹²,
 G. Mirabelli^{133a}, T. Mitani¹⁷², J. Mitrevski¹⁰⁰, V.A. Mitsou¹⁶⁸, A. Miucci⁴⁹, P.S. Miyagawa¹⁴⁰,
 J.U. Mjörnmark⁸¹, T. Moe^{147a,147b}, K. Mochizuki⁸⁵, S. Mohapatra³⁵, W. Mohr⁴⁸, S. Molander^{147a,147b},
 R. Moles-Valls¹⁶⁸, K. Mönig⁴², C. Monini⁵⁵, J. Monk³⁶, E. Monnier⁸⁵, J. Montejo Berlingen¹²,
 F. Monticelli⁷¹, S. Monzani^{133a,133b}, R.W. Moore³, N. Morange¹¹⁷, D. Moreno¹⁶³, M. Moreno Llácer⁵⁴,
 P. Morettini^{50a}, M. Morgenstern⁴⁴, M. Morii⁵⁷, V. Morisbak¹¹⁹, S. Moritz⁸³, A.K. Morley¹⁴⁸,
 G. Mornacchi³⁰, J.D. Morris⁷⁶, A. Morton⁵³, L. Morvaj¹⁰³, M. Mosidze^{51b}, J. Moss¹¹¹, K. Motohashi¹⁵⁸,
 R. Mount¹⁴⁴, E. Mountricha²⁵, S.V. Mouraviev^{96,*}, E.J.W. Moyse⁸⁶, S. Muanza⁸⁵, R.D. Mudd¹⁸,
 F. Mueller¹⁰¹, J. Mueller¹²⁵, K. Mueller²¹, R.S.P. Mueller¹⁰⁰, T. Mueller²⁸, D. Muenstermann⁴⁹,
 P. Mullen⁵³, Y. Munwes¹⁵⁴, J.A. Murillo Quijada¹⁸, W.J. Murray^{171,131}, H. Musheghyan⁵⁴, E. Musto¹⁵³,
 A.G. Myagkov^{130,ac}, M. Myska¹²⁸, O. Nackenhorst⁵⁴, J. Nadal⁵⁴, K. Nagai¹²⁰, R. Nagai¹⁵⁸, Y. Nagai⁸⁵,
 K. Nagano⁶⁶, A. Nagarkar¹¹¹, Y. Nagasaka⁵⁹, K. Nagata¹⁶¹, M. Nagel¹⁰¹, E. Nagy⁸⁵, A.M. Nairz³⁰,

Y. Nakahama³⁰, K. Nakamura⁶⁶, T. Nakamura¹⁵⁶, I. Nakano¹¹², H. Namasivayam⁴¹, G. Nanava²¹,
 R.F. Naranjo Garcia⁴², R. Narayan^{58b}, T. Nattermann²¹, T. Naumann⁴², G. Navarro¹⁶³, R. Nayyar⁷,
 H.A. Neal⁸⁹, P.Yu. Nechaeva⁹⁶, T.J. Neep⁸⁴, P.D. Nef¹⁴⁴, A. Negri^{121a,121b}, M. Negrini^{20a},
 S. Nektarijevic¹⁰⁶, C. Nellist¹¹⁷, A. Nelson¹⁶⁴, S. Nemecek¹²⁷, P. Nemethy¹¹⁰, A.A. Nepomuceno^{24a},
 M. Nessi^{30,ad}, M.S. Neubauer¹⁶⁶, M. Neumann¹⁷⁶, R.M. Neves¹¹⁰, P. Nevski²⁵, P.R. Newman¹⁸,
 D.H. Nguyen⁶, R.B. Nickerson¹²⁰, R. Nicolaidou¹³⁷, B. Nicquevert³⁰, J. Nielsen¹³⁸, N. Nikiforou³⁵,
 A. Nikiforov¹⁶, V. Nikolaenko^{130,ac}, I. Nikolic-Audit⁸⁰, K. Nikolopoulos¹⁸, P. Nilsson²⁵,
 Y. Ninomiya¹⁵⁶, A. Nisati^{133a}, R. Nisius¹⁰¹, T. Nobe¹⁵⁸, M. Nomachi¹¹⁸, I. Nomidis²⁹, S. Norberg¹¹³,
 M. Nordberg³⁰, O. Novgorodova⁴⁴, S. Nowak¹⁰¹, M. Nozaki⁶⁶, L. Nozka¹¹⁵, K. Ntekas¹⁰,
 G. Nunes Hanninger⁸⁸, T. Nunnemann¹⁰⁰, E. Nurse⁷⁸, F. Nuti⁸⁸, B.J. O'Brien⁴⁶, F. O'grady⁷,
 D.C. O'Neil¹⁴³, V. O'Shea⁵³, F.G. Oakham^{29,d}, H. Oberlack¹⁰¹, T. Obermann²¹, J. Ocariz⁸⁰, A. Ochi⁶⁷,
 I. Ochoa⁷⁸, S. Oda⁷⁰, S. Odaka⁶⁶, H. Ogren⁶¹, A. Oh⁸⁴, S.H. Oh⁴⁵, C.C. Ohm¹⁵, H. Ohman¹⁶⁷,
 H. Oide³⁰, W. Okamura¹¹⁸, H. Okawa¹⁶¹, Y. Okumura³¹, T. Okuyama¹⁵⁶, A. Olariu^{26a},
 A.G. Olchevski⁶⁵, S.A. Olivares Pino⁴⁶, D. Oliveira Damazio²⁵, E. Oliver Garcia¹⁶⁸, A. Olszewski³⁹,
 J. Olszowska³⁹, A. Onofre^{126a,126e}, P.U.E. Onyisi^{31,q}, C.J. Oram^{160a}, M.J. Oreglia³¹, Y. Oren¹⁵⁴,
 D. Orestano^{135a,135b}, N. Orlando¹⁵⁵, C. Oropeza Barrera⁵³, R.S. Orr¹⁵⁹, B. Osculati^{50a,50b}, R. Ospanov⁸⁴,
 G. Otero y Garzon²⁷, H. Otono⁷⁰, M. Ouchrif^{136d}, E.A. Ouellette¹⁷⁰, F. Ould-Saada¹¹⁹, A. Ouraou¹³⁷,
 K.P. Oussoren¹⁰⁷, Q. Ouyang^{33a}, A. Ovcharova¹⁵, M. Owen⁵³, R.E. Owen¹⁸, V.E. Ozcan^{19a}, N. Ozturk⁸,
 K. Pachal¹²⁰, A. Pacheco Pages¹², C. Padilla Aranda¹², M. Pagáčová⁴⁸, S. Pagan Griso¹⁵, E. Paganis¹⁴⁰,
 C. Pahl¹⁰¹, F. Paige²⁵, P. Pais⁸⁶, K. Pajchel¹¹⁹, G. Palacino^{160b}, S. Palestini³⁰, M. Palka^{38b}, D. Pallin³⁴,
 A. Palma^{126a,126b}, Y.B. Pan¹⁷⁴, E. Panagiotopoulou¹⁰, C.E. Pandini⁸⁰, J.G. Panduro Vazquez⁷⁷,
 P. Pani^{147a,147b}, N. Panikashvili⁸⁹, S. Panitkin²⁵, D. Pantea^{26a}, L. Paolozzi^{134a,134b},
 Th.D. Papadopoulou¹⁰, K. Papageorgiou¹⁵⁵, A. Paramonov⁶, D. Paredes Hernandez¹⁵⁵, M.A. Parker²⁸,
 K.A. Parker¹⁴⁰, F. Parodi^{50a,50b}, J.A. Parsons³⁵, U. Parzefall⁴⁸, E. Pasqualucci^{133a}, S. Passaggio^{50a},
 F. Pastore^{135a,135b,*}, Fr. Pastore⁷⁷, G. Pásztor²⁹, S. Patariaia¹⁷⁶, N.D. Patel¹⁵¹, J.R. Pater⁸⁴, T. Pauly³⁰,
 J. Pearce¹⁷⁰, L.E. Pedersen³⁶, M. Pedersen¹¹⁹, S. Pedraza Lopez¹⁶⁸, R. Pedro^{126a,126b},
 S.V. Peleganchuk^{109,c}, D. Pelikan¹⁶⁷, H. Peng^{33b}, B. Penning³¹, J. Penwell⁶¹, D.V. Perepelitsa²⁵,
 E. Perez Codina^{160a}, M.T. Pérez García-Estañ¹⁶⁸, L. Perini^{91a,91b}, H. Pernegger³⁰, S. Perrella^{104a,104b},
 R. Peschke⁴², V.D. Peshekhonov⁶⁵, K. Peters³⁰, R.F.Y. Peters⁸⁴, B.A. Petersen³⁰, T.C. Petersen³⁶,
 E. Petit⁴², A. Petridis^{147a,147b}, C. Petridou¹⁵⁵, E. Petrolo^{133a}, F. Petrucci^{135a,135b}, N.E. Pettersson¹⁵⁸,
 R. Pezoa^{32b}, P.W. Phillips¹³¹, G. Piacquadio¹⁴⁴, E. Pianori¹⁷¹, A. Picazio⁴⁹, E. Piccaro⁷⁶,
 M. Piccinini^{20a,20b}, M.A. Pickering¹²⁰, R. Piegaia²⁷, D.T. Pignotti¹¹¹, J.E. Pilcher³¹, A.D. Pilkington⁷⁸,
 J. Pina^{126a,126b,126d}, M. Pinamonti^{165a,165c,ae}, J.L. Pinfold³, A. Pingel³⁶, B. Pinto^{126a}, S. Pires⁸⁰,
 M. Pitt¹⁷³, C. Pizio^{91a,91b}, L. Plazak^{145a}, M.-A. Pleier²⁵, V. Pleskot¹²⁹, E. Plotnikova⁶⁵,
 P. Plucinski^{147a,147b}, D. Pluth⁶⁴, R. Poettgen⁸³, L. Poggioli¹¹⁷, D. Pohl²¹, G. Polesello^{121a},
 A. Policicchio^{37a,37b}, R. Polifka¹⁵⁹, A. Polini^{20a}, C.S. Pollard⁵³, V. Polychronakos²⁵, K. Pommès³⁰,
 L. Pontecorvo^{133a}, B.G. Pope⁹⁰, G.A. Popeneciu^{26b}, D.S. Popovic¹³, A. Poppleton³⁰, S. Pospisil¹²⁸,
 K. Potamianos¹⁵, I.N. Potrap⁶⁵, C.J. Potter¹⁵⁰, C.T. Potter¹¹⁶, G. Poulard³⁰, J. Poveda³⁰,
 V. Pozdnyakov⁶⁵, P. Pralavorio⁸⁵, A. Pranko¹⁵, S. Prasad³⁰, S. Prell⁶⁴, D. Price⁸⁴, J. Price⁷⁴, L.E. Price⁶,
 M. Primavera^{73a}, S. Prince⁸⁷, M. Proissl⁴⁶, K. Prokofiev^{60c}, F. Prokoshin^{32b}, E. Protopapadaki¹³⁷,
 S. Protopopescu²⁵, J. Proudfoot⁶, M. Przybycien^{38a}, E. Ptacek¹¹⁶, D. Puddu^{135a,135b}, E. Pueschel⁸⁶,
 D. Puldon¹⁴⁹, M. Purohit^{25,af}, P. Puzo¹¹⁷, J. Qian⁸⁹, G. Qin⁵³, Y. Qin⁸⁴, A. Quadt⁵⁴, D.R. Quarrie¹⁵,
 W.B. Quayle^{165a,165b}, M. Queitsch-Maitland⁸⁴, D. Quilty⁵³, V. Radeka²⁵, V. Radescu⁴²,
 S.K. Radhakrishnan¹⁴⁹, P. Radloff¹¹⁶, P. Rados⁸⁸, F. Ragusa^{91a,91b}, G. Rahal¹⁷⁹, S. Rajagopalan²⁵,
 M. Rammensee³⁰, C. Rangel-Smith¹⁶⁷, F. Rauscher¹⁰⁰, S. Rave⁸³, T.C. Rave⁴⁸, T. Ravenscroft⁵³,
 M. Raymond³⁰, A.L. Read¹¹⁹, N.P. Readioff⁷⁴, D.M. Rebuffi^{121a,121b}, A. Redelbach¹⁷⁵, G. Redlinger²⁵,
 R. Reece¹³⁸, K. Reeves⁴¹, L. Rehnisch¹⁶, H. Reisin²⁷, M. Relich¹⁶⁴, C. Rembser³⁰, H. Ren^{33a},

A. Renaud¹¹⁷, M. Rescigno^{133a}, S. Resconi^{91a}, O.L. Rezanova^{109,c}, P. Reznicek¹²⁹, R. Rezvani⁹⁵,
 R. Richter¹⁰¹, E. Richter-Was^{38b}, M. Ridel⁸⁰, P. Rieck¹⁶, C.J. Riegel¹⁷⁶, J. Rieger⁵⁴, M. Rijssenbeek¹⁴⁹,
 A. Rimoldi^{121a,121b}, L. Rinaldi^{20a}, E. Ritsch⁶², I. Riu¹², F. Rizatdinova¹¹⁴, E. Rizvi⁷⁶, S.H. Robertson^{87,k},
 A. Robichaud-Veronneau⁸⁷, D. Robinson²⁸, J.E.M. Robinson⁸⁴, A. Robson⁵³, C. Roda^{124a,124b},
 L. Rodrigues³⁰, S. Roe³⁰, O. Røhne¹¹⁹, S. Rolli¹⁶², A. Romaniouk⁹⁸, M. Romano^{20a,20b},
 S.M. Romano Saez³⁴, E. Romero Adam¹⁶⁸, N. Rompotis¹³⁹, M. Ronzani⁴⁸, L. Roos⁸⁰, E. Ros¹⁶⁸,
 S. Rosati^{133a}, K. Rosbach⁴⁸, P. Rose¹³⁸, P.L. Rosendahl¹⁴, O. Rosenthal¹⁴², V. Rossetti^{147a,147b},
 E. Rossi^{104a,104b}, L.P. Rossi^{50a}, R. Rosten¹³⁹, M. Rotaru^{26a}, I. Roth¹⁷³, J. Rothberg¹³⁹, D. Rousseau¹¹⁷,
 C.R. Royon¹³⁷, A. Rozanov⁸⁵, Y. Rozen¹⁵³, X. Ruan^{146c}, F. Rubbo¹², I. Rubinsky⁴², V.I. Rud⁹⁹,
 C. Rudolph⁴⁴, M.S. Rudolph¹⁵⁹, F. Rühr⁴⁸, A. Ruiz-Martinez³⁰, Z. Rurikova⁴⁸, N.A. Rusakovich⁶⁵,
 A. Ruschke¹⁰⁰, H.L. Russell¹³⁹, J.P. Rutherford⁷, N. Ruthmann⁴⁸, Y.F. Ryabov¹²³, M. Rybar¹²⁹,
 G. Rybkin¹¹⁷, N.C. Ryder¹²⁰, A.F. Saavedra¹⁵¹, G. Sabato¹⁰⁷, S. Sacerdoti²⁷, A. Saddique³,
 H.F.W. Sadrozinski¹³⁸, R. Sadykov⁶⁵, F. Safai Tehrani^{133a}, M. Saimpert¹³⁷, H. Sakamoto¹⁵⁶,
 Y. Sakurai¹⁷², G. Salamanna^{135a,135b}, A. Salamon^{134a}, M. Saleem¹¹³, D. Salek¹⁰⁷,
 P.H. Sales De Bruin¹³⁹, D. Salihagic¹⁰¹, A. Salnikov¹⁴⁴, J. Salt¹⁶⁸, D. Salvatore^{37a,37b}, F. Salvatore¹⁵⁰,
 A. Salvucci¹⁰⁶, A. Salzburger³⁰, D. Sampsonidis¹⁵⁵, A. Sanchez^{104a,104b}, J. Sánchez¹⁶⁸,
 V. Sanchez Martinez¹⁶⁸, H. Sandaker¹⁴, R.L. Sandbach⁷⁶, H.G. Sander⁸³, M.P. Sanders¹⁰⁰,
 M. Sandhoff¹⁷⁶, C. Sandoval¹⁶³, R. Sandstroem¹⁰¹, D.P.C. Sankey¹³¹, A. Sansoni⁴⁷, C. Santoni³⁴,
 R. Santonico^{134a,134b}, H. Santos^{126a}, I. Santoyo Castillo¹⁵⁰, K. Sapp¹²⁵, A. Saponov⁶⁵,
 J.G. Saraiva^{126a,126d}, B. Sarrazin²¹, O. Sasaki⁶⁶, Y. Sasaki¹⁵⁶, K. Sato¹⁶¹, G. Sauvage^{5,*}, E. Sauvan⁵,
 G. Savage⁷⁷, P. Savard^{159,d}, C. Sawyer¹²⁰, L. Sawyer^{79,n}, D.H. Saxon⁵³, J. Saxon³¹, C. Sbarra^{20a},
 A. Sbrizzi^{20a,20b}, T. Scanlon⁷⁸, D.A. Scannicchio¹⁶⁴, M. Scarcella¹⁵¹, V. Scarfone^{37a,37b},
 J. Schaarschmidt¹⁷³, P. Schacht¹⁰¹, D. Schaefer³⁰, R. Schaefer⁴², J. Schaeffer⁸³, S. Schaepe²¹,
 S. Schaetzel^{58b}, U. Schäfer⁸³, A.C. Schaffer¹¹⁷, D. Schaile¹⁰⁰, R.D. Schamberger¹⁴⁹, V. Scharf^{58a},
 V.A. Schegelsky¹²³, D. Scheirich¹²⁹, M. Schernau¹⁶⁴, C. Schiavi^{50a,50b}, C. Schillo⁴⁸, M. Schioppa^{37a,37b},
 S. Schlenker³⁰, E. Schmidt⁴⁸, K. Schmieden³⁰, C. Schmitt⁸³, S. Schmitt^{58b}, B. Schneider^{160a},
 Y.J. Schnellbach⁷⁴, U. Schnoor⁴⁴, L. Schoeffel¹³⁷, A. Schoening^{58b}, B.D. Schoenrock⁹⁰,
 A.L.S. Schorlemmer⁵⁴, M. Schott⁸³, D. Schouten^{160a}, J. Schovancova⁸, S. Schramm¹⁵⁹, M. Schreyer¹⁷⁵,
 C. Schroeder⁸³, N. Schuh⁸³, M.J. Schultens²¹, H.-C. Schultz-Coulon^{58a}, H. Schulz¹⁶, M. Schumacher⁴⁸,
 B.A. Schumm¹³⁸, Ph. Schune¹³⁷, C. Schwanenberger⁸⁴, A. Schwartzman¹⁴⁴, T.A. Schwarz⁸⁹,
 Ph. Schwegler¹⁰¹, Ph. Schwemling¹³⁷, R. Schwiendorfer⁹⁰, J. Schwindling¹³⁷, T. Schwindt²¹,
 M. Schwoerer⁵, F.G. Sciacca¹⁷, E. Scifo¹¹⁷, G. Sciolla²³, F. Scuri^{124a,124b}, F. Scutti²¹, J. Searcy⁸⁹,
 G. Sedov⁴², E. Sedykh¹²³, P. Seema²¹, S.C. Seidel¹⁰⁵, A. Seiden¹³⁸, F. Seifert¹²⁸, J.M. Seixas^{24a},
 G. Sekhniaidze^{104a}, S.J. Sekula⁴⁰, K.E. Selbach⁴⁶, D.M. Seliverstov^{123,*}, N. Semprini-Cesari^{20a,20b},
 C. Serfon³⁰, L. Serin¹¹⁷, L. Serkin⁵⁴, T. Serre⁸⁵, R. Seuster^{160a}, H. Severini¹¹³, T. Sfiligoi⁷⁵, F. Sforza¹⁰¹,
 A. Sfyrla³⁰, E. Shabalina⁵⁴, M. Shamim¹¹⁶, L.Y. Shan^{33a}, R. Shang¹⁶⁶, J.T. Shank²², M. Shapiro¹⁵,
 P.B. Shatalov⁹⁷, K. Shaw^{165a,165b}, A. Shcherbakova^{147a,147b}, C.Y. Shehu¹⁵⁰, P. Sherwood⁷⁸, L. Shi^{152,ag},
 S. Shimizu⁶⁷, C.O. Shimmin¹⁶⁴, M. Shimojima¹⁰², M. Shiyakova⁶⁵, A. Shmeleva⁹⁶, D. Shoaleh Saadi⁹⁵,
 M.J. Shochet³¹, S. Shojaii^{91a,91b}, S. Shrestha¹¹¹, E. Shulga⁹⁸, M.A. Shupe⁷, S. Shushkevich⁴²,
 P. Sicho¹²⁷, O. Sidiropoulou¹⁷⁵, D. Sidorov¹¹⁴, A. Sidoti^{20a,20b}, F. Siegert⁴⁴, Dj. Sijacki¹³,
 J. Silva^{126a,126d}, Y. Silver¹⁵⁴, D. Silverstein¹⁴⁴, S.B. Silverstein^{147a}, V. Simak¹²⁸, O. Simard⁵,
 Lj. Simic¹³, S. Simion¹¹⁷, E. Simioni⁸³, B. Simmons⁷⁸, D. Simon³⁴, R. Simoniello^{91a,91b}, P. Sinervo¹⁵⁹,
 N.B. Sinev¹¹⁶, G. Siragusa¹⁷⁵, A. Sircar⁷⁹, A.N. Sisakyan^{65,*}, S.Yu. Sivoklokov⁹⁹, J. Sjölin^{147a,147b},
 T.B. Sjørnsen¹⁴, M.B. Skinner⁷², H.P. Skottowe⁵⁷, P. Skubic¹¹³, M. Slater¹⁸, T. Slavicek¹²⁸,
 M. Slawinska¹⁰⁷, K. Sliwa¹⁶², V. Smakhtin¹⁷³, B.H. Smart⁴⁶, L. Smestad¹⁴, S.Yu. Smirnov⁹⁸,
 Y. Smirnov⁹⁸, L.N. Smirnova^{99,ah}, O. Smirnova⁸¹, K.M. Smith⁵³, M.N.K. Smith³⁵, M. Smizanska⁷²,
 K. Smolek¹²⁸, A.A. Snesarev⁹⁶, G. Snidero⁷⁶, S. Snyder²⁵, R. Sobie^{170,k}, F. Socher⁴⁴, A. Soffer¹⁵⁴,

D.A. Soh^{152,ag}, C.A. Solans³⁰, M. Solar¹²⁸, J. Solc¹²⁸, E.Yu. Soldatov⁹⁸, U. Soldevila¹⁶⁸,
 A.A. Solodkov¹³⁰, A. Soloshenko⁶⁵, O.V. Solovyanov¹³⁰, V. Solovyev¹²³, P. Sommer⁴⁸, H.Y. Song^{33b},
 N. Soni¹, A. Sood¹⁵, A. Sopczak¹²⁸, B. Sopko¹²⁸, V. Sopko¹²⁸, V. Sorin¹², D. Sosa^{58b}, M. Sosebee⁸,
 C.L. Sotiropoulou¹⁵⁵, R. Soualah^{165a,165c}, P. Soueid⁹⁵, A.M. Soukharev^{109,c}, D. South⁴²,
 S. Spagnolo^{73a,73b}, F. Spanò⁷⁷, W.R. Spearman⁵⁷, F. Spettel¹⁰¹, R. Spighi^{20a}, G. Spigo³⁰, L.A. Spiller⁸⁸,
 M. Spousta¹²⁹, T. Spreitzer¹⁵⁹, R.D. St. Denis^{53,*}, S. Staerz⁴⁴, J. Stahlman¹²², R. Stamen^{58a}, S. Stamm¹⁶,
 E. Stanecka³⁹, C. Stanescu^{135a}, M. Stanescu-Bellu⁴², M.M. Stanitzki⁴², S. Stapnes¹¹⁹,
 E.A. Starchenko¹³⁰, J. Stark⁵⁵, P. Staroba¹²⁷, P. Starovoitov⁴², R. Staszewski³⁹, P. Stavina^{145a,*},
 P. Steinberg²⁵, B. Stelzer¹⁴³, H.J. Stelzer³⁰, O. Stelzer-Chilton^{160a}, H. Stenzel⁵², S. Stern¹⁰¹,
 G.A. Stewart⁵³, J.A. Stillings²¹, M.C. Stockton⁸⁷, M. Stoebe⁸⁷, G. Stoica^{26a}, P. Stolte⁵⁴, S. Stonjek¹⁰¹,
 A.R. Stradling⁸, A. Straessner⁴⁴, M.E. Stramaglia¹⁷, J. Strandberg¹⁴⁸, S. Strandberg^{147a,147b},
 A. Strandlie¹¹⁹, E. Strauss¹⁴⁴, M. Strauss¹¹³, P. Strizenc^{145b}, R. Ströhmer¹⁷⁵, D.M. Strom¹¹⁶,
 R. Stroynowski⁴⁰, A. Strubig¹⁰⁶, S.A. Stucci¹⁷, B. Stugu¹⁴, N.A. Styles⁴², D. Su¹⁴⁴, J. Su¹²⁵,
 R. Subramaniam⁷⁹, A. Succurro¹², Y. Sugaya¹¹⁸, C. Suhr¹⁰⁸, M. Suk¹²⁸, V.V. Sulim⁹⁶, S. Sultansoy^{4c},
 T. Sumida⁶⁸, S. Sun⁵⁷, X. Sun^{33a}, J.E. Sundermann⁴⁸, K. Suruliz¹⁵⁰, G. Susinno^{37a,37b}, M.R. Sutton¹⁵⁰,
 Y. Suzuki⁶⁶, M. Svatos¹²⁷, S. Swedish¹⁶⁹, M. Swiatlowski¹⁴⁴, I. Sykora^{145a}, T. Sykora¹²⁹, D. Ta⁹⁰,
 C. Taccini^{135a,135b}, K. Tackmann⁴², J. Taenzer¹⁵⁹, A. Taffard¹⁶⁴, R. Tafirout^{160a}, N. Taiblum¹⁵⁴,
 H. Takai²⁵, R. Takashima⁶⁹, H. Takeda⁶⁷, T. Takeshita¹⁴¹, Y. Takubo⁶⁶, M. Talby⁸⁵, A.A. Talyshev^{109,c},
 J.Y.C. Tam¹⁷⁵, K.G. Tan⁸⁸, J. Tanaka¹⁵⁶, R. Tanaka¹¹⁷, S. Tanaka¹³², S. Tanaka⁶⁶, A.J. Tanasijczuk¹⁴³,
 B.B. Tannenwald¹¹¹, N. Tannoury²¹, S. Tapprogge⁸³, S. Tarem¹⁵³, F. Tarrade²⁹, G.F. Tartarelli^{91a},
 P. Tas¹²⁹, M. Tasevsky¹²⁷, T. Tashiro⁶⁸, E. Tassi^{37a,37b}, A. Tavares Delgado^{126a,126b}, Y. Tayalati^{136d},
 F.E. Taylor⁹⁴, G.N. Taylor⁸⁸, W. Taylor^{160b}, F.A. Teischinger³⁰, M. Teixeira Dias Castanheira⁷⁶,
 P. Teixeira-Dias⁷⁷, K.K. Temming⁴⁸, H. Ten Kate³⁰, P.K. Teng¹⁵², J.J. Teoh¹¹⁸, F. Tepel¹⁷⁶, S. Terada⁶⁶,
 K. Terashi¹⁵⁶, J. Terron⁸², S. Terzo¹⁰¹, M. Testa⁴⁷, R.J. Teuscher^{159,k}, J. Therhaag²¹,
 T. Thevenaux-Pelzer³⁴, J.P. Thomas¹⁸, J. Thomas-Wilsker⁷⁷, E.N. Thompson³⁵, P.D. Thompson¹⁸,
 R.J. Thompson⁸⁴, A.S. Thompson⁵³, L.A. Thomsen³⁶, E. Thomson¹²², M. Thomson²⁸, W.M. Thong⁸⁸,
 R.P. Thun^{89,*}, F. Tian³⁵, M.J. Tibbetts¹⁵, R.E. Ticse Torres⁸⁵, V.O. Tikhomirov^{96,ai}, Yu.A. Tikhonov^{109,c},
 S. Timoshenko⁹⁸, E. Tiouchichine⁸⁵, P. Tipton¹⁷⁷, S. Tisserant⁸⁵, T. Todorov^{5,*}, S. Todorova-Nova¹²⁹,
 J. Tojo⁷⁰, S. Tokár^{145a}, K. Tokushuku⁶⁶, K. Tollefson⁹⁰, E. Tolley⁵⁷, L. Tomlinson⁸⁴, M. Tomoto¹⁰³,
 L. Tompkins^{144,aj}, K. Toms¹⁰⁵, N.D. Topilin⁶⁵, E. Torrence¹¹⁶, H. Torres¹⁴³, E. Torró Pastor¹⁶⁸,
 J. Toth^{85,ak}, F. Touchard⁸⁵, D.R. Tovey¹⁴⁰, H.L. Tran¹¹⁷, T. Trefzger¹⁷⁵, L. Tremblet³⁰, A. Tricoli³⁰,
 I.M. Trigger^{160a}, S. Trincaz-Duvoid⁸⁰, M.F. Tripiana¹², W. Trischuk¹⁵⁹, B. Trocme⁵⁵, C. Troncon^{91a},
 M. Trottier-McDonald¹⁵, M. Trovatelli^{135a,135b}, P. True⁹⁰, M. Trzebinski³⁹, A. Trzupek³⁹,
 C. Tsarouchas³⁰, J.C.-L. Tseng¹²⁰, P.V. Tsiarehka⁹², D. Tsionou¹⁵⁵, G. Tsipolitis¹⁰, N. Tsirintanis⁹,
 S. Tsiskaridze¹², V. Tsiskaridze⁴⁸, E.G. Tskhadadze^{51a}, I.I. Tsukerman⁹⁷, V. Tsulaia¹⁵, S. Tsuno⁶⁶,
 D. Tsybychev¹⁴⁹, A. Tudorache^{26a}, V. Tudorache^{26a}, A.N. Tuna¹²², S.A. Tupputi^{20a,20b},
 S. Turchikhin^{99,ah}, D. Turecek¹²⁸, R. Turra^{91a,91b}, A.J. Turvey⁴⁰, P.M. Tuts³⁵, A. Tykhonov⁴⁹,
 M. Tylmad^{147a,147b}, M. Tyndel¹³¹, I. Ueda¹⁵⁶, R. Ueno²⁹, M. Ughetto⁸⁵, M. Ugland¹⁴, M. Uhlenbrock²¹,
 F. Ukegawa¹⁶¹, G. Unal³⁰, A. Undrus²⁵, G. Unel¹⁶⁴, F.C. Ungaro⁴⁸, Y. Unno⁶⁶, C. Unverdorben¹⁰⁰,
 J. Urban^{145b}, P. Urquijo⁸⁸, P. Urrejola⁸³, G. Usai⁸, A. Usanova⁶², L. Vacavant⁸⁵, V. Vacek¹²⁸,
 B. Vachon⁸⁷, N. Valencic¹⁰⁷, S. Valentini^{20a,20b}, A. Valero¹⁶⁸, L. Valery¹², S. Valkar¹²⁹,
 E. Valladolid Gallego¹⁶⁸, S. Vallecorsa⁴⁹, J.A. Valls Ferrer¹⁶⁸, W. Van Den Wollenberg¹⁰⁷,
 P.C. Van Der Deijl¹⁰⁷, R. van der Geer¹⁰⁷, H. van der Graaf¹⁰⁷, R. Van Der Leeuw¹⁰⁷, N. van Eldik³⁰,
 P. van Gemmeren⁶, J. Van Nieuwkoop¹⁴³, I. van Vulpen¹⁰⁷, M.C. van Woerden³⁰, M. Vanadia^{133a,133b},
 W. Vandelli³⁰, R. Vanguri¹²², A. Vaniachine⁶, F. Vannucci⁸⁰, G. Vardanyan¹⁷⁸, R. Vari^{133a}, E.W. Varnes⁷,
 T. Varol⁴⁰, D. Varouchas⁸⁰, A. Vartapetian⁸, K.E. Varvell¹⁵¹, F. Vazeille³⁴, T. Vazquez Schroeder⁵⁴,
 J. Veatch⁷, F. Veloso^{126a,126c}, T. Velz²¹, S. Veneziano^{133a}, A. Ventura^{73a,73b}, D. Ventura⁸⁶, M. Venturi¹⁷⁰,

N. Venturi¹⁵⁹, A. Venturini²³, V. Vercesi^{121a}, M. Verducci^{133a,133b}, W. Verkerke¹⁰⁷, J.C. Vermeulen¹⁰⁷, A. Vest⁴⁴, M.C. Vetterli^{143,d}, O. Viazlo⁸¹, I. Vichou¹⁶⁶, T. Vickey^{146c,al}, O.E. Vickey Boeriu^{146c}, G.H.A. Viehhauser¹²⁰, S. Viel¹⁵, R. Vigne³⁰, M. Villa^{20a,20b}, M. Villaplana Perez^{91a,91b}, E. Vilucchi⁴⁷, M.G. Vincter²⁹, V.B. Vinogradov⁶⁵, J. Virzi¹⁵, I. Vivarelli¹⁵⁰, F. Vives Vaque³, S. Vlachos¹⁰, D. Vladoiu¹⁰⁰, M. Vlasak¹²⁸, M. Vogel^{32a}, P. Vokac¹²⁸, G. Volpi^{124a,124b}, M. Volpi⁸⁸, H. von der Schmitt¹⁰¹, H. von Radziewski⁴⁸, E. von Toerne²¹, V. Vorobel¹²⁹, K. Vorobev⁹⁸, M. Vos¹⁶⁸, R. Voss³⁰, J.H. Vossebeld⁷⁴, N. Vranjes¹³, M. Vranjes Milosavljevic¹³, V. Vrba¹²⁷, M. Vreeswijk¹⁰⁷, R. Vuillermet³⁰, I. Vukotic³¹, Z. Vykydal¹²⁸, P. Wagner²¹, W. Wagner¹⁷⁶, H. Wahlberg⁷¹, S. Wahrenmund⁴⁴, J. Wakabayashi¹⁰³, J. Walder⁷², R. Walker¹⁰⁰, W. Walkowiak¹⁴², C. Wang^{33c}, F. Wang¹⁷⁴, H. Wang¹⁵, H. Wang⁴⁰, J. Wang⁴², J. Wang^{33a}, K. Wang⁸⁷, R. Wang¹⁰⁵, S.M. Wang¹⁵², T. Wang²¹, X. Wang¹⁷⁷, C. Wanotayaroj¹¹⁶, A. Warburton⁸⁷, C.P. Ward²⁸, D.R. Wardrope⁷⁸, M. Warsinsky⁴⁸, A. Washbrook⁴⁶, C. Wasicki⁴², P.M. Watkins¹⁸, A.T. Watson¹⁸, I.J. Watson¹⁵¹, M.F. Watson¹⁸, G. Watts¹³⁹, S. Watts⁸⁴, B.M. Waugh⁷⁸, S. Webb⁸⁴, M.S. Weber¹⁷, S.W. Weber¹⁷⁵, J.S. Webster³¹, A.R. Weidberg¹²⁰, B. Weinert⁶¹, J. Weingarten⁵⁴, C. Weiser⁴⁸, H. Weits¹⁰⁷, P.S. Wells³⁰, T. Wenaus²⁵, D. Wendland¹⁶, T. Wengler³⁰, S. Wenig³⁰, N. Vermes²¹, M. Werner⁴⁸, P. Werner³⁰, M. Wessels^{58a}, J. Wetter¹⁶², K. Whalen²⁹, A.M. Wharton⁷², A. White⁸, M.J. White¹, R. White^{32b}, S. White^{124a,124b}, D. Whiteson¹⁶⁴, D. Wicke¹⁷⁶, F.J. Wickens¹³¹, W. Wiedenmann¹⁷⁴, M. Wielers¹³¹, P. Wienemann²¹, C. Wiglesworth³⁶, L.A.M. Wiik-Fuchs²¹, A. Wildauer¹⁰¹, H.G. Wilkens³⁰, H.H. Williams¹²², S. Williams¹⁰⁷, C. Willis⁹⁰, S. Willocq⁸⁶, A. Wilson⁸⁹, J.A. Wilson¹⁸, I. Wingerter-Seez⁵, F. Winklmeier¹¹⁶, B.T. Winter²¹, M. Wittgen¹⁴⁴, J. Wittkowski¹⁰⁰, S.J. Wollstadt⁸³, M.W. Wolter³⁹, H. Wolters^{126a,126c}, B.K. Wosiek³⁹, J. Wotschack³⁰, M.J. Woudstra⁸⁴, K.W. Wozniak³⁹, M. Wu⁵⁵, S.L. Wu¹⁷⁴, X. Wu⁴⁹, Y. Wu⁸⁹, T.R. Wyatt⁸⁴, B.M. Wynne⁴⁶, S. Xella³⁶, D. Xu^{33a}, L. Xu^{33b,am}, B. Yabsley¹⁵¹, S. Yacoob^{146b,an}, R. Yakabe⁶⁷, M. Yamada⁶⁶, Y. Yamaguchi¹¹⁸, A. Yamamoto⁶⁶, S. Yamamoto¹⁵⁶, T. Yamanaka¹⁵⁶, K. Yamauchi¹⁰³, Y. Yamazaki⁶⁷, Z. Yan²², H. Yang^{33e}, H. Yang¹⁷⁴, Y. Yang¹⁵², S. Yanush⁹³, L. Yao^{33a}, W-M. Yao¹⁵, Y. Yasu⁶⁶, E. Yatsenko⁴², K.H. Yau Wong²¹, J. Ye⁴⁰, S. Ye²⁵, I. Yeletsikh⁶⁵, A.L. Yen⁵⁷, E. Yildirim⁴², K. Yorita¹⁷², R. Yoshida⁶, K. Yoshihara¹²², C. Young¹⁴⁴, C.J.S. Young³⁰, S. Youssef²², D.R. Yu¹⁵, J. Yu⁸, J.M. Yu⁸⁹, J. Yu¹¹⁴, L. Yuan⁶⁷, A. Yurkewicz¹⁰⁸, I. Yusuff^{28,ao}, B. Zabinski³⁹, R. Zaidan⁶³, A.M. Zaitsev^{130,ac}, A. Zaman¹⁴⁹, S. Zambito²³, L. Zanello^{133a,133b}, D. Zanzi⁸⁸, C. Zeitnitz¹⁷⁶, M. Zeman¹²⁸, A. Zemla^{38a}, K. Zengel²³, O. Zenin¹³⁰, T. Ženiš^{145a}, D. Zerwas¹¹⁷, D. Zhang⁸⁹, F. Zhang¹⁷⁴, J. Zhang⁶, L. Zhang¹⁵², R. Zhang^{33b}, X. Zhang^{33d}, Z. Zhang¹¹⁷, X. Zhao⁴⁰, Y. Zhao^{33d,117}, Z. Zhao^{33b}, A. Zhemchugov⁶⁵, J. Zhong¹²⁰, B. Zhou⁸⁹, C. Zhou⁴⁵, L. Zhou³⁵, L. Zhou⁴⁰, N. Zhou¹⁶⁴, C.G. Zhu^{33d}, H. Zhu^{33a}, J. Zhu⁸⁹, Y. Zhu^{33b}, X. Zhuang^{33a}, K. Zhukov⁹⁶, A. Zibell¹⁷⁵, D. Ziemska⁶¹, N.I. Zimine⁶⁵, C. Zimmermann⁸³, R. Zimmermann²¹, S. Zimmermann⁴⁸, Z. Zinonos⁵⁴, M. Zinser⁸³, M. Ziolkowski¹⁴², L. Živković¹³, G. Zobernig¹⁷⁴, A. Zoccoli^{20a,20b}, M. zur Nedden¹⁶, G. Zurzolo^{104a,104b}, L. Zwalinski³⁰.

¹ Department of Physics, University of Adelaide, Adelaide, Australia

² Physics Department, SUNY Albany, Albany NY, United States of America

³ Department of Physics, University of Alberta, Edmonton AB, Canada

⁴ (a) Department of Physics, Ankara University, Ankara; (b) Istanbul Aydin University, Istanbul; (c)

Division of Physics, TOBB University of Economics and Technology, Ankara, Turkey

⁵ LAPP, CNRS/IN2P3 and Université Savoie Mont Blanc, Annecy-le-Vieux, France

⁶ High Energy Physics Division, Argonne National Laboratory, Argonne IL, United States of America

⁷ Department of Physics, University of Arizona, Tucson AZ, United States of America

⁸ Department of Physics, The University of Texas at Arlington, Arlington TX, United States of America

⁹ Physics Department, University of Athens, Athens, Greece

¹⁰ Physics Department, National Technical University of Athens, Zografou, Greece

- ¹¹ Institute of Physics, Azerbaijan Academy of Sciences, Baku, Azerbaijan
- ¹² Institut de Física d'Altes Energies and Departament de Física de la Universitat Autònoma de Barcelona, Barcelona, Spain
- ¹³ Institute of Physics, University of Belgrade, Belgrade, Serbia
- ¹⁴ Department for Physics and Technology, University of Bergen, Bergen, Norway
- ¹⁵ Physics Division, Lawrence Berkeley National Laboratory and University of California, Berkeley CA, United States of America
- ¹⁶ Department of Physics, Humboldt University, Berlin, Germany
- ¹⁷ Albert Einstein Center for Fundamental Physics and Laboratory for High Energy Physics, University of Bern, Bern, Switzerland
- ¹⁸ School of Physics and Astronomy, University of Birmingham, Birmingham, United Kingdom
- ¹⁹ ^(a) Department of Physics, Bogazici University, Istanbul; ^(b) Department of Physics Engineering, Gaziantep University, Gaziantep; ^(c) Department of Physics, Dogus University, Istanbul, Turkey
- ²⁰ ^(a) INFN Sezione di Bologna; ^(b) Dipartimento di Fisica e Astronomia, Università di Bologna, Bologna, Italy
- ²¹ Physikalisches Institut, University of Bonn, Bonn, Germany
- ²² Department of Physics, Boston University, Boston MA, United States of America
- ²³ Department of Physics, Brandeis University, Waltham MA, United States of America
- ²⁴ ^(a) Universidade Federal do Rio De Janeiro COPPE/EE/IF, Rio de Janeiro; ^(b) Electrical Circuits Department, Federal University of Juiz de Fora (UFJF), Juiz de Fora; ^(c) Federal University of Sao Joao del Rei (UFSJ), Sao Joao del Rei; ^(d) Instituto de Fisica, Universidade de Sao Paulo, Sao Paulo, Brazil
- ²⁵ Physics Department, Brookhaven National Laboratory, Upton NY, United States of America
- ²⁶ ^(a) National Institute of Physics and Nuclear Engineering, Bucharest; ^(b) National Institute for Research and Development of Isotopic and Molecular Technologies, Physics Department, Cluj Napoca; ^(c) University Politehnica Bucharest, Bucharest; ^(d) West University in Timisoara, Timisoara, Romania
- ²⁷ Departamento de Física, Universidad de Buenos Aires, Buenos Aires, Argentina
- ²⁸ Cavendish Laboratory, University of Cambridge, Cambridge, United Kingdom
- ²⁹ Department of Physics, Carleton University, Ottawa ON, Canada
- ³⁰ CERN, Geneva, Switzerland
- ³¹ Enrico Fermi Institute, University of Chicago, Chicago IL, United States of America
- ³² ^(a) Departamento de Física, Pontificia Universidad Católica de Chile, Santiago; ^(b) Departamento de Física, Universidad Técnica Federico Santa María, Valparaíso, Chile
- ³³ ^(a) Institute of High Energy Physics, Chinese Academy of Sciences, Beijing; ^(b) Department of Modern Physics, University of Science and Technology of China, Anhui; ^(c) Department of Physics, Nanjing University, Jiangsu; ^(d) School of Physics, Shandong University, Shandong; ^(e) Department of Physics and Astronomy, Shanghai Key Laboratory for Particle Physics and Cosmology, Shanghai Jiao Tong University, Shanghai; ^(f) Physics Department, Tsinghua University, Beijing 100084, China
- ³⁴ Laboratoire de Physique Corpusculaire, Clermont Université and Université Blaise Pascal and CNRS/IN2P3, Clermont-Ferrand, France
- ³⁵ Nevis Laboratory, Columbia University, Irvington NY, United States of America
- ³⁶ Niels Bohr Institute, University of Copenhagen, Kobenhavn, Denmark
- ³⁷ ^(a) INFN Gruppo Collegato di Cosenza, Laboratori Nazionali di Frascati; ^(b) Dipartimento di Fisica, Università della Calabria, Rende, Italy
- ³⁸ ^(a) AGH University of Science and Technology, Faculty of Physics and Applied Computer Science, Krakow; ^(b) Marian Smoluchowski Institute of Physics, Jagiellonian University, Krakow, Poland
- ³⁹ Institute of Nuclear Physics Polish Academy of Sciences, Krakow, Poland
- ⁴⁰ Physics Department, Southern Methodist University, Dallas TX, United States of America

41 Physics Department, University of Texas at Dallas, Richardson TX, United States of America
42 DESY, Hamburg and Zeuthen, Germany
43 Institut für Experimentelle Physik IV, Technische Universität Dortmund, Dortmund, Germany
44 Institut für Kern- und Teilchenphysik, Technische Universität Dresden, Dresden, Germany
45 Department of Physics, Duke University, Durham NC, United States of America
46 SUPA - School of Physics and Astronomy, University of Edinburgh, Edinburgh, United Kingdom
47 INFN Laboratori Nazionali di Frascati, Frascati, Italy
48 Fakultät für Mathematik und Physik, Albert-Ludwigs-Universität, Freiburg, Germany
49 Section de Physique, Université de Genève, Geneva, Switzerland
50 ^(a) INFN Sezione di Genova; ^(b) Dipartimento di Fisica, Università di Genova, Genova, Italy
51 ^(a) E. Andronikashvili Institute of Physics, Iv. Javakhishvili Tbilisi State University, Tbilisi; ^(b) High Energy Physics Institute, Tbilisi State University, Tbilisi, Georgia
52 II Physikalisches Institut, Justus-Liebig-Universität Giessen, Giessen, Germany
53 SUPA - School of Physics and Astronomy, University of Glasgow, Glasgow, United Kingdom
54 II Physikalisches Institut, Georg-August-Universität, Göttingen, Germany
55 Laboratoire de Physique Subatomique et de Cosmologie, Université Grenoble-Alpes, CNRS/IN2P3, Grenoble, France
56 Department of Physics, Hampton University, Hampton VA, United States of America
57 Laboratory for Particle Physics and Cosmology, Harvard University, Cambridge MA, United States of America
58 ^(a) Kirchhoff-Institut für Physik, Ruprecht-Karls-Universität Heidelberg, Heidelberg; ^(b) Physikalisches Institut, Ruprecht-Karls-Universität Heidelberg, Heidelberg; ^(c) ZITI Institut für technische Informatik, Ruprecht-Karls-Universität Heidelberg, Mannheim, Germany
59 Faculty of Applied Information Science, Hiroshima Institute of Technology, Hiroshima, Japan
60 ^(a) Department of Physics, The Chinese University of Hong Kong, Shatin, N.T., Hong Kong; ^(b) Department of Physics, The University of Hong Kong, Hong Kong; ^(c) Department of Physics, The Hong Kong University of Science and Technology, Clear Water Bay, Kowloon, Hong Kong, China
61 Department of Physics, Indiana University, Bloomington IN, United States of America
62 Institut für Astro- und Teilchenphysik, Leopold-Franzens-Universität, Innsbruck, Austria
63 University of Iowa, Iowa City IA, United States of America
64 Department of Physics and Astronomy, Iowa State University, Ames IA, United States of America
65 Joint Institute for Nuclear Research, JINR Dubna, Dubna, Russia
66 KEK, High Energy Accelerator Research Organization, Tsukuba, Japan
67 Graduate School of Science, Kobe University, Kobe, Japan
68 Faculty of Science, Kyoto University, Kyoto, Japan
69 Kyoto University of Education, Kyoto, Japan
70 Department of Physics, Kyushu University, Fukuoka, Japan
71 Instituto de Física La Plata, Universidad Nacional de La Plata and CONICET, La Plata, Argentina
72 Physics Department, Lancaster University, Lancaster, United Kingdom
73 ^(a) INFN Sezione di Lecce; ^(b) Dipartimento di Matematica e Fisica, Università del Salento, Lecce, Italy
74 Oliver Lodge Laboratory, University of Liverpool, Liverpool, United Kingdom
75 Department of Physics, Jožef Stefan Institute and University of Ljubljana, Ljubljana, Slovenia
76 School of Physics and Astronomy, Queen Mary University of London, London, United Kingdom
77 Department of Physics, Royal Holloway University of London, Surrey, United Kingdom
78 Department of Physics and Astronomy, University College London, London, United Kingdom
79 Louisiana Tech University, Ruston LA, United States of America

- ⁸⁰ Laboratoire de Physique Nucléaire et de Hautes Energies, UPMC and Université Paris-Diderot and CNRS/IN2P3, Paris, France
- ⁸¹ Fysiska institutionen, Lunds universitet, Lund, Sweden
- ⁸² Departamento de Física Teórica C-15, Universidad Autónoma de Madrid, Madrid, Spain
- ⁸³ Institut für Physik, Universität Mainz, Mainz, Germany
- ⁸⁴ School of Physics and Astronomy, University of Manchester, Manchester, United Kingdom
- ⁸⁵ CPPM, Aix-Marseille Université and CNRS/IN2P3, Marseille, France
- ⁸⁶ Department of Physics, University of Massachusetts, Amherst MA, United States of America
- ⁸⁷ Department of Physics, McGill University, Montreal QC, Canada
- ⁸⁸ School of Physics, University of Melbourne, Victoria, Australia
- ⁸⁹ Department of Physics, The University of Michigan, Ann Arbor MI, United States of America
- ⁹⁰ Department of Physics and Astronomy, Michigan State University, East Lansing MI, United States of America
- ⁹¹ ^(a) INFN Sezione di Milano; ^(b) Dipartimento di Fisica, Università di Milano, Milano, Italy
- ⁹² B.I. Stepanov Institute of Physics, National Academy of Sciences of Belarus, Minsk, Republic of Belarus
- ⁹³ National Scientific and Educational Centre for Particle and High Energy Physics, Minsk, Republic of Belarus
- ⁹⁴ Department of Physics, Massachusetts Institute of Technology, Cambridge MA, United States of America
- ⁹⁵ Group of Particle Physics, University of Montreal, Montreal QC, Canada
- ⁹⁶ P.N. Lebedev Institute of Physics, Academy of Sciences, Moscow, Russia
- ⁹⁷ Institute for Theoretical and Experimental Physics (ITEP), Moscow, Russia
- ⁹⁸ National Research Nuclear University MEPhI, Moscow, Russia
- ⁹⁹ D.V. Skobeltsyn Institute of Nuclear Physics, M.V. Lomonosov Moscow State University, Moscow, Russia
- ¹⁰⁰ Fakultät für Physik, Ludwig-Maximilians-Universität München, München, Germany
- ¹⁰¹ Max-Planck-Institut für Physik (Werner-Heisenberg-Institut), München, Germany
- ¹⁰² Nagasaki Institute of Applied Science, Nagasaki, Japan
- ¹⁰³ Graduate School of Science and Kobayashi-Maskawa Institute, Nagoya University, Nagoya, Japan
- ¹⁰⁴ ^(a) INFN Sezione di Napoli; ^(b) Dipartimento di Fisica, Università di Napoli, Napoli, Italy
- ¹⁰⁵ Department of Physics and Astronomy, University of New Mexico, Albuquerque NM, United States of America
- ¹⁰⁶ Institute for Mathematics, Astrophysics and Particle Physics, Radboud University Nijmegen/Nikhef, Nijmegen, Netherlands
- ¹⁰⁷ Nikhef National Institute for Subatomic Physics and University of Amsterdam, Amsterdam, Netherlands
- ¹⁰⁸ Department of Physics, Northern Illinois University, DeKalb IL, United States of America
- ¹⁰⁹ Budker Institute of Nuclear Physics, SB RAS, Novosibirsk, Russia
- ¹¹⁰ Department of Physics, New York University, New York NY, United States of America
- ¹¹¹ Ohio State University, Columbus OH, United States of America
- ¹¹² Faculty of Science, Okayama University, Okayama, Japan
- ¹¹³ Homer L. Dodge Department of Physics and Astronomy, University of Oklahoma, Norman OK, United States of America
- ¹¹⁴ Department of Physics, Oklahoma State University, Stillwater OK, United States of America
- ¹¹⁵ Palacký University, RCPTM, Olomouc, Czech Republic
- ¹¹⁶ Center for High Energy Physics, University of Oregon, Eugene OR, United States of America

- ¹¹⁷ LAL, Université Paris-Sud and CNRS/IN2P3, Orsay, France
- ¹¹⁸ Graduate School of Science, Osaka University, Osaka, Japan
- ¹¹⁹ Department of Physics, University of Oslo, Oslo, Norway
- ¹²⁰ Department of Physics, Oxford University, Oxford, United Kingdom
- ¹²¹ ^(a) INFN Sezione di Pavia; ^(b) Dipartimento di Fisica, Università di Pavia, Pavia, Italy
- ¹²² Department of Physics, University of Pennsylvania, Philadelphia PA, United States of America
- ¹²³ National Research Centre "Kurchatov Institute" B.P.Konstantinov Petersburg Nuclear Physics Institute, St. Petersburg, Russia
- ¹²⁴ ^(a) INFN Sezione di Pisa; ^(b) Dipartimento di Fisica E. Fermi, Università di Pisa, Pisa, Italy
- ¹²⁵ Department of Physics and Astronomy, University of Pittsburgh, Pittsburgh PA, United States of America
- ¹²⁶ ^(a) Laboratório de Instrumentação e Física Experimental de Partículas - LIP, Lisboa; ^(b) Faculdade de Ciências, Universidade de Lisboa, Lisboa; ^(c) Department of Physics, University of Coimbra, Coimbra; ^(d) Centro de Física Nuclear da Universidade de Lisboa, Lisboa; ^(e) Departamento de Física, Universidade do Minho, Braga; ^(f) Departamento de Física Teórica y del Cosmos and CAFPE, Universidad de Granada, Granada (Spain); ^(g) Dep Física and CEFITEC of Faculdade de Ciências e Tecnologia, Universidade Nova de Lisboa, Caparica, Portugal
- ¹²⁷ Institute of Physics, Academy of Sciences of the Czech Republic, Praha, Czech Republic
- ¹²⁸ Czech Technical University in Prague, Praha, Czech Republic
- ¹²⁹ Faculty of Mathematics and Physics, Charles University in Prague, Praha, Czech Republic
- ¹³⁰ State Research Center Institute for High Energy Physics, Protvino, Russia
- ¹³¹ Particle Physics Department, Rutherford Appleton Laboratory, Didcot, United Kingdom
- ¹³² Ritsumeikan University, Kusatsu, Shiga, Japan
- ¹³³ ^(a) INFN Sezione di Roma; ^(b) Dipartimento di Fisica, Sapienza Università di Roma, Roma, Italy
- ¹³⁴ ^(a) INFN Sezione di Roma Tor Vergata; ^(b) Dipartimento di Fisica, Università di Roma Tor Vergata, Roma, Italy
- ¹³⁵ ^(a) INFN Sezione di Roma Tre; ^(b) Dipartimento di Matematica e Fisica, Università Roma Tre, Roma, Italy
- ¹³⁶ ^(a) Faculté des Sciences Ain Chock, Réseau Universitaire de Physique des Hautes Energies - Université Hassan II, Casablanca; ^(b) Centre National de l'Energie des Sciences Techniques Nucleaires, Rabat; ^(c) Faculté des Sciences Semlalia, Université Cadi Ayyad, LPHEA-Marrakech; ^(d) Faculté des Sciences, Université Mohamed Premier and LPTPM, Oujda; ^(e) Faculté des sciences, Université Mohammed V-Agdal, Rabat, Morocco
- ¹³⁷ DSM/IRFU (Institut de Recherches sur les Lois Fondamentales de l'Univers), CEA Saclay (Commissariat à l'Energie Atomique et aux Energies Alternatives), Gif-sur-Yvette, France
- ¹³⁸ Santa Cruz Institute for Particle Physics, University of California Santa Cruz, Santa Cruz CA, United States of America
- ¹³⁹ Department of Physics, University of Washington, Seattle WA, United States of America
- ¹⁴⁰ Department of Physics and Astronomy, University of Sheffield, Sheffield, United Kingdom
- ¹⁴¹ Department of Physics, Shinshu University, Nagano, Japan
- ¹⁴² Fachbereich Physik, Universität Siegen, Siegen, Germany
- ¹⁴³ Department of Physics, Simon Fraser University, Burnaby BC, Canada
- ¹⁴⁴ SLAC National Accelerator Laboratory, Stanford CA, United States of America
- ¹⁴⁵ ^(a) Faculty of Mathematics, Physics & Informatics, Comenius University, Bratislava; ^(b) Department of Subnuclear Physics, Institute of Experimental Physics of the Slovak Academy of Sciences, Kosice, Slovak Republic
- ¹⁴⁶ ^(a) Department of Physics, University of Cape Town, Cape Town; ^(b) Department of Physics,

- University of Johannesburg, Johannesburg; ^(c) School of Physics, University of the Witwatersrand, Johannesburg, South Africa
- ¹⁴⁷ ^(a) Department of Physics, Stockholm University; ^(b) The Oskar Klein Centre, Stockholm, Sweden
- ¹⁴⁸ Physics Department, Royal Institute of Technology, Stockholm, Sweden
- ¹⁴⁹ Departments of Physics & Astronomy and Chemistry, Stony Brook University, Stony Brook NY, United States of America
- ¹⁵⁰ Department of Physics and Astronomy, University of Sussex, Brighton, United Kingdom
- ¹⁵¹ School of Physics, University of Sydney, Sydney, Australia
- ¹⁵² Institute of Physics, Academia Sinica, Taipei, Taiwan
- ¹⁵³ Department of Physics, Technion: Israel Institute of Technology, Haifa, Israel
- ¹⁵⁴ Raymond and Beverly Sackler School of Physics and Astronomy, Tel Aviv University, Tel Aviv, Israel
- ¹⁵⁵ Department of Physics, Aristotle University of Thessaloniki, Thessaloniki, Greece
- ¹⁵⁶ International Center for Elementary Particle Physics and Department of Physics, The University of Tokyo, Tokyo, Japan
- ¹⁵⁷ Graduate School of Science and Technology, Tokyo Metropolitan University, Tokyo, Japan
- ¹⁵⁸ Department of Physics, Tokyo Institute of Technology, Tokyo, Japan
- ¹⁵⁹ Department of Physics, University of Toronto, Toronto ON, Canada
- ¹⁶⁰ ^(a) TRIUMF, Vancouver BC; ^(b) Department of Physics and Astronomy, York University, Toronto ON, Canada
- ¹⁶¹ Faculty of Pure and Applied Sciences, University of Tsukuba, Tsukuba, Japan
- ¹⁶² Department of Physics and Astronomy, Tufts University, Medford MA, United States of America
- ¹⁶³ Centro de Investigaciones, Universidad Antonio Narino, Bogota, Colombia
- ¹⁶⁴ Department of Physics and Astronomy, University of California Irvine, Irvine CA, United States of America
- ¹⁶⁵ ^(a) INFN Gruppo Collegato di Udine, Sezione di Trieste, Udine; ^(b) ICTP, Trieste; ^(c) Dipartimento di Chimica, Fisica e Ambiente, Università di Udine, Udine, Italy
- ¹⁶⁶ Department of Physics, University of Illinois, Urbana IL, United States of America
- ¹⁶⁷ Department of Physics and Astronomy, University of Uppsala, Uppsala, Sweden
- ¹⁶⁸ Instituto de Física Corpuscular (IFIC) and Departamento de Física Atómica, Molecular y Nuclear and Departamento de Ingeniería Electrónica and Instituto de Microelectrónica de Barcelona (IMB-CNM), University of Valencia and CSIC, Valencia, Spain
- ¹⁶⁹ Department of Physics, University of British Columbia, Vancouver BC, Canada
- ¹⁷⁰ Department of Physics and Astronomy, University of Victoria, Victoria BC, Canada
- ¹⁷¹ Department of Physics, University of Warwick, Coventry, United Kingdom
- ¹⁷² Waseda University, Tokyo, Japan
- ¹⁷³ Department of Particle Physics, The Weizmann Institute of Science, Rehovot, Israel
- ¹⁷⁴ Department of Physics, University of Wisconsin, Madison WI, United States of America
- ¹⁷⁵ Fakultät für Physik und Astronomie, Julius-Maximilians-Universität, Würzburg, Germany
- ¹⁷⁶ Fachbereich C Physik, Bergische Universität Wuppertal, Wuppertal, Germany
- ¹⁷⁷ Department of Physics, Yale University, New Haven CT, United States of America
- ¹⁷⁸ Yerevan Physics Institute, Yerevan, Armenia
- ¹⁷⁹ Centre de Calcul de l'Institut National de Physique Nucléaire et de Physique des Particules (IN2P3), Villeurbanne, France
- ^a Also at Department of Physics, King's College London, London, United Kingdom
- ^b Also at Institute of Physics, Azerbaijan Academy of Sciences, Baku, Azerbaijan
- ^c Also at Novosibirsk State University, Novosibirsk, Russia

- d* Also at TRIUMF, Vancouver BC, Canada
- e* Also at Department of Physics, California State University, Fresno CA, United States of America
- f* Also at Department of Physics, University of Fribourg, Fribourg, Switzerland
- g* Also at Departamento de Fisica e Astronomia, Faculdade de Ciencias, Universidade do Porto, Portugal
- h* Also at Tomsk State University, Tomsk, Russia
- i* Also at CPPM, Aix-Marseille Université and CNRS/IN2P3, Marseille, France
- j* Also at Università di Napoli Parthenope, Napoli, Italy
- k* Also at Institute of Particle Physics (IPP), Canada
- l* Also at Particle Physics Department, Rutherford Appleton Laboratory, Didcot, United Kingdom
- m* Also at Department of Physics, St. Petersburg State Polytechnical University, St. Petersburg, Russia
- n* Also at Louisiana Tech University, Ruston LA, United States of America
- o* Also at Institucio Catalana de Recerca i Estudis Avancats, ICREA, Barcelona, Spain
- p* Also at Department of Physics, National Tsing Hua University, Taiwan
- q* Also at Department of Physics, The University of Texas at Austin, Austin TX, United States of America
- r* Also at Institute of Theoretical Physics, Ilia State University, Tbilisi, Georgia
- s* Also at CERN, Geneva, Switzerland
- t* Also at Georgian Technical University (GTU), Tbilisi, Georgia
- u* Also at Ochadai Academic Production, Ochanomizu University, Tokyo, Japan
- v* Also at Manhattan College, New York NY, United States of America
- w* Also at Hellenic Open University, Patras, Greece
- x* Also at Institute of Physics, Academia Sinica, Taipei, Taiwan
- y* Also at LAL, Université Paris-Sud and CNRS/IN2P3, Orsay, France
- z* Also at Academia Sinica Grid Computing, Institute of Physics, Academia Sinica, Taipei, Taiwan
- aa* Also at School of Physics, Shandong University, Shandong, China
- ab* Also at Dipartimento di Fisica, Sapienza Università di Roma, Roma, Italy
- ac* Also at Moscow Institute of Physics and Technology State University, Dolgoprudny, Russia
- ad* Also at Section de Physique, Université de Genève, Geneva, Switzerland
- ae* Also at International School for Advanced Studies (SISSA), Trieste, Italy
- af* Also at Department of Physics and Astronomy, University of South Carolina, Columbia SC, United States of America
- ag* Also at School of Physics and Engineering, Sun Yat-sen University, Guangzhou, China
- ah* Also at Faculty of Physics, M.V.Lomonosov Moscow State University, Moscow, Russia
- ai* Also at National Research Nuclear University MEPhI, Moscow, Russia
- aj* Also at Department of Physics, Stanford University, Stanford CA, United States of America
- ak* Also at Institute for Particle and Nuclear Physics, Wigner Research Centre for Physics, Budapest, Hungary
- al* Also at Department of Physics, Oxford University, Oxford, United Kingdom
- am* Also at Department of Physics, The University of Michigan, Ann Arbor MI, United States of America
- an* Also at Discipline of Physics, University of KwaZulu-Natal, Durban, South Africa
- ao* Also at University of Malaya, Department of Physics, Kuala Lumpur, Malaysia
- * Deceased